

**THE SYNTHESIS AND CHARACTERIZATION OF CU(I) NETWORKS WITH
HETEROCYCLIC BRIDGING LIGANDS**

A Thesis

Presented to

The Faculty of the Department of Chemistry
The College of William and Mary in Virginia

In Partial Fulfillment

Of the Requirements for the Degree of
Master of Arts

by

Jonathan Timothy Maeyer

2001

APPROVAL SHEET

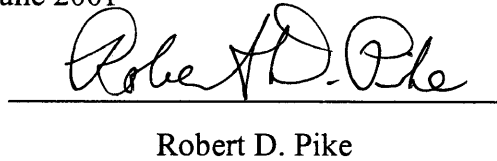
This thesis is submitted in partial fulfillment of

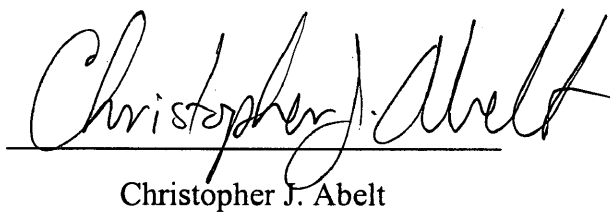
The requirements for the degree of

Master of Arts


Author

Approved, June 2001


Robert D. Pike


Christopher J. Abelt

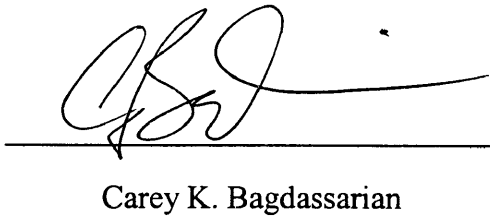

Carey K. Bagdassarian

TABLE OF CONTENTS

Acknowledgements	<i>vii</i>
List of Tables	<i>viii</i>
List of Figures	<i>ix</i>
Abstract	<i>xii</i>
Introduction	2
Experimental	
General Methods.....	11
Materials	11
General Syntheses	11
Preparation of $[\text{Cu}(\text{Pam})(\text{PPh}_3)_2]^+ \text{BF}_4^-$	11
Preparation of $[\text{Cu}_2(\text{Pdca})(\text{PPh}_3)_4]^{2+} 2 \text{BF}_4^-$	12
Preparation of $[\text{Cu}(\text{D-Pca})(\text{PPh}_3)_2]$	12
Preparation of $[(\text{CuCl})\text{Pdz}]$	12
Preparation of $[(\text{CuI})_2\text{Pym}]$	13
Preparation of $[(\text{CuI})_2(\text{PPh}_3)_2\text{Pdz}]$	13
Preparation of $[(\text{CuBr})_2\text{Trz}]$	13
Preparation of $[(\text{CuCl})_2(\text{P}(\text{OPh})_3)_2\text{Trz}]$	14
Stability Test for $[(\text{CuI})_x(\text{Pdz})]$ $x = 1,2$	14
Atomic Absorption Analysis.....	15
Thermogravimetric Analysis.....	15
Results and Discussion	
Pyrazine Acids and Amides	16

Results with Pyrazine Carboxylic Acid (Pca).....	24
[Cu(Pca)(PPh ₃) ₂] ⁺ BF ₄ ⁻	24
[Cu(D-Pca)(PPh ₃) ₂].....	25
Results with Pyrazine Dicarboxylic Acid (Pdca).....	26
[Cu ₂ (Pdca)(PPh ₃) ₄] ²⁺ 2 BF ₄ ⁻	26
[Cu ₂ (D-Pdca)(PPh ₃) ₄] ⁺ BF ₄ ⁻	28
Results with Pyrazine Carboxamide (Pam)	29
[Cu(Pam)(PPh ₃) ₂] ⁺ BF ₄ ⁻	29
[Cu ₂ (D-Pam)(PPh ₃) ₄] ⁺ BF ₄ ⁻	30
Results with Pyrazine Dicarboxamide (Pdam)	31
[Cu ₂ (Pdam)(PPh ₃) ₄] ²⁺ 2 BF ₄ ⁻	31
[Cu ₂ (D-Pdam)(PPh ₃) ₄] ⁺ BF ₄ ⁻	32
Pyrimidine, Pyridazine, and Triazine Halide Complexes	34
Pyrimidine.....	43
[(CuCl) ₂ Pym]	43
[(CuBr) ₂ Pym]	45
[(CuI) ₂ Pym].....	46
[(CuCl) ₂ (PPh ₃) ₂ Pym]	49
[(CuCl) ₂ (P(OPh) ₃) ₂ Pym].....	50
[(CuBr) ₂ (PPh ₃) ₂ Pym]	51
[(CuBr) ₂ (P(OPh) ₃) ₂ Pym].....	53
[(CuI) ₂ (PPh ₃) ₂ Pym].....	54
[(CuI) ₂ (P(OPh) ₃) ₂ Pym]	56

Pyridazine.....	56
[(CuCl)Pd _z].....	56
[(CuBr)Pd _z]	57
[(CuI)Pd _z]	60
[(CuI) ₂ Pd _z]	62
[(CuCl) ₂ (PPh ₃) ₂ Pd _z]	63
[(CuCl)(P(OPh) ₃)Pd _z].....	65
[(CuBr)(PPh ₃)Pd _z]	66
[(CuBr)(P(OPh) ₃)Pd _z]	68
[(CuI)(PPh ₃)Pd _z].....	70
[(CuI) ₂ (P(OPh) ₃) ₂ Pd _z]	71
Triazine	71
[(CuCl) ₂ Trz].....	71
[(CuCl) ₃ Trz].....	73
[(CuBr) ₃ (Trz) ₂].....	74
[(CuBr) ₂ Trz].....	75
[(CuBr) ₃ Trz].....	76
[(CuI) ₂ Trz]	78
[(CuCl) ₃ (PPh ₃) ₃ Trz]	80
[(CuCl) ₂ (P(OPh) ₃) ₂ Trz]	81
[(CuBr) ₂ (PPh ₃) ₂ Trz].....	82
[(CuBr) ₂ (P(OPh) ₃) ₂ Trz]	84
[(CuI) ₂ (PPh ₃) ₂ Trz]	85

$[(\text{CuI})_3(\text{P}(\text{OPh})_3)_3\text{Trz}]$	86
Conclusion	89
Appendix A	91
References	94
Vita	96

ACKNOWLEDGEMENTS

The author wishes to express his sincere gratitude to Dr. Robert D. Pike for his endless patience, expert supervision, and forgiving humor. He would also like to thank Dr. Christopher J. Abelt and Dr. Carey K. Bagdassarian for their critique of this manuscript. The author conveys his appreciation to his family, Lucy Ann, Ulrich, Nicole, and Heidi Maeyer, for their constant support. He is very grateful to his close friends, especially Erkyel Aklu, for their kindness and strength. The author would like to give particular recognition to Jenine Cole for her encouragement and keeping him focused. He would also like to give special thanks to Don and Susie Beck for providing him with a home away from home.

LIST OF TABLES

Table		Page
1.	Dielectric Constants of Some Solvents.....	23
2.	Average chain length data for acid and amide oligomers	23
3.	Synthetic and Analytical Data for [(CuX) _n B _m] Complexes (n=1,2,3; m=1,2)..	38
4.	Synthetic and Analytical Data for [(CuX) _n (L) _n B] Complexes (n = 1,2,3).....	39
5.	Thermogravimetric Decomposition Results for [(CuX) _n B _m] Complexes.....	41
6.	Thermogravimetric Decomposition Results for [(CuX) _n (L) _n B] Complexes....	42
7.	Thermodynamic Stability Test for [(CuI) ₂ Pym]	48
8.	Thermodynamic Stability Test for [(CuBr)Pdz]	59
9.	Thermodynamic Stability Test for [(CuI) _x Pdz] (x = 1,2).....	62
10.	Thermal Stability Test of [(CuI) ₂ Trz]	79

LIST OF FIGURES

Figure	Page
1. Examples of organic polymers.....	2
2. Examples of inorganic materials.....	3
3. Some known structures of [CuXL].....	5
4. Examples of bidentate and tridentate bridging ligands.....	6
5. Some [(CuX) _n B] oligomers (n = ½, 1, or 2).....	8
6. Formula for the average polymer number using ¹ H NMR.....	16
7. Ratio of Phosphine to Bridging Protons (R) vs. Average Chain Length (N)....	17
8. Calculation of Average Chain Length Using AAS.....	18
9. Examples of Bridging Ligands.....	19
10. Proposed Sheet Polymer of [Cu(Pca)(PPh ₃) ₂] _n ⁿ⁺ n BF ₄ ⁻	20
11. Thermogravimetric Analysis of [Cu(Pca)(PPh ₃) ₂] ⁺ BF ₄ ⁻	25
12. Thermogravimetric Analysis of [Cu(D-Pca)(PPh ₃) ₂].....	26
13. Thermogravimetric Analysis of [Cu ₂ (Pdca)(PPh ₃) ₄] ²⁺ 2 BF ₄ ⁻	27
14. Thermogravimetric Analysis of [Cu ₂ (D-Pdca)(PPh ₃) ₄] ⁺ BF ₄ ⁻	29
15. Thermogravimetric Analysis of [Cu(Pam)(PPh ₃) ₂] ⁺ BF ₄ ⁻	30
16. Thermogravimetric Analysis of [Cu ₂ (D-Pam)(PPh ₃) ₄] ⁺ BF ₄ ⁻	31
17. Thermogravimetric Analysis of [Cu ₂ (Pdam)(PPh ₃) ₄] ²⁺ 2 BF ₄ ⁻	32
18. Thermogravimetric Analysis of [Cu ₂ (D-Pdam)(PPh ₃) ₄] ⁺ BF ₄ ⁻	33
19. Thermogravimetric Analysis of CuCl.....	36
20. Thermogravimetric Analysis of CuBr.....	37
21. Thermogravimetric Analysis of CuI.....	37

22.	Thermogravimetric Analysis of [(CuCl) ₂ Pym]	44
23.	Thermogravimetric Analysis of [(CuBr) ₂ Pym]	46
24.	Thermogravimetric Analysis of [(CuI) ₂ Pym]	48
25.	Thermogravimetric Analysis of [(CuCl) ₂ (PPh ₃) ₂ Pym]	50
26.	Thermogravimetric Analysis of [(CuCl) ₂ (P(OPh) ₃) ₂ Pym]	51
27.	Thermogravimetric Analysis of [(CuBr) ₂ (PPh ₃) ₂ Pym]	52
28.	Thermogravimetric Analysis of [(CuBr) ₂ (P(OPh) ₃) ₂ Pym]	54
29.	Thermogravimetric Analysis of [(CuI) ₂ (PPh ₃) ₂ Pym]	55
30.	Thermogravimetric Analysis of [(CuCl)Pd ₂]	57
31.	Thermogravimetric Analysis of [(CuBr)Pd ₂]	59
32.	Thermogravimetric Analysis of [(CuI)Pd ₂]	61
33.	Thermogravimetric Analysis of [(CuI) ₂ Pd ₂]	63
34.	Thermogravimetric Analysis of [(CuCl) ₂ (PPh ₃) ₂ Pd ₂]	65
35.	Thermogravimetric Analysis of [(CuCl)(P(OPh) ₃)Pd ₂]	66
36.	Thermogravimetric Analysis of [(CuBr)(PPh ₃)Pd ₂]	68
37.	Thermogravimetric Analysis of [(CuBr)(P(OPh) ₃)Pd ₂]	69
38.	Thermogravimetric Analysis of [(CuI)(PPh ₃)Pd ₂]	71
39.	Thermogravimetric Analysis of [(CuCl) ₂ Trz]	72
40.	Thermogravimetric Analysis of [(CuCl) ₃ Trz]	74
41.	Thermogravimetric Analysis of [(CuBr) ₃ (Trz) ₂]	75
42.	Thermogravimetric Analysis of [(CuBr) ₂ Trz]	76
43.	Thermogravimetric Analysis of [(CuBr) ₃ Trz]	77
44.	Thermogravimetric Analysis of [(CuI) ₂ Trz]	79

45.	Thermogravimetric Analysis of $[(\text{CuCl})_3(\text{PPh}_3)_3\text{Trz}]$	81
46.	Thermogravimetric Analysis of $[(\text{CuCl})_2(\text{P}(\text{OPh})_3)_2\text{Trz}]$	82
47.	Thermogravimetric Analysis of $[(\text{CuBr})_2(\text{PPh}_3)_2\text{Trz}]$	83
48.	Thermogravimetric Analysis of $[(\text{CuBr})_2(\text{P}(\text{OPh})_3)_2\text{Trz}]$	85
49.	Thermogravimetric Analysis of $[(\text{CuI})_2(\text{PPh}_3)_2\text{Trz}]$	86
50.	Thermogravimetric Analysis of $[(\text{CuI})(\text{P}(\text{OPh})_3)]_3\text{Trz}]$	88
A1.	Proton NMR of $[\text{Cu}(\text{Pca})(\text{PPh}_3)_2]^+ \text{BF}_4^-$	91
A2.	Proton NMR of $[\text{Cu}(\text{D-Pca})(\text{PPh}_3)_2]$	92
A3.	Proton NMR of $[\text{Cu}_2(\text{Pdca})(\text{PPh}_3)_4]^{2+} 2 \text{BF}_4^-$	93

ABSTRACT

Overall, a total of thirty-seven network compounds of copper(I) were synthesized as part of this project. The compounds were analyzed by AAS and TGA to confirm their composition.

Thirteen complexes of CuX ($X = \text{Cl, Br, I}$) with heterocyclic bridging ligands (pyrimidine (Pym), pyridazine (Pdz), and triazine (Trz)) have been synthesized. The pyrimidine compounds all show the $[(\text{CuX})_2\text{Pym}]$ stoichiometry. The pyridazine bridge forms $[(\text{CuX})\text{Pdz}]$ for all three halides, as well as forming $[(\text{CuI})_2\text{Pdz}]$. Triazine forms $[(\text{CuX})_2\text{Trz}]$ for all three halides, $[(\text{CuX})_3\text{Trz}]$ for the Cl and Br derivatives, and Br also forms a $[(\text{CuBr})_3(\text{Trz})_2]$ stoichiometry. Several of these systems were analyzed using thermodynamic stability tests to confirm stoichiometries.

Sixteen compounds of the type $[(\text{CuX})_n\text{L}_n\text{B}]$ ($X = \text{Cl, Br, I}$; $\text{L} =$ triphenylphosphine (PPh_3), triphenylphosphite (P(OPh)_3); $\text{B} = \text{Pym, Pdz, Trz}$) have been prepared. The compounds formed with the bridging ligand pyrimidine, all exhibit the $[(\text{CuX})_2\text{L}_2\text{Pym}]$ stoichiometry, with the exception that the CuI-P(OPh)_3 product does not form. The pyridazine complexes formed are of the type, $[(\text{CuX})\text{LB}]$. The only exceptions to this rule is the formation of $[(\text{CuCl})_2(\text{PPh}_3)_2\text{Pdz}]$ and the inability to form a CuI-P(OPh)_3 compound. Complexes of the type $[(\text{CuX})_2\text{L}_2\text{Trz}]$ are formed for all combinations except for the CuCl-PPh_3 and CuI-P(OPh)_3 analogs which form $[(\text{CuX})_3\text{L}_3\text{Trz}]$ stoichiometries.

Eight oligomeric compounds with the formula $[\text{Cu}_n\text{L}_n\text{B}]$ ($\text{L} = \text{PPh}_3$; $\text{B} =$ pyrazine carboxylic acid (Pca) and its deprotonated analog: (D-Pca), pyrazine dicarboxylic acid (Pdca) and (D-Pdca), pyrazine carboxamide (Pam) and (D-Pam), pyrazine dicarboxamide (Pdam) and (D-Pdam). The complexes from Pca, Pam, and D-Pca formed long oligomers of the type $[\text{CuB}(\text{PPh}_3)_2]$. The remaining bridging ligands formed dimers of the type $[\text{Cu}_2\text{B}(\text{PPh}_3)_4]$. These compounds were characterized using AAS, TGA, and ^1H NMR.

**THE SYNTHESIS AND CHARACTERIZATION OF CU(I) NETWORKS
WITH HETEROCYCLIC BRIDGING LIGANDS**

INTRODUCTION

Organic polymers and inorganic materials have been studied extensively for many years. Until recently, materials scientists have worked almost exclusively in these areas. Organic polymers consist of long covalently bonded chains produced from low molecular weight monomers, which contain mostly carbon, hydrogen, oxygen, and nitrogen. Polymers are usually lightweight, non-conductive, colorless, and of low-to-moderate thermal stability. Examples of organic polymers include poly(vinyl chloride) (PVC) and polyformaldehyde (Figure 1). In contrast, inorganic materials can be covalently or ionically bonded, and tend to form more highly networked structures, such as three-dimensional (3-D) lattices (Figure 2). Unary materials, such as copper, silicon, sulfur, diamond, and graphite are formed from a single element. Common rock salt, NaCl and cubic zinc sulfide are examples of binary lattices. Ternary lattice structures, such as FeCuS₂, also exist. The complexity of the lattice tends to increase with the number of elemental substituents.

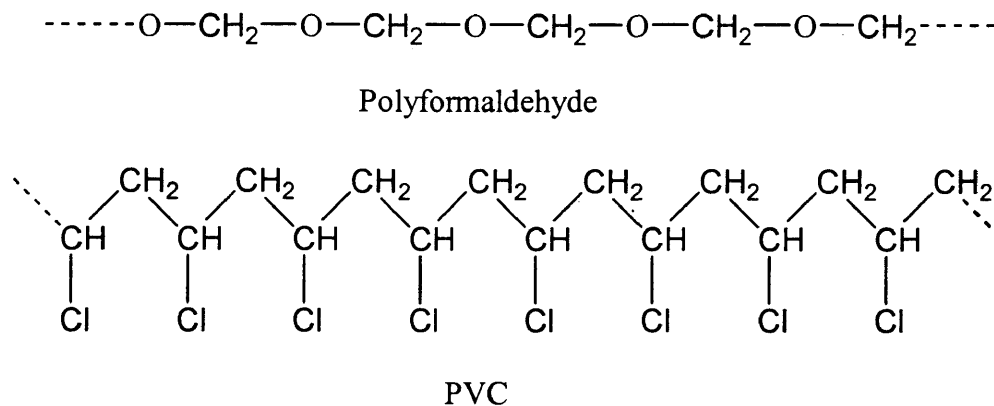
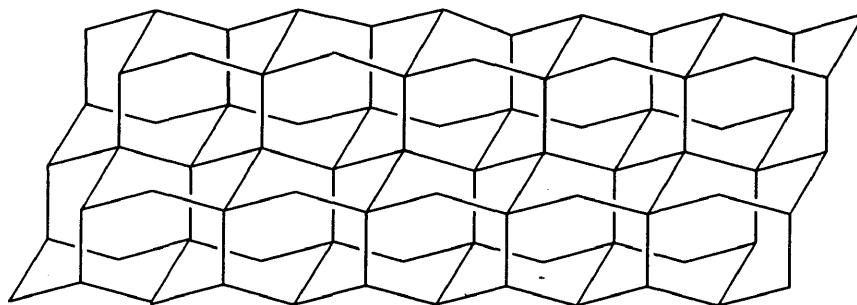
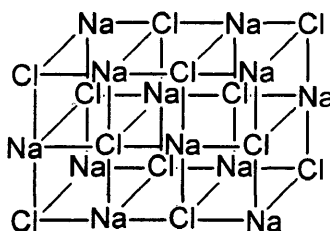


Figure 1. Examples of organic polymers.



Diamond



NaCl, rock salt

Figure 2. Examples of inorganic materials.

Only recently, scientists have begun to conduct research at the interface of organic and inorganic materials. Metal-organic network compounds consist of metal ions connected by organic ligands. Network-forming, ‘bridging’, ligands are bifunctional (bidentate), or greater, and are geometrically unable to chelate. The resulting networks can comprise a wide array of differing structural types, including one, two, and three-dimensional networks. The long-range framework of a metal-organic network is called the ‘supramolecular’ structure. Chemical and structural characterization of these highly complex, and often insoluble, networks can be very difficult. X-ray crystallography has proved to be a key tool in such efforts.

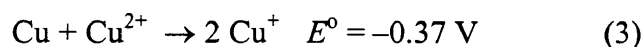
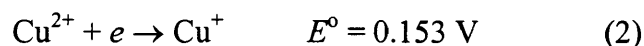
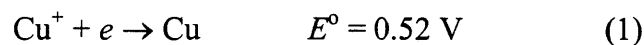
One-dimensional metal-organic structures include infinite straight chain polymers, ladder polymers, and short chain ‘capped’ oligomers. Capping ligands are

monodentate, or chelating polydentate, and therefore inhibit chain growth by blocking a metal coordination site. Two examples of monodentate capping ligands we have employed in the following study are triphenylphosphine (PPh_3) and triphenylphosphite (P(OPh)_3). Many two- and three-dimensional network geometries are known, including a variety of sheets and lattices.

There are many potential applications for the chemistry of networked supermolecules incorporating transition metals. For example, the channels and cavities formed in the network crystal lattice might provide catalytic sites for size- or shape-specific reactions. These materials may also have molecular sieve properties, due to ease of molecular or ionic diffusion effects. The large cavities may form strong, low-density materials.¹

Of the transition metals, the group 11 elements are of particular interest. They have high thermal and electrical conductivities. They are known as the 'coinage metals' due to their high malleability and metallic sheen. Of particular use to us is the +1 oxidation state of copper. The copper(I) state has a filled d^{10} valence electron configuration. Its compounds are usually colorless, except when charge transfer is occurring. The usually green or blue compounds of copper(II) have a partially-filled d^9 valence electron configuration. Copper(I) is more polarizable than copper(II), and as a 'softer' electrophile, is apt to bond with soft nucleophiles, such as those of phosphorus, sulfur, and unsaturated nitrogen. Copper(II) tends to bond to harder nucleophiles, oxygen for example. Copper(I) usually prefers four- or three-coordination, but can sometimes be two-coordinate. Due to the lack of crystal field effects, four-coordinate copper(I) always shows roughly tetrahedral geometry.

The relative stabilities of the copper(I) and copper(II) oxidation states in solution strongly depends on the copper's environment. Most copper(I) complexes are unstable in water and become oxidized to copper(II). Likewise, in a solvent such as acetonitrile, copper(II) complexes can be reduced to copper(I) species. These stabilities are indicated by the following aqueous copper reduction potential data:



The crystal structures of the copper(I) halides ($\text{CuX} = \text{CuCl}, \text{CuBr}, \text{CuI}$) are known. They form diamond-like (cubic ZnS) networks having four-coordinate copper and halide centers. When capping ligands (L) are incorporated into the copper halide networks, a variety of molecular and polymeric structures $[\text{CuXL}_n]$ are formed.² Some known structures are dimers, cubanes, stepped tetramers, split stairs, infinite stairs, and displaced stairs (Figure 3).

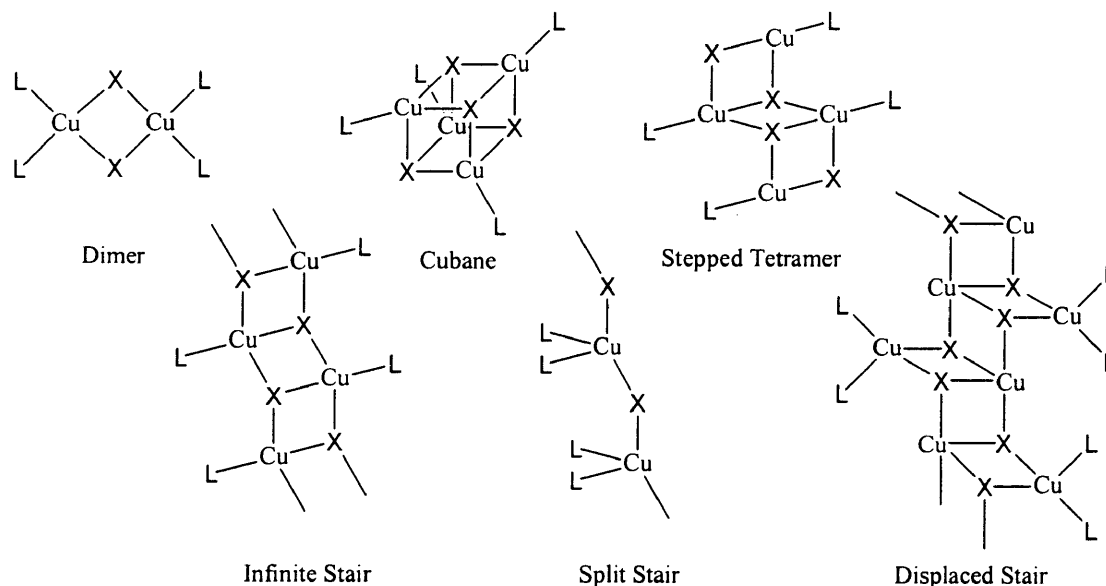


Figure 3. Some known structures of $[\text{CuXL}]$.

The soft-soft bonding interaction can be seen in the formation of these capped structures. The phosphorus of the phosphine or phosphite can donate its lone pair of electrons to the copper(I). The same is true for the interaction between copper(I) and unsaturated aromatic nitrogens. The lone pairs of nitrogen readily donate their electron pair to copper(I) to form stable complexes. An aromatic ring containing two or more non-chelating, polydentate nitrogens are capable of bridging two or more copper centers. These bridging compounds are usually more highly networked and multidimensional than their capped counterparts. We are interested in three of these pyrazine (Pyz) type bridging ligands: pyridazine (Pdz), pyrimidine (Pym), and triazine (Trz) (Figure 4).

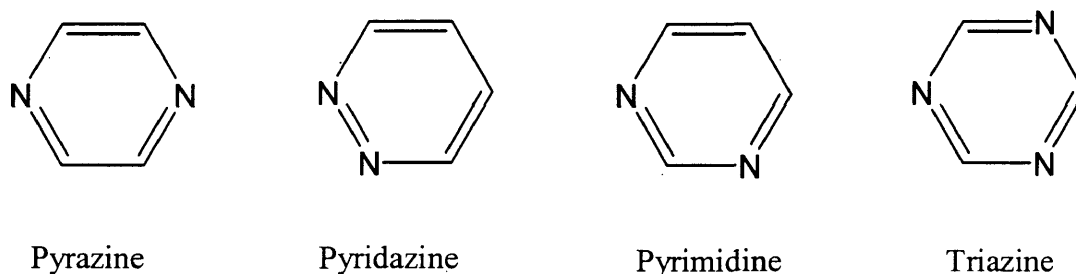
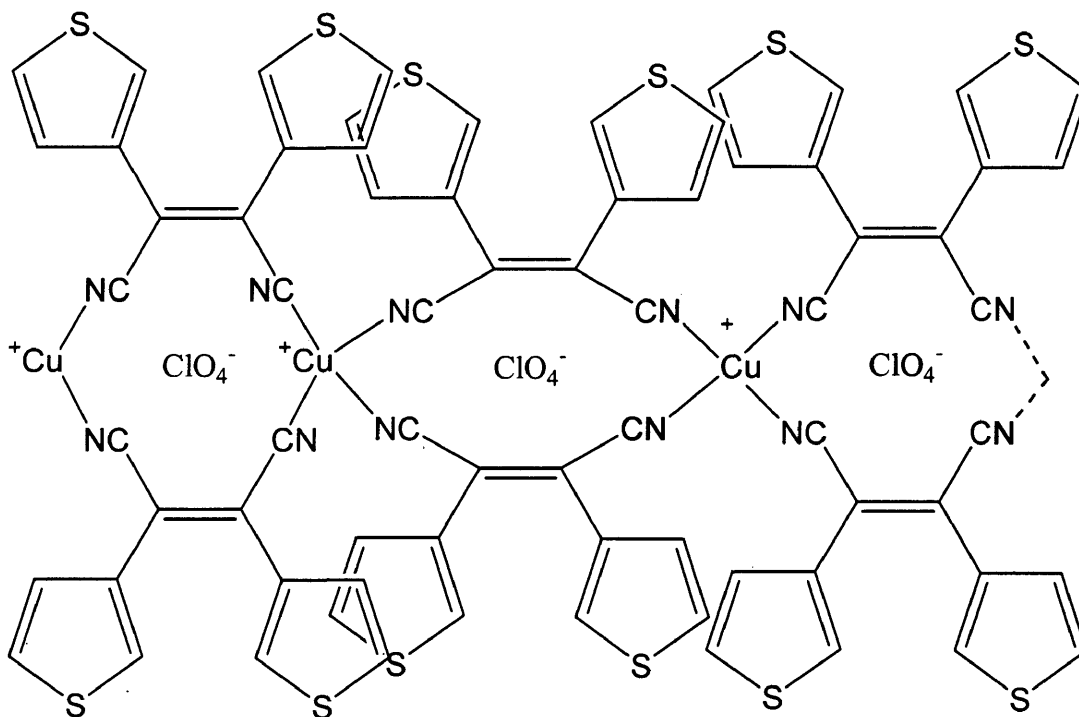


Figure 4. Examples of bidentate and tridentate bridging ligands.

Some examples of bridging ligands in CuX chemistry are directly comparable to some of the [CuXL] structures mentioned before. Complexes can be formed consisting of a bridging ligand with copper(I) without the halide bridge. These are accompanied by spectator anions in place of the halides. These spectator ions tend to occupy empty spaces in the crystal structure without significantly affecting the bonding of the molecule.³ When using a bidentate bridging ligand these complexes formed usually have the formula [CuB₂]⁺. In the presence of a capping ligand these structures can form one

dimensional polymers $[\text{CuBL}_2]^+$ and two dimensional sheets $[\text{Cu}_2\text{B}_3\text{L}_2]^+$. An example of this chemistry is $[\text{Cu}(\text{cis-L})_2]^+ \text{ClO}_4^-$ (L = 1,2-bis(2,4,5-trimethyl-3-thienyl)ethane) 1.⁴



1

Complexes can be formed that are bridged through both halides and bridging ligands. These complexes exhibit extensive networking capabilities, due to their complexity. The complex $[(\text{CuBr})\text{Pyz}]$ forms a two-dimensional sheet with copper(I) being bridged by both bromide and pyrazine. This is comparable to a zigzag polymer bridged by a pyrazine at every copper(I).⁵ The $[(\text{CuI})(\text{Py})_2]$ complex (Py = pyridine) follows the same guidelines, it is directly comparable to a $[\text{CuXL}]$ structure except it is capped by pyridine.⁶ The $[(\text{CuI})_2(\text{Quin})]$ complex (Quin = quinoxaline) is similar to the $[\text{CuXL}]$ stair step polymer (Figure 5). Each stair step is bridged at the copper(I) to form a more networked, two-dimensional structure.⁵ It is thus possible to see the increase in dimensionality by the introduction of bridging ligands.

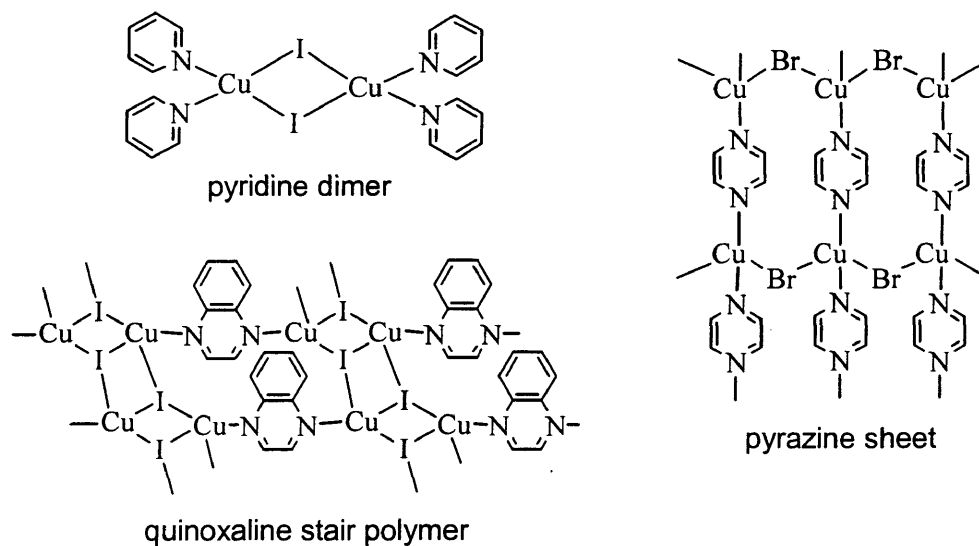
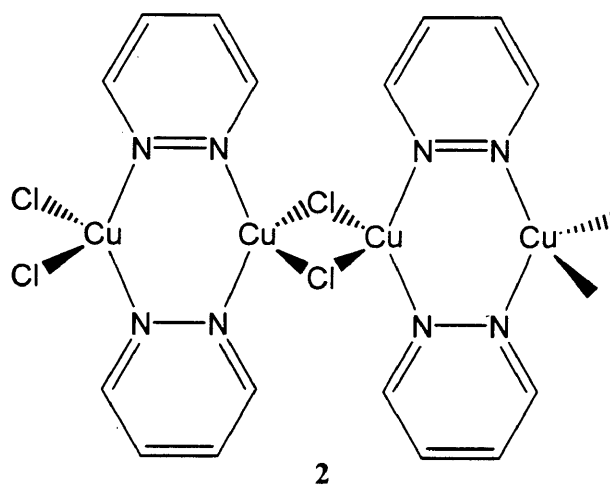


Figure 5. Some $[(\text{CuX})_n\text{B}]$ oligomers ($n = \frac{1}{2}, 1, \text{ or } 2$).

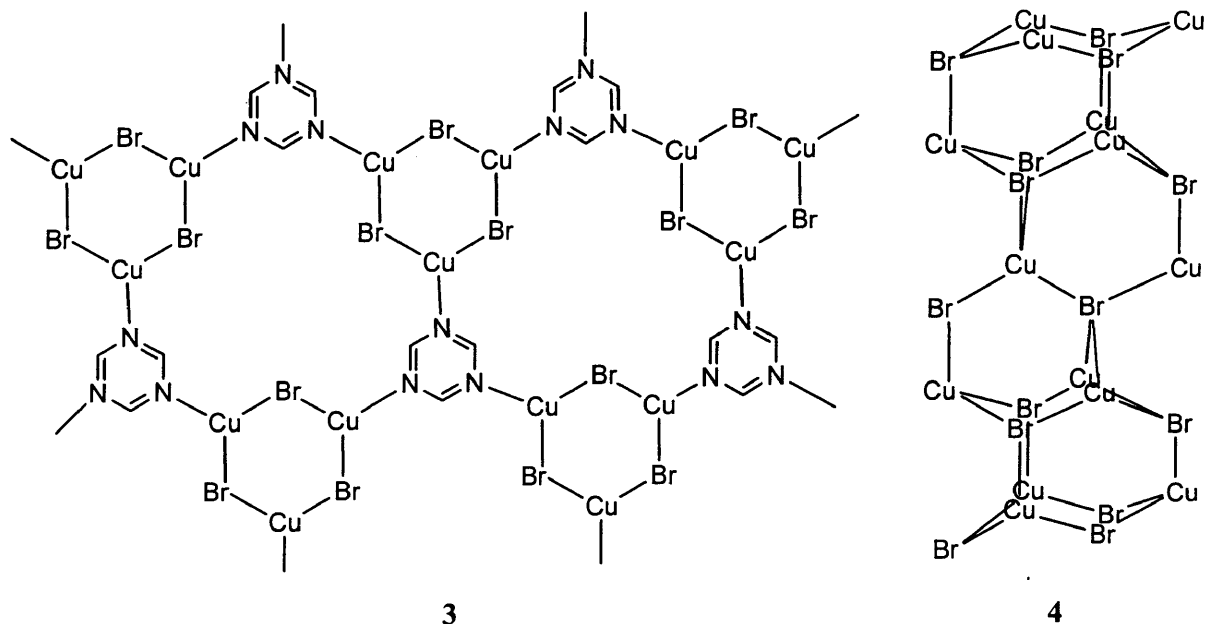
Some related research has been conducted in the copper halide chemistry incorporating bridging ligands. Previously, $[(\text{CuX})\text{PdZ}]$, where $\text{X} = \text{Cl}, \text{Br}, \text{ and } \text{I}$, had been discovered as well as a $[(\text{CuI})_2\text{PdZ}]$ complex. The compound $[\text{CuCl}(\text{PdZ})]$ **2** forms an unusual polymeric structure. There is a substructure within the polymer that consists of four aromatic nitrogens, from two pyridazines, and two coppers to form a six membered ring. The same source reported forming $[(\text{CuBr})_2(\text{Pym})_2]$.⁷ A $[(\text{CuI})_2\text{Pym}]$ complex with a CuI staircase chain was reported as well.⁸



Using pseudo-halides can duplicate this bridging action observed in these molecules. These pseudo-halides carry an overall negative charge and are bidentate. Some examples of these bridging molecules are thiocyanate (SCN^-) and azide (N_3^-). This bonding is analogous to halide bridging as can be observed in the complexes, $[\text{Cu}_2(\text{SCN})_2\text{Bpy}]$ and $[\text{Cu}(\text{N}_3)\text{PyZ}]$.^{9,10}

The addition of the 'capping' ligands (L), triphenylphosphine (PPh_3) and triphenylphosphite (P(OPh)_3), to these stair step polymers should result in $[(\text{CuX})\text{LB}]$ (1:1:1) oligomers, $[(\text{CuX})_2\text{L}_2\text{B}]$ (2:2:1) oligomers, and even $[(\text{CuX})_3\text{L}_3\text{B}]$ dendrimers when B = triazine. Similar materials have been formed including $[(\text{CuCl})_2(\text{PPh}_3)_2\text{Bpy}]$ and $[(\text{CuCl})_2(\text{PPh}_3)_2\text{PyZ}]$.^{11,12}

When a potentially tridentate ligand such as triazine is introduced, the possible structures that can form are vast. Triazine has the capability to bond with all three, two, or only one of its nitrogens. When incorporated with copper halides the networking can become extensive. Triazine is known to form two structures when complexed with CuX , ($\text{X} = \text{Br}, \text{I}$) either $[(\text{CuX})_2\text{Trz}]$ or $[(\text{CuX})_3\text{Trz}]$. A molecular structure of $[(\text{CuBr})_3\text{Trz}]$ is shown in the schemes below. Scheme 3 is a cross-section of the complex that displays the bonding of the compound on the triazine plane. In this diagram, several CuBr six-membered rings are shown linked by tridentate triazines with threefold symmetry. These CuBr rings are actually vertical columns, 4 that give the molecule its networking characteristics.¹³



The $[(\text{CuI})_2\text{Trz}]$ complex consists of bidentate bridging triazine to form a two dimensional layer. Only two of the nitrogens of triazine bond to the CuI layer leaving one nitrogen with its electron pair. It can be seen that the accumulation of copper halide bridging with a tridentate bridging ligand results in very complex supermolecular structures.

This thesis presents a study of metal-organic chemistry and introduces $[(\text{CuX})_n\text{B}]$ and $[(\text{CuXL})_n\text{B}]$ chemistry ($\text{X} = \text{Cl}, \text{Br}, \text{I}$; $\text{L} = \text{PPh}_3, \text{P}(\text{OPh})_3$; $n = 1, 1.5, 2, 3$; $\text{B} =$ various bidentate and tridentate ligands). Several compounds of the type, $[\text{CuBL}_2]^+ \text{BF}_4^-$ and $[\text{Cu}_2\text{BL}_4]^{2+} 2 \text{BF}_4^-$, are also studied. The presence of the capping ligand in the formation of less networked linear oligomers are described. Several known molecules were synthesized and analyzed. In addition, numerous new compounds have been synthesized and will be introduced to the reader.

EXPERIMENTAL

General Methods. All syntheses were carried out under nitrogen atmosphere. Flame atomic absorption spectroscopy (AAS) was performed with a Perkin-Elmer 1100B spectrophotometer. Microanalyses for C, H, and N were carried out by Atlantic Microlabs, Inc., Norcross, GA. All TGA analyses were conducted on a Shimadzu TGA-50 instrument.

Materials. All ligands were purchased from Aldrich or Acros and were used as received. Copper(I) chloride and bromide were freshly recrystallized from aqueous HCl or HBr. Copper(I) iodide was recrystallized from hot acetonitrile. Ultrex nitric acid was purchased from Baker Chemical.

General Syntheses. The following syntheses are representative reactions. There are a whole series of parallel reactions that involve other bridging ligands at the same ratios.

Preparation of $[\text{Cu}(\text{Pam})(\text{PPh}_3)_2]^+ \text{BF}_4^-$. $[\text{Cu}(\text{NCCH}_3)_4]^+ \text{BF}_4^-$ (0.5025 g, 1.598 mmol) and PPh_3 (0.8390 g, 3.199 mmol) are added to a 100 mL round bottom flask and dissolved in 40 mL of acetone. Pyrazinamide (0.2005 g, 1.629 mmol) is added to the reaction flask to form an orange solution. This is refluxed for 17 h. It is then concentrated to 5 mL. A yellow powder is formed on addition of a large volume of diethyl ether. The product is collected via filtration, washed with diethyl ether, and then dried under vacuum (1.159 g, 1.453 mmol, 91%).

Preparation of $[\text{Cu}_2(\text{Pdca})(\text{PPh}_3)_4]^{2+} 2 \text{BF}_4^-$. $[\text{Cu}(\text{NCCH}_3)_4]^+ \text{BF}_4^-$ (0.7134 g, 2.2679 mmol) and two equivalents of PPh_3 (1.191 g, 4.540 mmol) are added to a 100 mL round bottom flask and dissolved in 40 mL of acetone. One equivalent of pyrazine dicarboxylic acid (0.3855 g, 2.293 mmol) is added to the reaction flask to form a deep red solution with particles of free Pdca in suspension. After stirring for 2 h, the excess Pdca is collected by Buchner filtration. The red filtrate is then concentrated to 10 mL. The solution is transferred to a 125 mL Erlenmeyer flask and allowed to crystallize overnight at 0 °C. Red orange crystals are collected via Buchner filtration, washed with diethyl ether, and then dried under vacuum (1.097 g, 0.7225 mmol, 76%).

Preparation of $[\text{Cu}(\text{D-Pca})(\text{PPh}_3)_2]^+ \text{BF}_4^-$. $[\text{Cu}(\text{Pca})(\text{PPh}_3)_2]^+ \text{BF}_4^-$ (0.2543 g, 0.3183 mmol) and five equivalents of K_2CO_3 (0.2254 g, 1.6310 mmol) are added to a 100 mL round bottom flask and suspended in 50 mL of acetone. Excess K_2CO_3 remains suspended in a yellow solution. This is stirred at room temperature for 17 h. The suspended K_2CO_3 is collected via Buchner filtration and discarded. The yellow filtrate is concentrated to dryness and then redissolved in 15 mL of CH_2Cl_2 . Addition of a large volume of pentane forms a lemon yellow solid. This powder is collected via Buchner filtration, washed with pentane, and then vacuum dried (0.1529 g, 0.2150 mmol, 68%).

Preparation of $[(\text{CuCl})\text{Pdz}]$. CuCl (0.1820 g, 1.839 mmol) is added to a 100 mL beaker and dissolved in 40 mL of acetonitrile. This solution is filtered through paper into a 100 mL round bottom flask. One equivalent of pyridazine (0.1543 g, 1.927 mmol) is added to a 10 mL beaker and dissolved in 3 mL of chloroform. This solution is added to the reaction flask via syringe. Upon addition, a red brown precipitate forms immediately.

This suspension is stirred for one hour and then collected via frit filtration, washed with ether, and then vacuum dried (0.2562 g, 1.431 mmol, 78%).

Preparation of [(CuI)₂Pym]. CuI (0.7715 g, 4.051 mmol) is added to a 100 mL beaker and dissolved in 30 mL of acetonitrile. This is filtered through paper, to remove traces of Cu(II) species, into a 100 mL round bottom flask. This is stirred under nitrogen at 20 °C. One half equivalent of pyrimidine (0.1625 g, 2.029 mmol) is added to a 10 mL beaker and dissolved in 3 mL of acetonitrile. This solution is added to the reaction flask via syringe. Upon addition, a neon yellow precipitate forms immediately. This suspension is stirred for 2 h and then collected via frit filtration, washed with diethyl ether, and then vacuum dried (0.8307 g, 3.604 mmol, 89%).

Preparation of [(CuI)₂(PPh₃)₂Pdz]. CuI (0.3079 g, 1.617 mmol) is added to a 100 mL round bottom flask. One equivalent of PPh₃ (0.4264 g, 1.626 mmol) is added to the flask. This is suspended in 40 mL of CHCl₃ and stirred under nitrogen at 20 °C. One half of an equivalent of pyridazine (0.0680 g, 0.8490 mmol) is added to a 10 mL beaker and dissolved in 3 mL of chloroform. This solution is added to the reaction flask via syringe. Upon addition, an orange solution forms with a trace amount of orange powder, [(CuI)(Pdz)], in suspension. The reaction is stirred for 15 min. The powder is collected via paper filtration and discarded. The orange filtrate is concentrated to 10 mL. The orange-yellow solid product is formed upon addition of a large volume of diethyl ether. This is then collected by frit filtration, washed with diethyl ether, and then vacuum dried (0.5210 g, 1.057 mmol, 65%).

Preparation of [(CuBr)₂Trz]. CuBr (1.057 g, 7.366 mmol) is added to a 100 mL beaker and dissolved in 40 mL of acetonitrile. This is filtered through paper, to remove

traces of Cu(II) species, into a 100 mL round bottom flask. This is stirred under nitrogen at 20 °C. One half equivalent of triazine (0.3043 g, 3.753 mmol) is added to a 10 mL beaker and diluted with 3 mL of acetonitrile. The solution is added to the reaction flask via syringe. Upon addition, a red brown precipitate forms immediately. This suspension is stirred for 17 h, concentrated to 3 mL, collected via frit filtration, washed with diethyl ether, and then vacuum dried (1.056 g, 5.742 mmol, 78%).

Preparation of [(CuCl)₂(P(OPh)₃)₂Trz]. CuCl (0.3452 g, 3.487 mmol) is added to a 100 mL beaker. One equivalent of P(OPh)₃ (1.083g, 3.491 mmol) is added to a 5 mL beaker and dissolved in 3 mL of CHCl₃. The phosphite solution is then added to the beaker. The [(CuCl)(P(OPh)₃)] compound is formed in a 40 mL solution of chloroform. This is filtered through paper, to remove traces of Cu(II) species, into a 100 mL round bottom flask. One half of an equivalent of triazine (0.1422 g, 1.754 mmol) is added to a 5 mL beaker and diluted with 3 mL of chloroform. This solution is added to the reaction flask via syringe. Upon addition, a yellow solution forms with a trace amount of orange powder, [(CuCl)₂(Trz)], in suspension. The reaction is stirred for 10 minutes. The powder is collected via paper filtration and discarded. The yellow filtrate is concentrated to 5 mL. The yellow orange solid product is formed upon addition of a large volume of diethyl ether. This is then collected by frit filtration, washed with diethyl ether, and then vacuum dried (1.086 g, 2.414 mmol, 69%).

Stability Test for [(CuI)_x(PdZ)] x = 1,2. A 20 mM solution of CuI, a 20 mM solution of pyridazine, and a 40 mM solution of pyridazine are prepared in acetonitrile. These stock solutions are volumetrically pipetted into fifteen eight-dram vials to form solutions containing 10 mM CuI and PdZ concentrations ranging from 1.0 to 20 mM.

First, the pyridazine and acetonitrile solutions and additional acetonitrile are pipetted into the vials in the appropriate volumes. Next, the CuI solution is added to the prepared solutions of pyridazine. The mixtures are stirred for 19 h at 20 °C. The mixtures are also stirred in an oil bath at 70 °C.

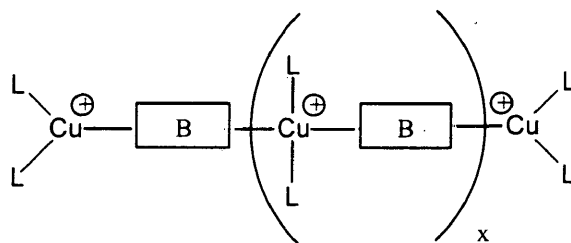
Atomic Absorption Analysis. Sample stock solutions are prepared by digesting 10-13 mg of complex in about 1 mL of Ultrex HNO₃ at room temperature and then heating the mixture at about 50 °C for 5 minutes. The samples are diluted to 100 mL with ultra filtered deionized water. Solutions for analysis are prepared by diluting 1 or 2 mL of the stock solutions to 25 mL with water. Standards are prepared by diluting a 1000 ppm stock solution of Cu(NO₃)₂ to 500, 1000, 1500, 2000, and 2500 ppb in dilute nitric acid. Absorption measurements are made at 324 nm.

Thermogravimetric Analysis. All TGA analyses are conducted under flowing nitrogen (40 mL/min) using a platinum pan. About 10 mg of copper(I) complex are subjected to a linear temperature ramp of 5 °C min⁻¹ up to 900 °C.

RESULTS AND DISCUSSION

Pyrazine Acids and Amides.

Previous work has been done with compounds with the formula $[\text{Cu}(\text{PPh}_3)_2(\text{B})]_n^+$ BF_4^- , where B = *o*-, *m*-, *p*-dicyanobenzene, 4,4'-dicyanobiphenyl, *p*-cyanopyridine, pyrazine, quinoxaline, and 4,4'-dipyridyl¹⁴. From this research we have learned that these compounds form zigzag oligomers consisting of about three to eight monomer units. The exception to this rule is *o*-dicyanobenzene, which forms a cyclic dimer. The *m*-dicyanobenzene is thought to form either a cyclic dimer or tetramer, but conclusive evidence is not available. To find the average length of a polymer we used two different methods. The first strategy, proton NMR, was utilized through a simple equation that compared the integrations of the phosphine protons and the protons of the bridge. The formula is shown in Figure 6.



N = Average Polymer Number

x = Number of Internal Repeat Units

Number of PPh₃ Protons in Oligomer = (60 + 30x)

$R = (\int \text{PPh}_3) / (\int \text{B}) = [(60 + 30x) / (b + bx)]$

$N = (x + 2)$

b = Number of Protons in B Ligand

$R = {}^1\text{H NMR Integration Ratio} = (\int \text{PPh}_3) / (\int \text{B})$

Number of B protons in Oligomer = (b + bx)

$x = [(60 - bR) / (bR - 30)]$

Figure 6. Formula for the average polymer number using ¹H NMR.

In the equation for the number of phosphine protons in the oligomer, sixty represents protons comprising the two $[\text{Cu}(\text{PPh}_3)_2]^+ \text{BF}_4^-$ caps (15 protons per triphenylphosphine). The $30x$ signifies that each repeat unit has 30 protons from two triphenylphosphines. The total number of phosphine protons, $(30x + 60)$, can be compared to the amount of protons present in the bridging ligand. Using the integral values of each distinctive peak from NMR (bridge and phosphine protons are discernible in NMR) a ratio of phosphine protons to bridge protons (R) can be calculated. This ratio can be used to solve the average polymer number for the oligomer. Three ^1H NMR spectra are shown in Appendix A. The actual length of the polymers formed can only be estimated up to about ten monomer units using this method due to uncertainty in the integration process (Figure 7). The ratio of phosphine protons to bridge protons (R) rapidly becomes indistinguishable as the average polymer number (N) increases.

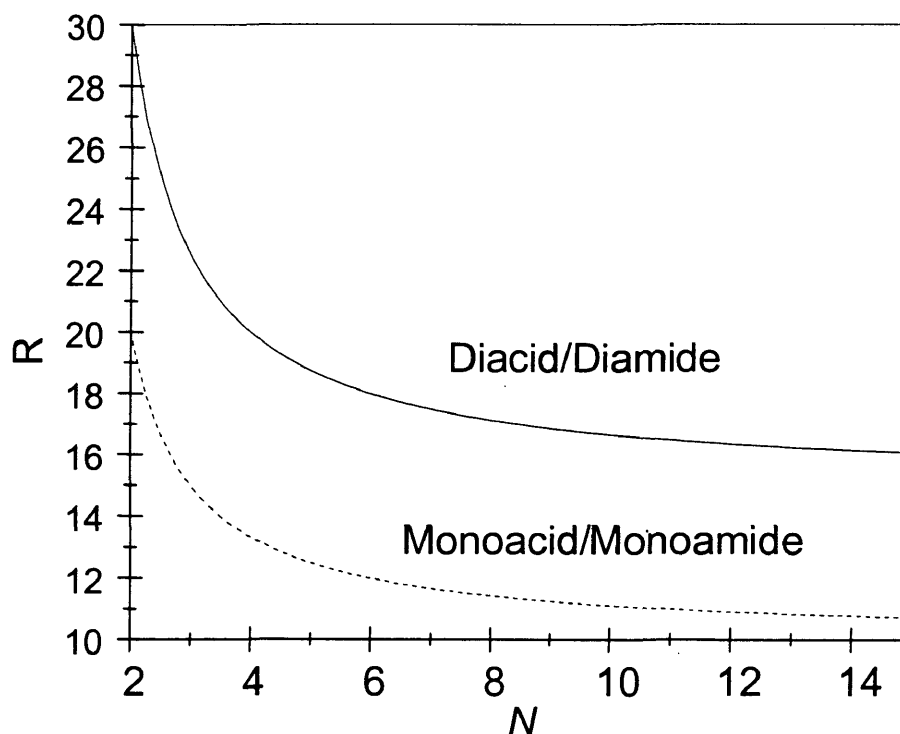
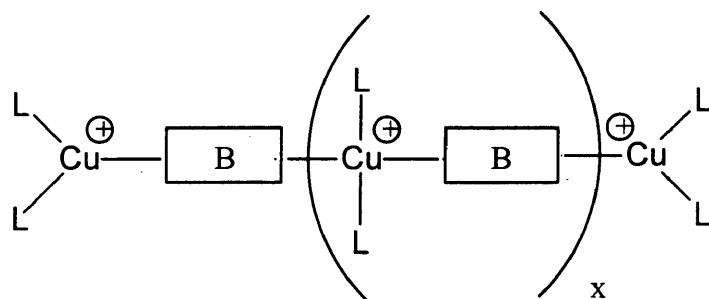


Figure 7. Ratio of Phosphine to Bridging Protons (R) vs. Average Chain Length (N).

Another method to find polymer length utilized the important data from atomic absorption spectroscopy (AAS). The actual copper percentage is found from the analysis of the sample oligomer. The theoretical copper percentages for the dimer and infinite polymer are calculated and then used to calculate the average chain length. Using AAS, it is possible to analyze our compounds for copper percentage by mass. Comparing the calculated theoretical copper percentages for dimers and infinite polymers to the experimental value can give an estimate of the polymer number. The actual copper percentage falls somewhere between the values of the dimer and polymer (Figure 8).



% Cu (experimental) = A	$A = ((2D) + (Px))/(x + 2)$
% Cu (dimer) = D	monomer units = x
% Cu (polymer) = P	$N = x + 2$
Average chain length = N	

Figure 8. Calculation of Average Chain Length Using AAS.

Data from these methods can be corroborated when used in conjunction with another tool, thermogravimetric analysis (TGA). Thermogravimetric analysis is used to follow the decomposition of the oligomers in a controlled environment. A molecule will lose mass with increasing temperature and the resulting data is graphed to show its degradation. This thermal degradation information is useful because the components of

the polymer are lost at different temperatures. Reconstruction of the fragments can help to map out the skeleton of the compound. The change in mass of the compound due to the loss of ligands can be confirmed from the TGA graph. In the $[\text{Cu}(\text{B})(\text{PPh}_3)_2]_n^{n+} n \text{BF}_4^-$ type oligomers, the bridging ligand is usually the component first to degrade. It is then quickly followed by the phosphine ligands, which tend to leave the compound simultaneously. The final material left is usually near the mass percentage of copper metal. This method, while not as conclusive as ^1H NMR and AAS, was a very useful tool in conjunction with these methods in solving the chemical composition of our metal-organic products.

The bridging ligands that were used are the pyrazine-based ligands: 2-pyrazine carboxylic acid (Pca), 2,3-pyrazine dicarboxylic acid (Pdca), pyrazinamide (Pam), 2,3-pyrazine dicarboxamide (Pdam) (Figure 9).

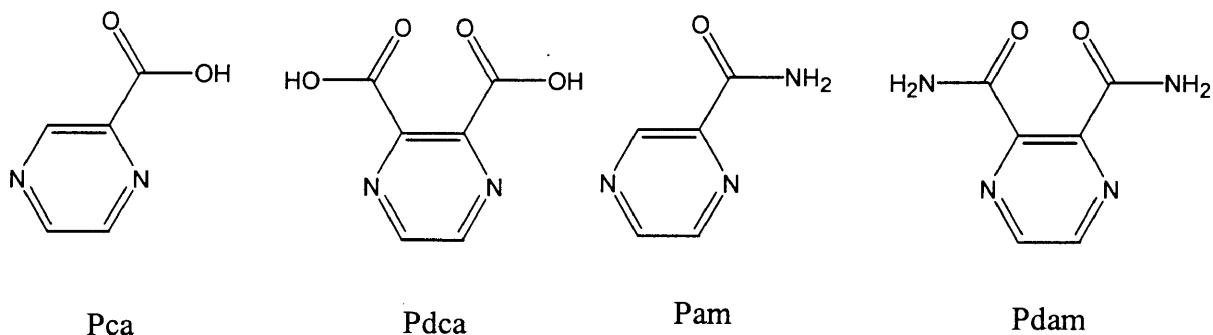


Figure 9. Examples of Bridging Ligands.

The products from our previous work with bridging bidentate ligands presumably were oligomers that extended in one dimension only. The four acid and amide ligands, although still bidentate, were hypothesized to have additional interactions of the acid and

amide substituents. Each carboxylic acid or carboxamide group can possibly interact with a carbonyl oxygen and a hydrogen of either a hydroxyl or an amine group through hydrogen-bonding. The expected result is a network of polymers bonding in two dimensions, probably forming a sheet structure (Figure 10). A similar non-'capped' molecule that exhibits hydrogen bonding is $[(\text{CuI})(\text{Pam})_2]$.¹⁵ In this complex, a CuI infinite stair backbone is formed, while perpendicular to the plane, packing of the crystal structure is obtained through the hydrogen bonding interactions. Another related compound, $[(\text{CuCl})_2(\text{TMT-TTF})]$, where TMT-TTF = Tetrakis(methylthio)tetrathiafulvalene, packs through a sulfur-sulfur interaction.¹⁶

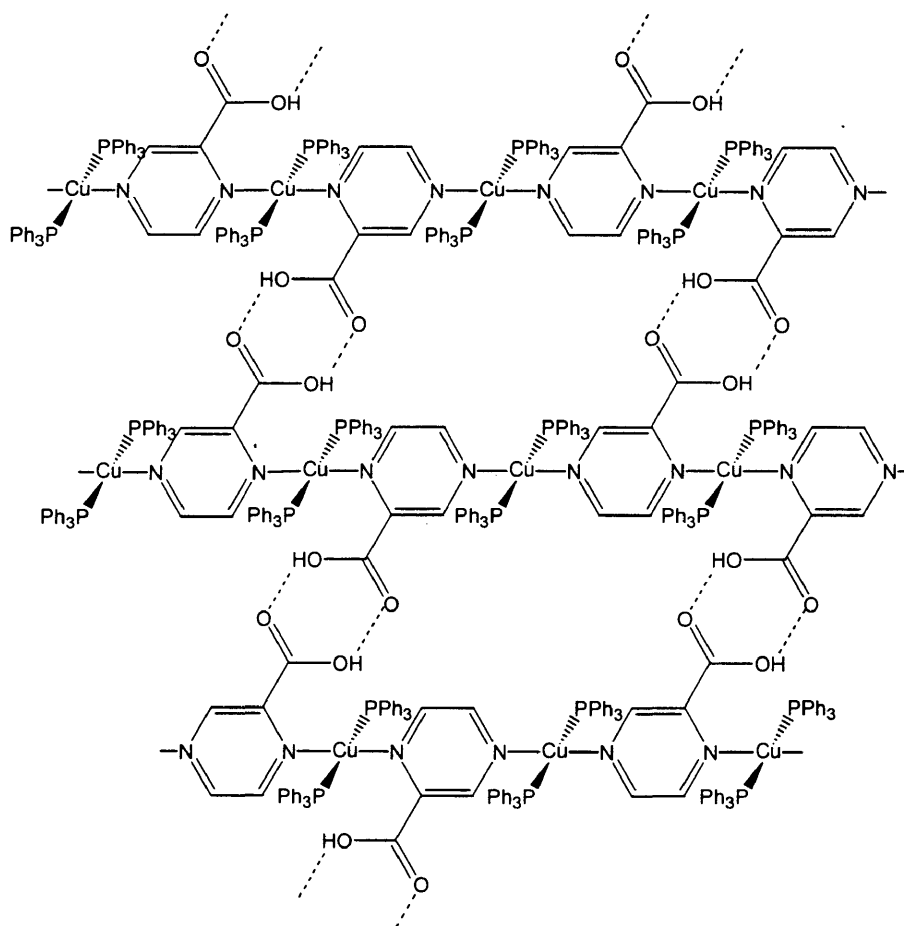


Figure 10. Proposed Sheet Polymer of $[\text{Cu}(\text{Pca})(\text{PPh}_3)_2]_n^{n+} n \text{BF}_4^-$.

The amine and hydroxyl protons of the pyrazine acids and amides can be deprotonated to form a new type of polymer. With the use of a Bronsted base, it should be possible to deprotonate each bridging ligand in the polymer. The result would be a lessening of the ionic character of the polymers. This reaction, (7), shows the reduction of charge and the elimination of the counter ion to form KBF_4 .

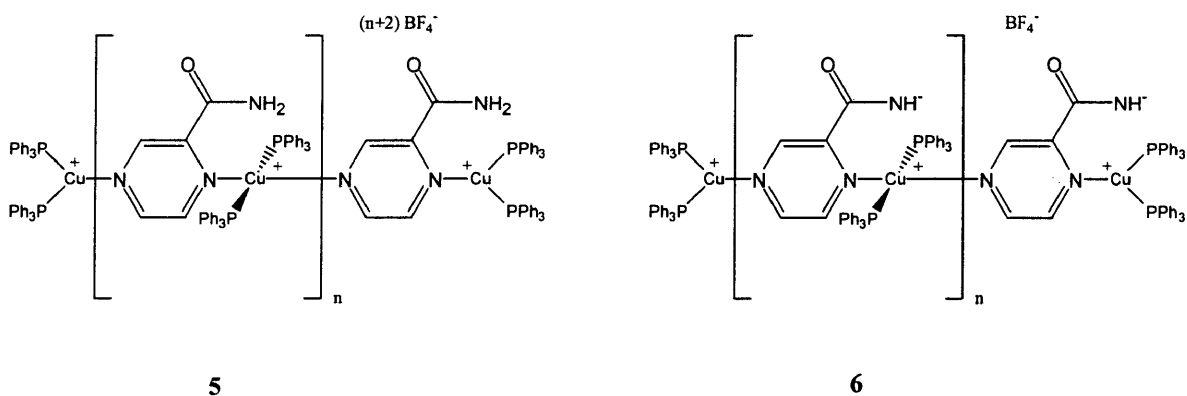


When deprotonation reactions were carried out using K_2CO_3 , an unusual phenomenon was observed. During the process of collecting the deprotonated compound from its suspension into a fritted filter, it was found that the glass of the filtering surface dissolved. Large holes in the fritted filters suggest that possibly HF is formed during the deprotonation process. The formation of this strong acid may be through a reaction between water and the KBF_4 formed in the prior mechanism (8). In the initial reaction to form KOH and HBF_4 , the equilibrium heavily favors the reactants. However, formation of gases in the subsequent reaction, drive the equilibrium in reaction (8). The HBF_4 that is created can decompose to form the destructive HF and BF_3 (9). The BF_3 leaves the reaction as a gas and the reaction must balance this loss by forming more HBF_4 . Only a small amount of the HF acid is required to destroy a fritted filter.



A clearer look at the ionic character change of these complexes is provided from a structural comparison between the protonated and deprotonated versions of the Pam polymer 5, 6. It can be seen that the Pam polymer has a much higher overall separation of charge than the D-Pam polymer. Each cation of the protonated polymer has a BF_4^-

counter ion within the crystal lattice. The counter ion must be small enough to fit in the limited space of the crystal lattice without causing too much stress on the system. In the case of the deprotonated system, space for only one counter ion is needed, allowing much more freedom of movement for the molecule. An interaction conceivably occurs between the nitrogen anion and the copper cation of each monomer of the oligomer forming a five-membered ring within the polymer.



This change in ionic character is reflected in differences in solubility of the protonated and deprotonated polymers. The protonated polymers are soluble in acetone and are precipitated with the addition of diethyl ether. It was found that the deprotonated polymers are slightly soluble in diethyl ether and, therefore, precipitation was difficult. The solution was to dissolve these materials in chloroform and then precipitate them using pentane.

Solubility is dependent on many factors, but one very important aspect is the dielectric constant of a solvent (Table 1). Polar solvents tend to dissolve polar solutes and the same is true for non-polar solvents and non-polar solutes. The solubility of the deprotonated polymer in acetone and chloroform is an indication of a decrease in ionic character of the species. Also, the slight solubility in ether of the D-Pam polymer agrees with the decrease in net charge.

Table 1. Dielectric constants of some solvents¹⁷.

Solvent	Dielectric Constant
Acetone	21.0
CH ₂ Cl ₂	8.9
CHCl ₃	4.8
Diethyl Ether	4.3
Pentane	1.8

A compilation of the ¹H NMR and AAS data used to analyze the compounds for N-values follows (Table 2). The ratios of phosphine protons to bridging protons (R) are used to determine the average chain length (N) for ¹H NMR (Figure 6). The copper percentages for each compound is used to calculate N for AAS (Figure 8). The AAS and ¹H NMR chain length determinations compare well for all of the samples excluding D-Pca, which showed a long oligomer from AAS and a short trimer from proton NMR.

Table 2. Average chain length data for acid and amide oligomers.

	R (NMR)	N (NMR)	% Cu (AAS)	N (AAS)
Pca	10.1	>10	8.01	20
Pdca	29.8	2	8.99	<2
Pam	9.5	>10	7.97	>100
Pdam	28.3	2.1	8.09	3.1
D-Pca	15.5	2.8	8.76	>100
D-Pdca	30.1	<2	9.65	<2
D-Pam	16.1	2.6	9.75	2.1
D-Pdam	34.3	<2	9.62	<2

Results with Pyrazine Carboxylic Acid (Pca)

$[\text{Cu}(\text{Pca})(\text{PPh}_3)_2]^+ \text{BF}_4^-$

A golden-yellow powder was formed from a reaction mixture of one equivalent of $[\text{Cu}(\text{NCCH}_3)_4]^+ \text{BF}_4^-$, one equivalent of Pca, and two equivalents of triphenylphosphine. Proton NMR data suggested an average chain length of greater than ten. From atomic absorption spectroscopy, the copper content of the compound was discovered to be 8.01 %, which compared well to the theoretical copper percentage of 7.95 %. The average chain length using the AAS method was found to be 20 units. TGA suggests that the polymer degraded with a slow loss of Pca initially followed by a rapid loss of phosphine, which was the major loss of mass (Figure 11). Each of these data suggests that this material was a long polymer. Attempts to synthesize a dimer from these components failed, and formed the long polymer instead.

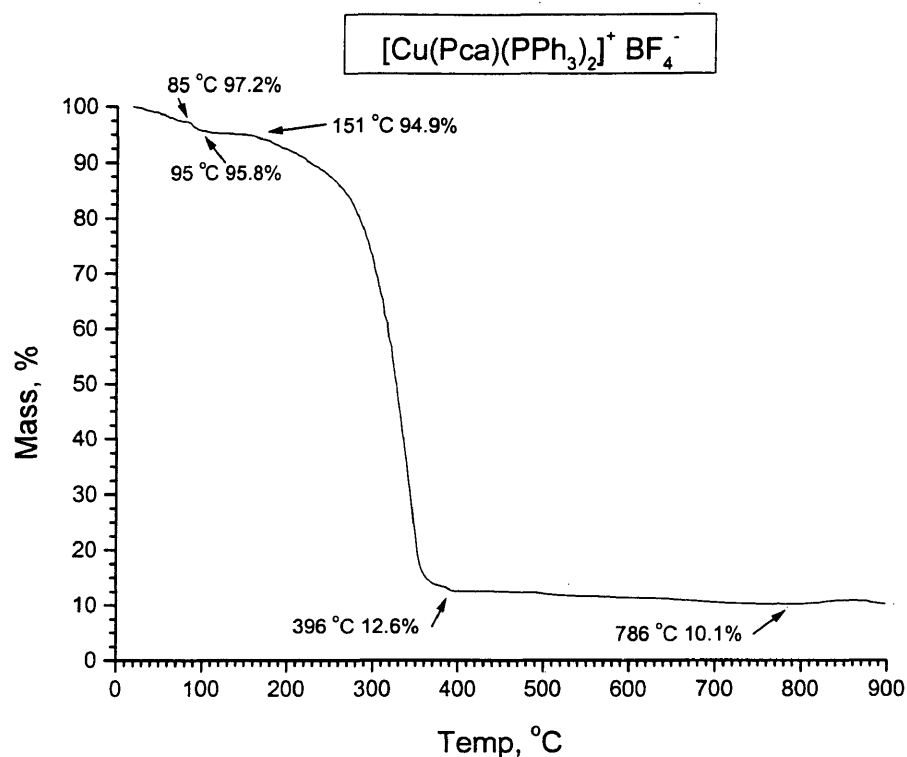


Figure 11. Thermogravimetric Analysis of [Cu(Pca)(PPh₃)₂]⁺ BF₄⁻.

[Cu(D-Pca)(PPh₃)₂]

Deprotonation of the golden-yellow long polymer of Pca using K₂CO₃ formed a yellow-green powder. The deprotonated polymer had an average chain length of 2.8 units according to ¹H NMR data. The percentage of copper was found to be 8.76 % by AAS, which compared well to the theoretical copper percentage of 8.94 %. The experimental copper percentage suggests an average chain length of over 100 units. TGA showed a large mass loss of the D-Pca and phosphine to 10.8 % of the original mass (Figure 12). This correlated well for the polymer with the theoretical mass percent of 8.94 % for the copper residue remaining after a loss of phosphine and bridging ligand. It was noticeable that NMR and AAS data did not seem to agree in the average chain length

determination. This was most likely due to the inaccuracy of the NMR chain length determination method. The AAS results of a long chain length are probably a more reliable determination of chain length.

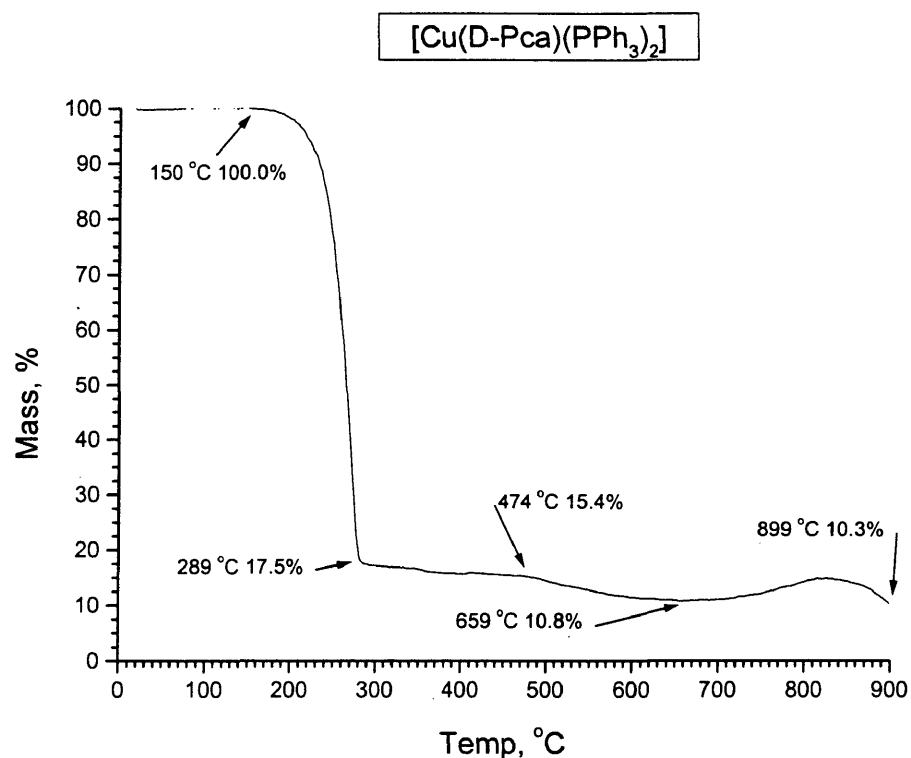


Figure 12. Thermogravimetric Analysis of [Cu(D-Pca)(PPh₃)₂].

Results with Pyrazine Dicarboxylic Acid (Pdca)



An attempted replication of the long Pca polymer using Pdca, repeatedly resulted in an oligomer with a much shorter chain length. Repeating the experiment using two equivalents of [Cu(NCCH₃)₄]⁺ BF₄⁻, one equivalent of Pdca, and four equivalents of triphenyl phosphine formed a red-orange crystalline powder. Analysis using ¹H NMR,

resulted in an average chain length of two units, suggesting a dimer. The Pdca dimer had an experimental composition of 8.99 % copper by mass and compared well to the theoretical value of 8.88 % copper by mass. This signified an average chain length of slightly less than two. The sample was analyzed by TGA and began to lose mass by 175 °C (Figure 13). The plateau formed by 232 °C resulted from the loss of the Pdca bridging ligand to form $[\text{Cu}_2(\text{PPh}_3)_2]^{2+} 2 \text{BF}_4^-$. At this temperature the phosphine began to be lost from the sample and by 364 °C had formed $\text{Cu}^+ \text{BF}_4^-$. The TGA information correlates well with the assumption that the compound was a dimer. It was evident that the preferred chain length for Pdca was that of a short oligomer, typically a dimer.

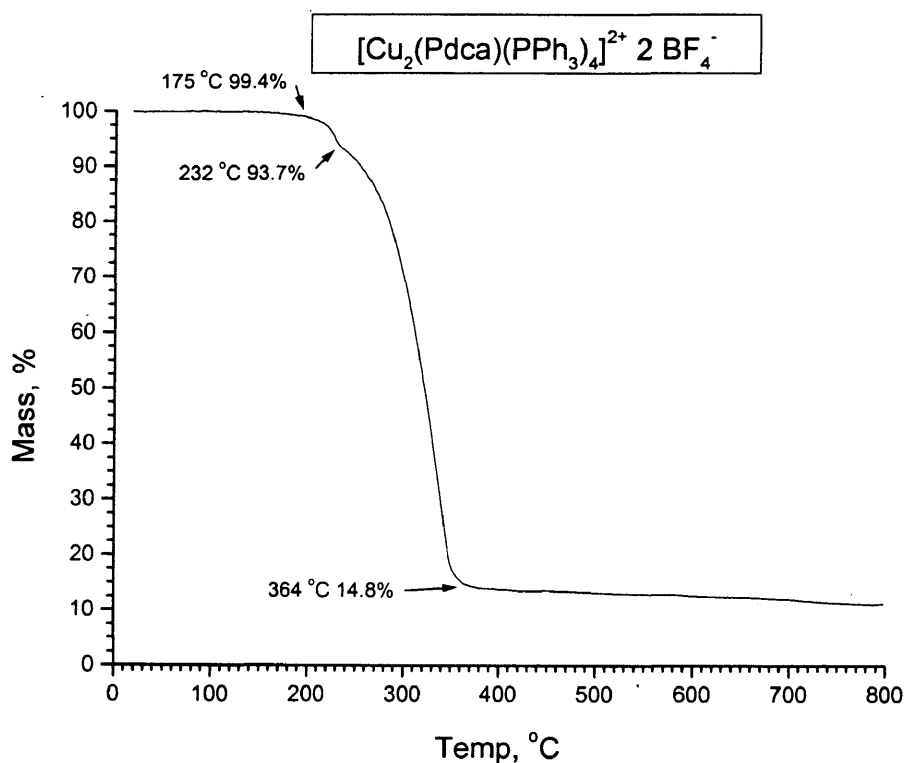


Figure 13. Thermogravimetric Analysis of $[\text{Cu}_2(\text{Pdca})(\text{PPh}_3)_4]^{2+} 2 \text{BF}_4^-$.



The deprotonation of the red-orange Pdca dimer using K_2CO_3 produced a yellow powder. The deprotonated Pdca oligomer had an average chain length that was calculated as being less than two using proton NMR analysis. The percent copper in the material was found to be 9.65 % from AAS. This value compared well to the theoretical copper percentage of 9.46 %. The same short chain length was found when using the AAS data to analyze the sample. The TGA of this sample showed a large loss in mass due to the loss of all the phosphine and the deprotonated Pdca by 128 °C (Figure 14). The theoretical percent mass of $\text{Cu}^+ \text{BF}_4^-$ was 15.9 %. In comparison the TGA value of 16.5 % was a good indication that the sample oligomer was a dimer. The infinite polymer $[\text{Cu}(\text{D-Pdca})(\text{PPh}_3)_2]^+ \text{BF}_4^-$ would recover a mass percent of 8.4 % for $\text{Cu}^+ \text{BF}_4^-$. The information gathered from these analyses shows that the deprotonated Pdca compound retains the short chain length of the original polymer.

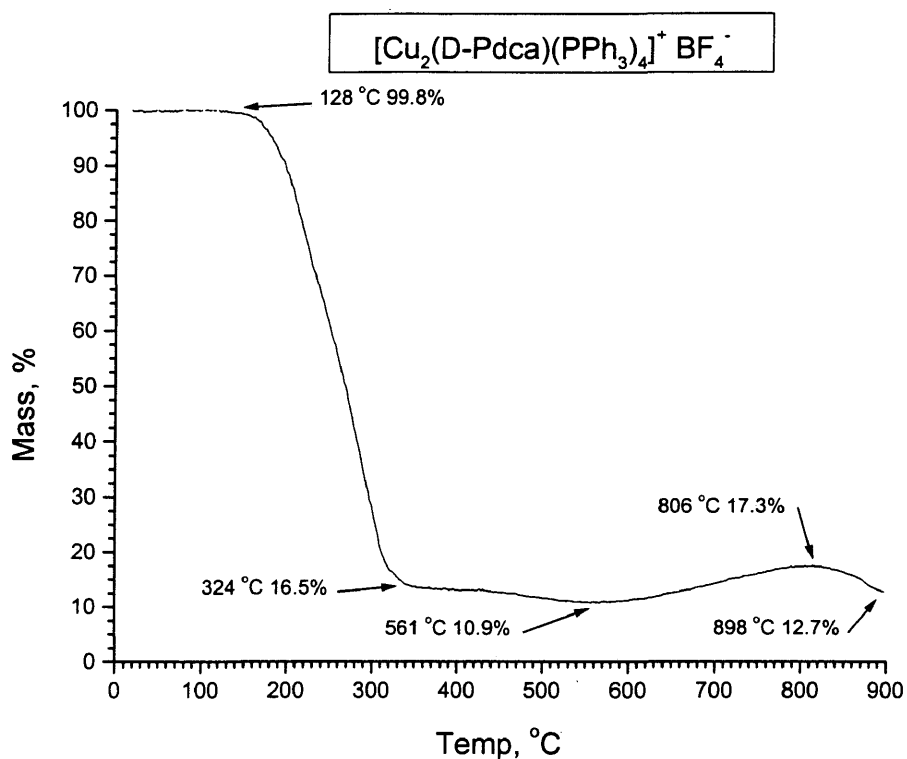


Figure 14. Thermogravimetric Analysis of $[\text{Cu}_2(\text{D-Pdca})(\text{PPh}_3)_4]^+ \text{BF}_4^-$.

Results with Pyrazine Carboxamide (Pam)

$[\text{Cu}(\text{Pam})(\text{PPh}_3)_2]^+ \text{BF}_4^-$

An attempt to synthesize a polymer similar to the long Pca oligomer resulted in a bright yellow powder. An average chain length that was greater than ten units was found using ^1H NMR analysis. An experimental value of 7.97 % copper was found for the sample using AAS. The theoretical copper percentage for an infinite polymer would be 7.96 %, and thus suggested a polymer length greater than ten. The same sample was studied by TGA and was found to begin degradation by 64 °C (Figure 15). Two smaller plateaus were formed before the large mass loss of phosphine was detected. The first phase formed by 112 °C was due to a loss of one half of a pyrazine carboxamide. At this

plateau, $[\text{Cu}(\text{Pam})_{0.5}(\text{PPh}_3)_2]^+ \text{BF}_4^-$ had been formed which is directly analogous to the Pdca dimer. By 197 °C, the remainder of the bridge had been lost, to form $[\text{Cu}(\text{PPh}_3)_2]^+ \text{BF}_4^-$. At this temperature the phosphine begins to degrade and has been lost by 375 °C. Taken all together, the data suggest that the product of this reaction was a long oligomer whose chain length exceeds the range that can be determined by our analytical methods.

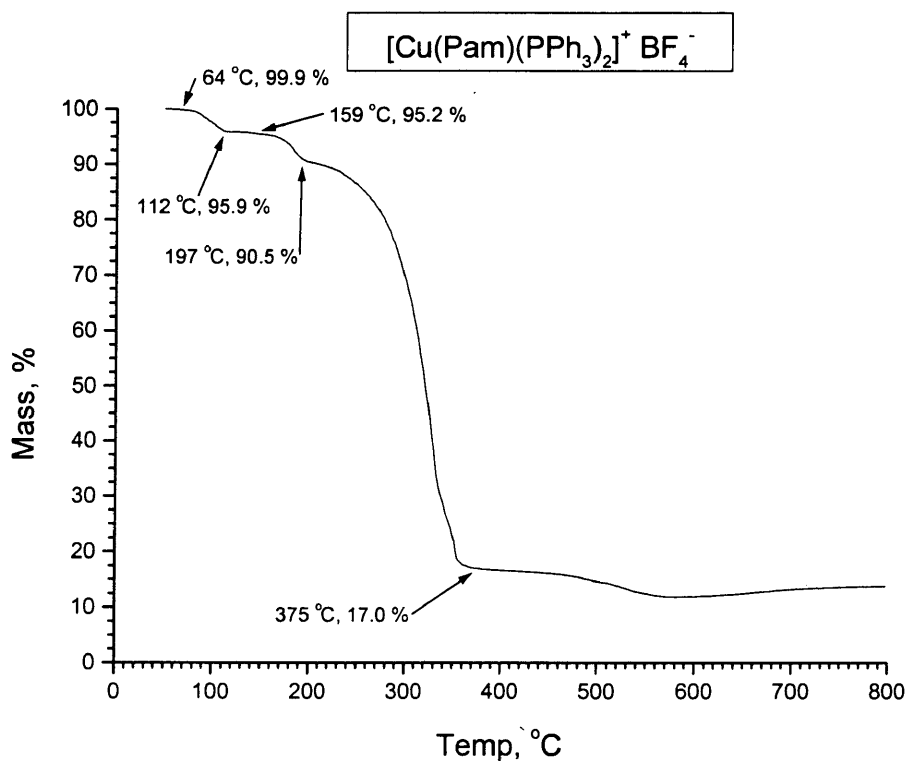


Figure 15. Thermogravimetric Analysis of $[\text{Cu}(\text{Pam})(\text{PPh}_3)_2]^+ \text{BF}_4^-$.

$[\text{Cu}_2(\text{D-Pam})(\text{PPh}_3)_4]^+ \text{BF}_4^-$

Upon deprotonation of the bright yellow Pam polymer, a mustard yellow powder was obtained. According to ^1H NMR analysis, this material loses its character as a long oligomer and showed an average chain length of 2.6 units. The data collected from AAS shows an oligomer with a copper percentage of 9.75 %. This was equivalent to a material

with an average chain length of 2.1 units, which was also much shorter than the protonated analog. The sample was analyzed by TGA with the assumption that the sample was a dimer (Figure 16). It was shown that a small mass percentage was lost by 143 °C that resembled a theoretical loss of the D-Pam from the dimer to form $[\text{Cu}_2(\text{PPh}_3)_4]^{2+} 2 \text{BF}_4^-$. At this temperature, the remainder of the phosphine began to be lost and had formed $\text{Cu}^+ \text{BF}_4^-$ by 715 °C. If the long polymer stoichiometry had been assumed the TGA results would have been quite inaccurate. The results of these analyses point to a short chain length oligomer between a dimer and a trimer.

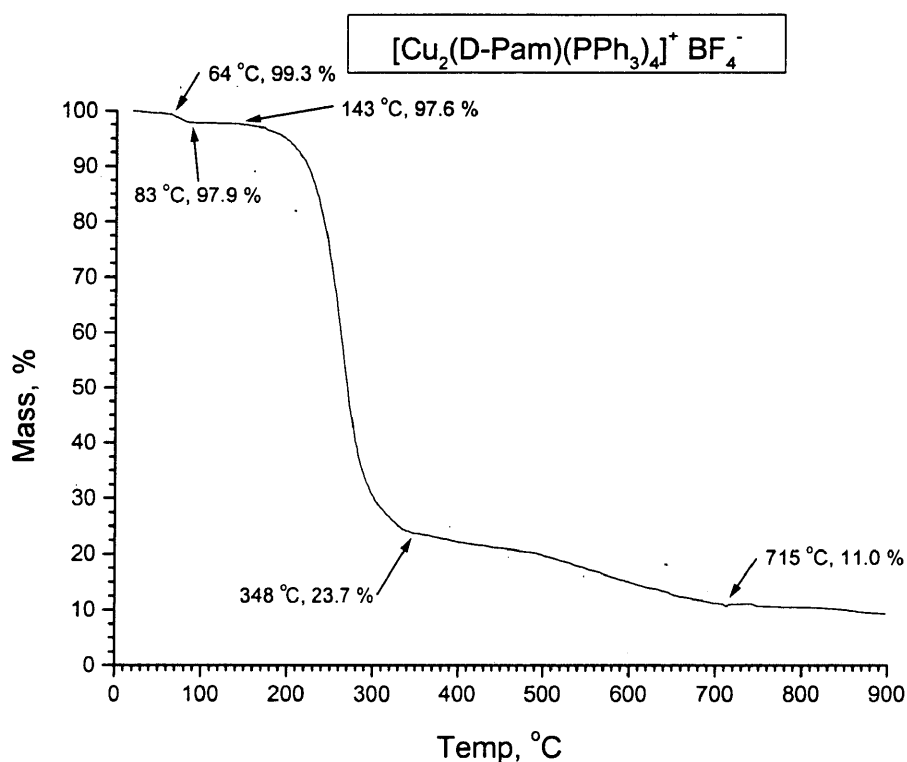


Figure 16. Thermogravimetric Analysis of $[\text{Cu}_2(\text{D-Pam})(\text{PPh}_3)_4]^+ \text{BF}_4^-$.

Results with Pyrazine Dicarboxamide (Pdam)



The synthesis of the Pdam polymer resulted in a yellow-orange powder. Upon ^1H NMR analysis, an average chain length of 2.1 units was determined. The same material was analyzed using AAS and a copper percentage of 8.09% was found. This correlates with an average chain length of 3.1 units. A TGA of this material was run to confirm that the average chain length was near a dimer (Figure 17). The sample began to degrade by 70 °C, and had lost all of the Pdam by 88 °C. This $[\text{Cu}_2(\text{Pdam})(\text{PPh}_3)_4]^{2+} 2 \text{BF}_4^-$ phase was stable to 166 °C, at which point it lost the phosphine to form $\text{Cu}^+ \text{BF}_4^-$. The Pdam oligomer seems to be very similar to the Pdca dimer studied previously. Thus the diacid and diamide both show a tendency to form only short chains.

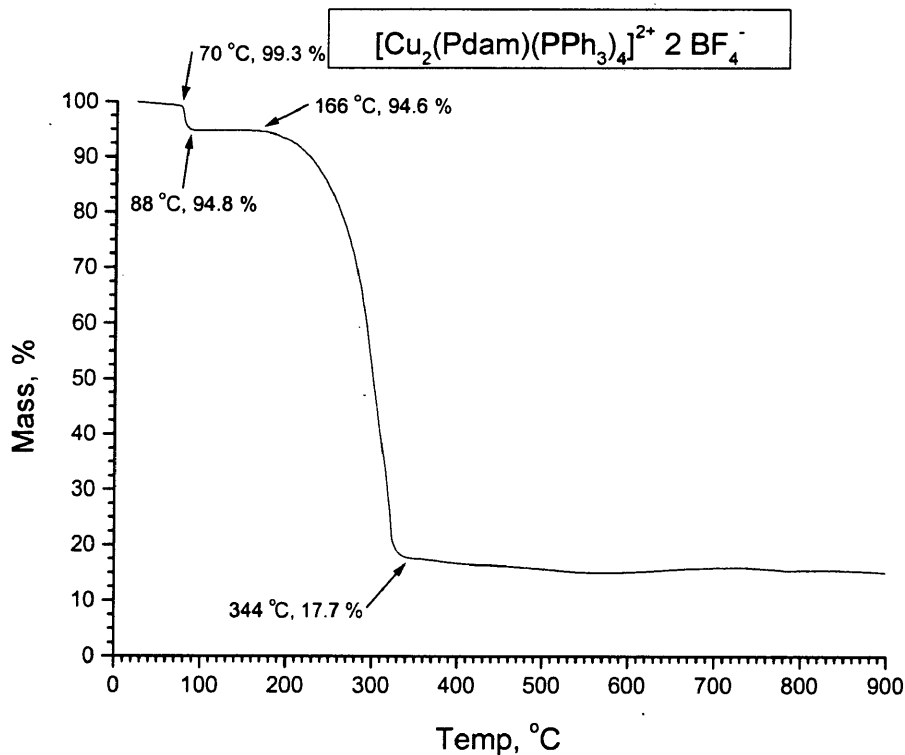
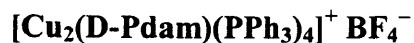


Figure 17. Thermogravimetric Analysis of $[\text{Cu}_2(\text{Pdam})(\text{PPh}_3)_4]^{2+} 2 \text{BF}_4^-$.



The deprotonation of the yellow-orange Pdam dimer forms a brick red powder when reacted with K_2CO_3 . Analysis of this red powder by ^1H NMR suggested an average chain length of less than two. The AAS analysis of the same material showed a copper percentage of 9.62%. This was also equal to an average chain length of less than two. The TGA of this material showed that the bridge and phosphine were lost near the same temperature and therefore they could not be differentiated (Figure 18). By 447°C , all of the phosphine and D-Pdca had been lost and $\text{Cu}^+ \text{BF}_4^-$ had been formed. The BF_4^- began to degrade and by 515°C , only copper metal remained. It may be concluded from the collected data that the protonated dimer retains its short chain length when deprotonated.

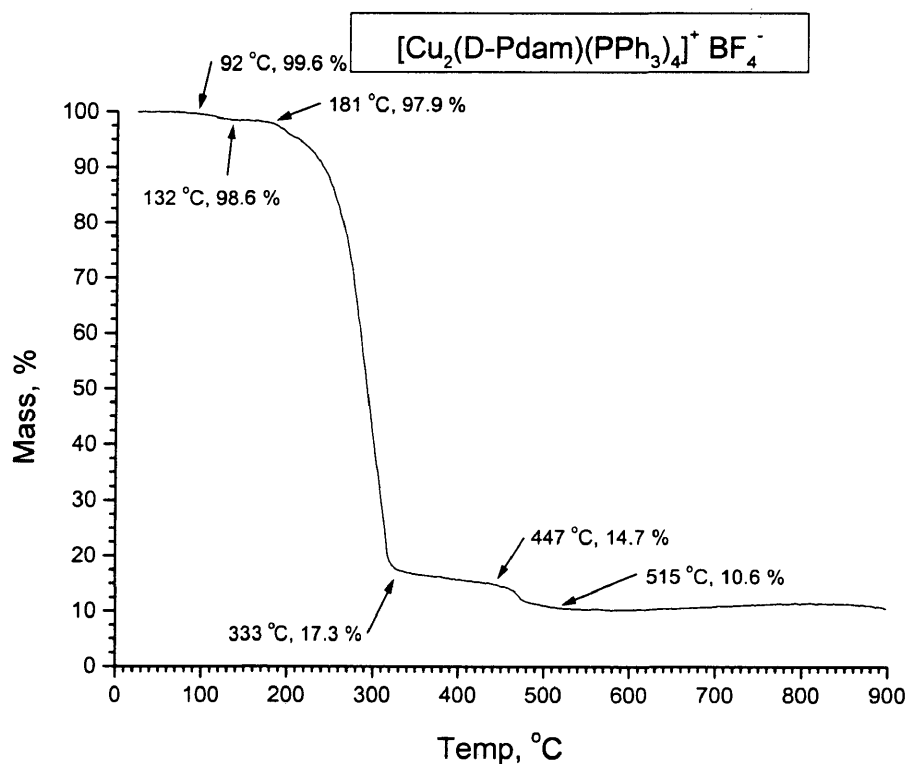


Figure 18. Thermogravimetric Analysis of $[\text{Cu}_2(\text{D-Pdam})(\text{PPh}_3)_4]^+ \text{BF}_4^-$.

Pyrimidine, Pyridazine, and Triazine Halide Complexes

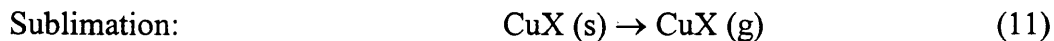
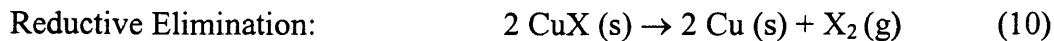
Copper halide coordination chemistry, which was briefly described in the introduction, was the focus of the following section. Three non-linear bridging ligands, pyrimidine (Pym), pyridazine (Pdz), and triazine (Trz), were reacted with copper halides in an attempt to form the expected stair step networks. The products that were formed were analyzed using predominantly AAS and TGA. When the two analyses agreed well, compounds were further analyzed for carbon, hydrogen, and nitrogen by combustion analysis. In contrast to the TGA results for the complexes of the pyrazine acids and amides, the TGA's of the pyrimidine, pyridazine, and triazine materials were very helpful in confirming the stoichiometries of the compounds. The following two tables contain a compilation of the data for the compounds that were formed. The AAS and combustion analysis data (Tables 3 and 4) and TGA data (Tables 5 and 6) were successfully utilized in the identification of the compounds synthesized.

The TGA analyses of these compounds were expected to display a step-wise thermal degradation profile. The complexes would initially lose the bridging ligand, either in steps or all at once, forming $[\text{CuX}]$ or $[(\text{CuX})\text{L}]_n$ depending on whether a 'capping' ligand was present in the original compound. The $[(\text{CuX})\text{L}]_n$ compound would be stable for a limited temperature range and then form $[\text{CuX}]$ by the loss of the capping phosphine or phosphite. At this point, the remaining phase would be $[\text{CuX}]$ and should remain stable beyond the 900 °C limit of the TGA. The boiling points of CuCl, CuBr, and CuI are 1400 °C, 1345 °C, and 1290 °C respectively.¹⁸ However, it was found experimentally that the CuX phase of all of the TGA's began to lose considerable mass by 500 °C. For the compounds containing CuCl or CuBr, the final phase formed showed

a mass percentage less than that of the copper mass percentage based on the beginning mass of the material. This meant that a certain percentage of copper was being displaced from the system. The boiling point of copper at 1 atm is 2562 °C, well beyond the temperature ranges encountered in the TGA experiments.¹⁸ The thermal degradation of the CuX phase introduced some doubt of whether the compounds being analyzed were the expected conformation. To understand this phenomenon, TGA analyses of CuCl, CuBr and CuI were conducted.

Copper(I) chloride was found to be stable to 380 °C, at which point it lost about 94 % of its mass (Figure 19). The remaining mass was stable to 790 °C, whereupon the mass fell to zero. Copper(I) bromide began to degrade by 395 °C and lost about 91 % of its original mass (Figure 20). By 870 °C, the remaining mass began to slowly degrade. Copper(I) iodide began to degrade by 389 °C and formed a stable phase by 657 °C that represented 41.5 % of the original mass (Figure 21). This phase began to lose additional mass by 854 °C.

The initial thermal degradation of the copper halides can be explained using two mechanisms. The first is a reductive elimination of CuX, (reaction 10). In this reaction, the copper(I) is reduced and X₂ sublimates leaving copper metal. The second mechanism involves the direct sublimation of the copper halide. Sublimation of the copper halides can occur at temperatures well below their boiling point presumably due to a lowering of the vapor pressure of the system (reaction 11). The constant flow of nitrogen in the TGA environment resulted in the elimination of the small fraction of CuX that was in the vapor phase. The loss of this copper halide gas would force the equilibrium toward the production of more of the CuX in the vapor phase.



The evidence suggested that CuCl and CuBr were subject to both CuX thermal degradation pathways. A small percentage of the copper halide degrades through reductive elimination while the majority of the material sublimates. As a result, a small mass of what is presumably copper is left behind. On the other hand, the CuI was found to degrade through a reductive elimination process (reaction 10) to form copper metal.

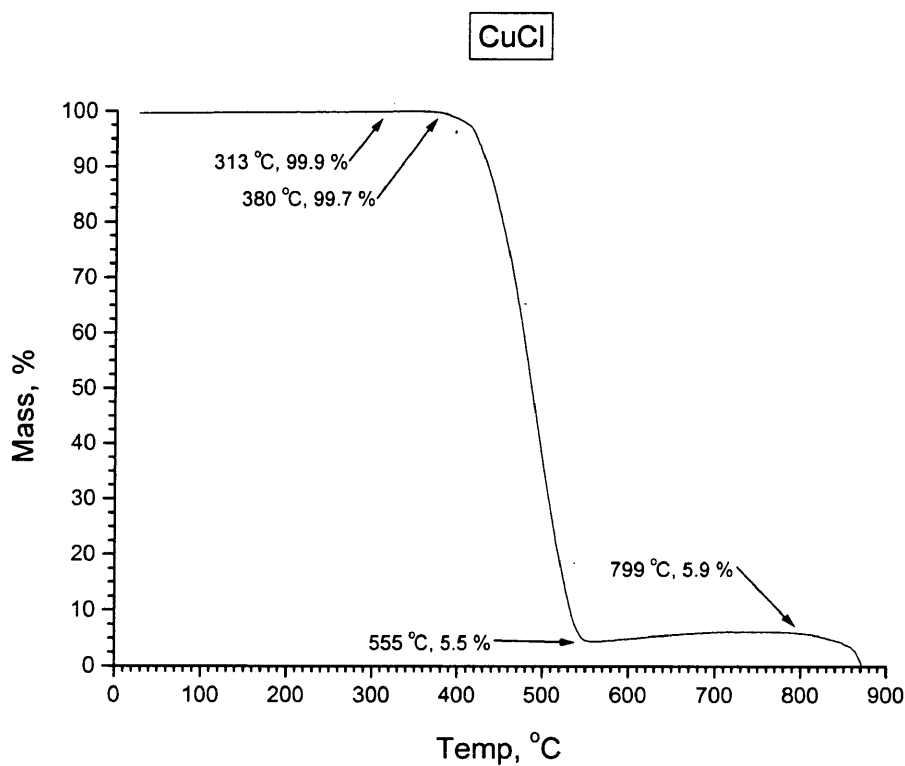


Figure 19. Thermogravimetric Analysis of CuCl.

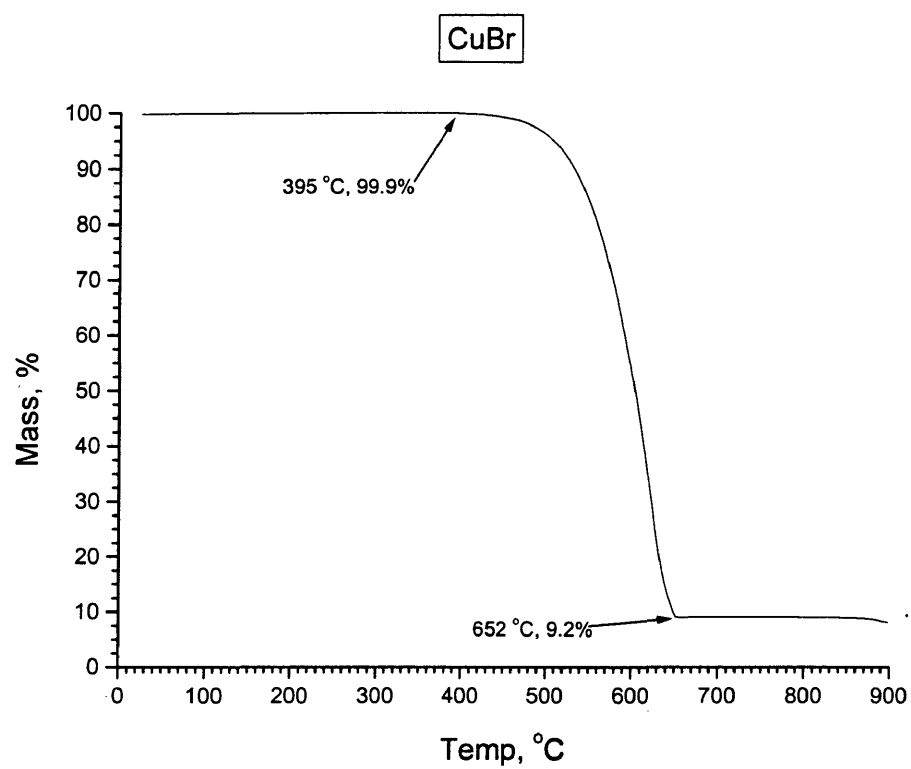


Figure 20. Thermogravimetric Analysis of CuBr.

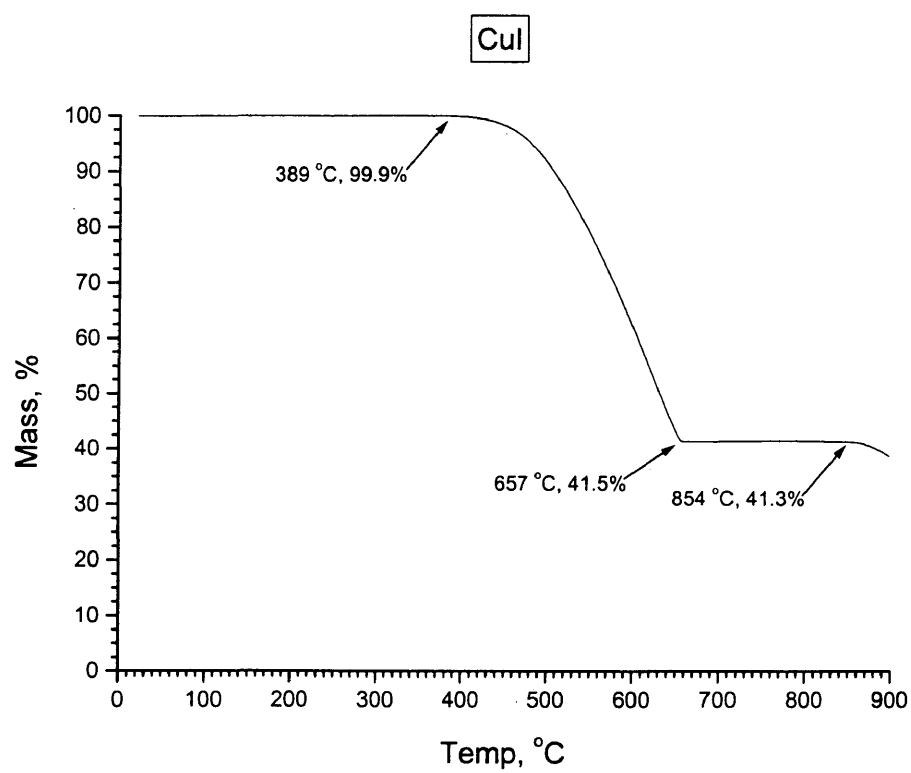


Figure 21. Thermogravimetric Analysis of CuI.

Table 3. Synthetic and Analytical Data for [(CuX)_nB_m] Complexes (n = 1,2,3; m=1,2).

Compound	Yield, %	Color	% (theory)	% (expt.)	% error
[(CuCl) ₂ Pym]	64	gold	Cu 45.70	43.33	5.2
[(CuBr) ₂ Pym]	79	olive	Cu 34.63	33.93	2.1
[(CuI) ₂ Pym]	89	neon yellow	Cu 27.57	27.28	1.1
			C 10.42	10.59	1.6
			H 0.87	0.89	2.3
			N 6.08	6.06	0.3
[(CuCl)PdZ]	79	dark red	Cu 35.48	36.38	2.5
[(CuBr)PdZ]	88	red-brown	Cu 28.43	27.87	2.0
			C 21.49	20.99	2.4
			H 1.80	1.72	4.7
			N 12.53	12.12	3.4
[(CuI)PdZ]	86	orange	Cu 23.49	22.65	3.7
[(CuI) ₂ PdZ]	95	yellow	Cu 27.57	27.84	1.0
[(CuCl) ₂ Trz]	70	orange-	Cu 45.54	46.22	1.5
		brown			
[(CuCl) ₃ Trz]	78	orange-	Cu 50.43	47.45	6.3
		brown	C 9.52	9.89	3.7
			H 0.80	1.00	20.0
			N 11.12	11.16	0.4
[(CuBr) ₃ (Trz) ₂]	20	red-brown	Cu 32.18	32.20	0.1
[(CuBr) ₂ Trz]	78	orange	Cu 34.54	35.00	1.3
			C 9.79	9.67	1.2
			H 0.82	0.92	10.9
			N 11.42	10.99	3.9
[(CuBr) ₃ Trz]	76	red-brown	Cu 37.28	37.19	0.2
[(CuI) ₂ Trz]	94	neon-yellow	Cu 27.51	27.58	0.3

Table 4. Synthetic and Analytical Data for [(CuX)_n(L)_nB] Complexes (n = 1,2,3).

Compound	% Yield	Color	% (theory)	% (expt.)	% error
[(CuCl) ₂ (PPh ₃) ₂ Pym]	89	pale yellow	Cu 15.83	16.94	6.6
			C 59.85	60.34	0.8
			H 4.24	4.27	0.7
			N 3.49	3.17	10.7
[(CuBr) ₂ (PPh ₃) ₂ Pym]	98	yellow	Cu 14.26	14.64	2.6
[(CuI) ₂ (PPh ₃) ₂ Pym]	36	neon yellow	Cu 12.90	13.11	1.6
			C 48.74	47.87	1.8
			H 3.48	3.45	0.9
			N 2.84	2.78	2.2
[(CuCl) ₂ (PPh ₃) ₂ Pdz]	72	light yellow	Cu 14.40	13.74	4.8
[(CuBr)(PPh ₃)Pdz]	63	light yellow orange	Cu 13.08	13.15	0.5
			C 54.39	53.84	1.0
			H 3.94	4.08	3.4
			N 5.77	5.57	3.6
[(CuI)(PPh ₃)Pdz]	65	yellow	Cu 11.93	12.62	5.5
[(CuCl) ₃ (PPh ₃) ₃ Trz]	80	yellow	Cu 16.37	16.39	0.1
[(CuBr) ₂ (PPh ₃) ₂ Trz]	81	yellow	Cu 14.24	14.52	2.0
			C 52.48	51.62	1.6
			H 3.73	3.69	1.1
			N 4.71	4.65	1.3
[(CuI) ₂ (PPh ₃) ₂ Trz]	84	light orange	Cu 12.88	12.80	0.6
			C 47.48	46.88	1.3
			H 3.37	3.35	0.6
			N 4.26	4.21	1.2
[(CuCl) ₂ (P(OPh) ₃) ₂ Pym]	42	light yellow	Cu 14.14	13.53	4.5

[(CuBr) ₂ (P(OPh) ₃) ₂ Pym]	71	light yellow	Cu	12.87	12.94	0.5			
			C	48.64	48.04	1.2			
			H	3.44	3.57	3.6			
			N	2.84	3.05	6.9			
[(CuCl)(P(OPh) ₃)Pd _z]	49	yellow	Cu	12.99	12.55	3.5			
[(CuBr)(P(OPh) ₃)Pd _z]	69	light yellow	Cu	11.90	12.08	1.5			
			C	49.50	48.61	1.8			
			H	3.59	3.52	2.0			
			N	5.25	5.11	2.7			
[(CuCl) ₂ (P(OPh) ₃) ₂ Trz]	69	yellow	Cu	14.13	13.93	1.4			
[(CuBr) ₂ (P(OPh) ₃) ₂ Trz]	51	orange	Cu	12.86	12.83	0.2			
		yellow							
		C					47.38	47.25	0.3
		H					3.36	3.36	0.0
[(CuI) ₃ (P(OPh) ₃) ₃ Trz]	65	cream	N	4.25	4.27	0.5			
			Cu	12.04	11.77	2.3			
			C	43.24	44.00	1.7			
			H	3.06	3.34	8.4			
			N	2.65	2.79	5.0			

Table 5. Thermogravimetric Decomposition Results for [(CuX)_nB_m] Complexes.

Complex	Temp, °C	Product	wt % (theory)	wt % (actual)
[(CuCl) ₂ Pym]	75–135	[(CuCl) ₄ Pym]	86	85
	135–205	[(CuCl) ₈ Pym]	78	77
[(CuBr) ₂ Pym]	145–255	CuBr	78	78
[(CuI) ₂ Pym]	155–235	CuI	83	83
[(CuCl)Pd _z]	100–185	[(CuCl) ₂ Pd _z]	78	78
	185–230	[(CuCl) ₃ Pd _z]	70	69
	230–425	CuCl	55	55
[(CuBr)Pd _z]	120–195	[(CuBr) ₂ Pd _z]	82	83
	195–260	[(CuBr) ₄ Pd _z]	73	74
	260–470	CuBr	64	68
[(CuI)Pd _z]	110–200	[(CuI) ₂ Pd _z]	85	83
	200–250	CuI	70	71
[(CuI) ₂ Pd _z]	170–250	CuI	83	83
[(CuCl) ₂ Trz]	110–160	[(CuCl) ₃ Trz]	91	90
	160–230	CuCl	71	72
[(CuCl) ₃ (Trz)]	120–175	[(CuCl) ₄ Trz]	95	96
	175–250	CuCl	79	77
[(CuBr) ₃ Trz ₂]	90–150	[(CuBr) ₂ Trz]	97	94
	145–175	[(CuBr) ₃ Trz]	92	89
	175–250	CuBr	78	77
[(CuBr) ₂ Trz]	105–165	[(CuBr) ₃ Trz]	93	93
	165–220	CuBr	78	79
[(CuBr) ₃ Trz]	75–150	[(CuBr) ₆ Trz]	92	95
	150–235	CuBr	84	82
[(CuI) ₂ Trz]	125–200	CuI	82	82

Table 6. Thermogravimetric Decomposition Results for [(CuX)_n(L)_nB] Complexes.

Complex	Temp, °C	Product	wt % (theory)	wt % (actual)
[(CuCl) ₂ (PPh ₃) ₂ Pym]	100–190	[(CuCl)(PPh ₃)]	90	90
[(CuBr) ₂ (PPh ₃) ₂ Pym]	75–95	[(CuBr) ₄ (PPh ₃) ₄ Pym]	96	98
	115–175	[(CuBr)(PPh ₃)]	91	95
	175–380	CuBr	32	30
[(CuI) ₂ (PPh ₃) ₂ Pym]	125–175	[(CuI)(PPh ₃)]	92	91
	210–405	CuI	39	41
[(CuCl) ₂ (PPh ₃) ₂ Pdz]	115–180	[(CuCl)(PPh ₃)]	90	92
	180–400	CuCl	24	25
[(CuBr)(PPh ₃)Pdz]	65–95	[(CuBr) ₂ (PPh ₃) ₂ Pdz]	92	94
	130–200	[(CuBr)(PPh ₃)]	84	79
	260–370	CuBr	30	31
[(CuI)(PPh ₃)Pdz]	70–110	[(CuI) ₂ (PPh ₃) ₂ Pdz]	92	92
	110–160	[(CuI)(PPh ₃)]	85	88
	200–380	CuI	36	35
[(CuCl) ₃ (PPh ₃) ₃ Trz]	100–140	[(CuCl) ₄ (PPh ₃) ₄ Trz]	98	97
	195–245	[(CuCl)(PPh ₃)]	93	93
	245–375	CuCl	25	32
[(CuBr) ₂ (PPh ₃) ₂ Trz]	115–150	[(CuBr)(PPh ₃)]	91	91
	240–370	CuBr	32	38
[(CuI) ₂ (PPh ₃) ₂ Trz]	120–165	[(CuI)(PPh ₃)]	92	91

	165–440	CuI	39	39
[(CuCl) ₂ (P(OPh) ₃) ₂ Pym]	105–210	[(CuCl)(P(OPh) ₃)]	91	91
	210–350	CuCl	22	23
[(CuBr) ₂ (P(OPh) ₃) ₂ Pym]	100–145	[(CuBr) ₄ (P(OPh) ₃) ₄ Pym]	96	96
	145–190	[(CuBr)(P(OPh) ₃)]	92	91
	190–280	CuBr	29	32
[(CuCl)(P(OPh) ₃)PdZ]	80–315	CuCl	20	28
[(CuBr)(P(OPh) ₃)PdZ]	75–330	CuBr	27	36
[(CuCl) ₂ (P(OPh) ₃) ₂ Trz]	40 – 90	[(CuCl) ₄ (P(OPh) ₃) ₄ Pym]	95	94
	90–170	[(CuCl)(P(OPh) ₃)]	91	89
	170–290	CuCl	22	23
[(CuBr) ₂ (P(OPh) ₃) ₂ Trz]	75–185	[(CuBr)(PPh ₃)]	92	92
	185–385	CuBr	29	36
	385–570	Cu	13	13
[(CuI) ₃ (P(OPh) ₃) ₃ Trz]	30–150	[(CuI)(P(OPh) ₃)]	93	93
	150–255	CuI	35	38

Pyrimidine

[(CuCl)₂Pym]

A golden powder in 26 % yield resulted from a reaction of two equivalents of CuCl and one equivalent of Pym dissolved in acetonitrile. The experimental copper percentage was analyzed using AAS to be 43.33 %. When compared to the value of the theoretical copper percentage, a 5.2 % relative error was calculated (Table 3). Using TGA (Figure 22) it was observed that decomposition of the material began sharply at 74

°C and continued to drop until it reached 134 °C (Table 5). At this point, 15 % of the original mass had sublimed. A theoretical mass loss of 14 % would account for a loss of one half of a pyrimidine. This left $[(\text{CuCl})_4\text{Pym}]$ as an intermediate phase. This continued to decompose shortly afterward and reached another plateau at 205 °C. The resultant compound, $[(\text{CuCl})_8\text{Pym}]$ was formed from the decomposition of another quarter unit of pyrimidine. This would theoretically be accompanied with an additional 8 % mass loss from the previous meta-stable state. This correlated with the mass loss data taken from the TGA.

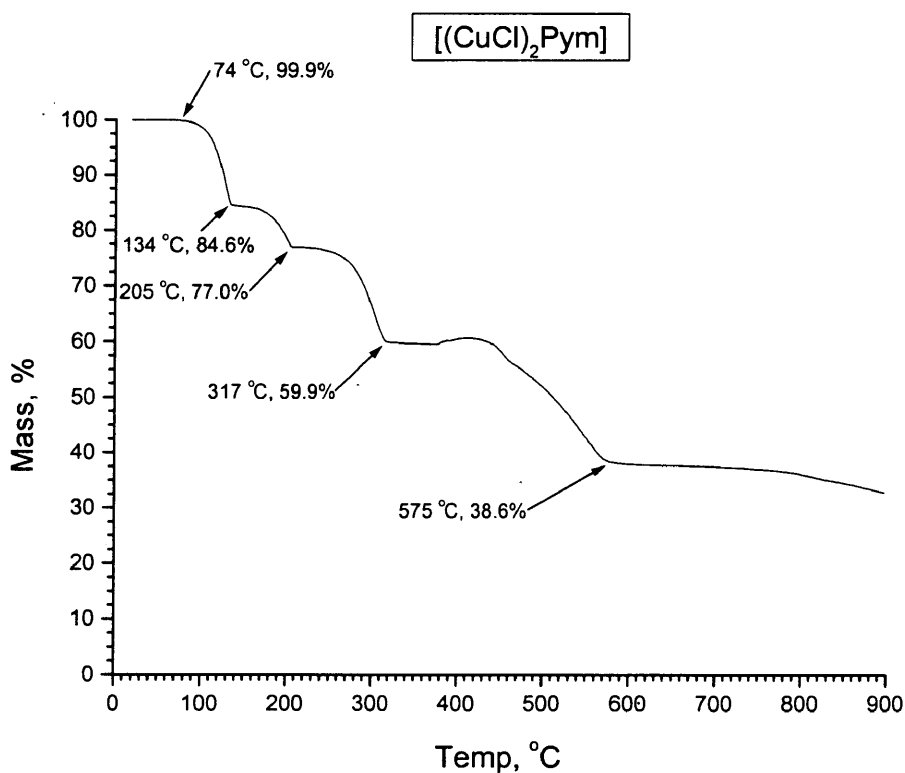


Figure 22. Thermogravimetric Analysis of $[(\text{CuCl})_2\text{Pym}]$.

[(CuBr)₂Pym]

A 68 % yield of an olive-yellow powder was produced from a reaction of two equivalents of CuBr and one equivalent of pyrimidine dissolved in acetonitrile. The resultant powder was analyzed using AAS, and a copper percentage of 33.93 % was discovered. The theoretical percent copper for [(CuBr)₂Pym] is 34.63 % (Table 3). TGA analysis of this compound displayed an initial mass loss at 146 °C (Table 5, Figure 23). The compound steadily decreased in mass until it reached a mass of 78 % at 253 °C, at which point it leveled off. The theoretical percent mass of CuBr is 78 %. This correlated to the loss of all the pyrimidine in the sample. The next mass loss occurred at 439 °C. This significant mass loss continued to 648 °C, and only 6.9 % of the original mass remained. This mass loss was due to the sublimation and reductive elimination of CuBr. This phase was 8.8 % of the mass of the CuBr phase, which compares well to the CuBr thermal degradation information stated previously.

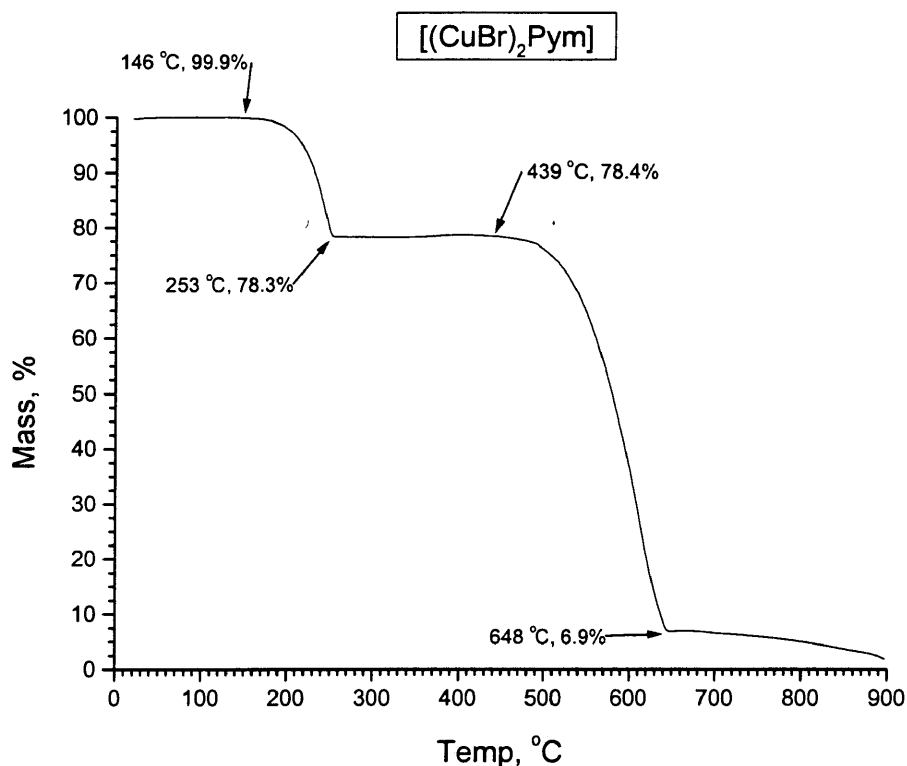


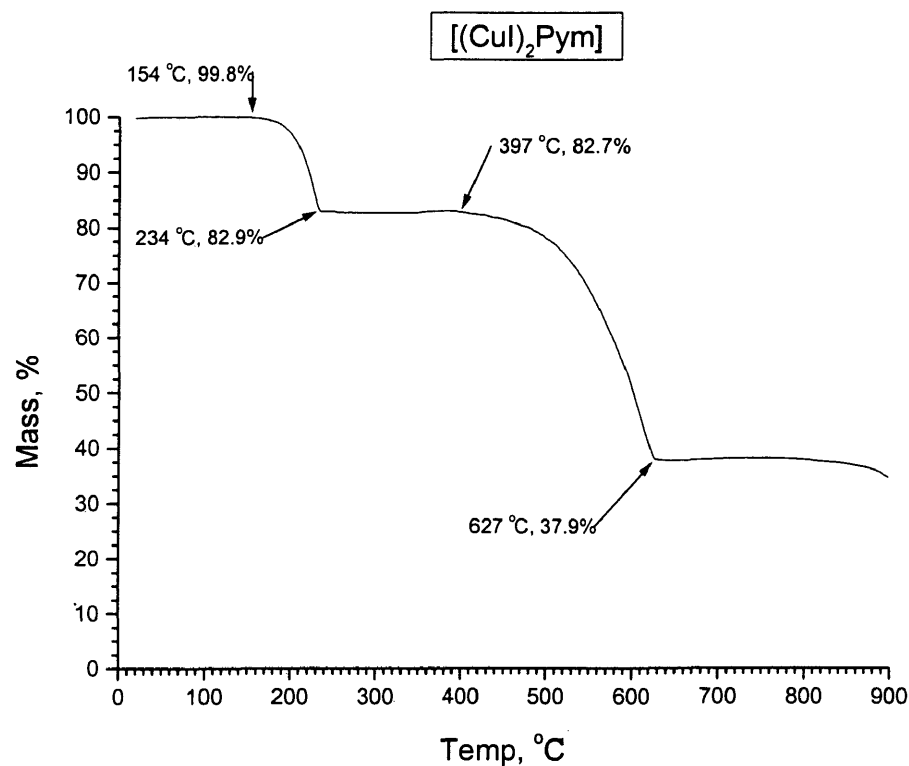
Figure 23. Thermogravimetric Analysis of $[(\text{CuBr})_2\text{Pym}]$.

$[(\text{CuI})_2\text{Pym}]$

A reaction of two equivalents of CuI and one equivalent of pyrimidine resulted in a neon yellow powder in 89 % yield. This compound was analyzed for copper using AAS. A copper amount of 27.28 % was determined. A theoretical copper percentage of 27.57 % corresponded to $[(\text{CuI})_2\text{Pym}]$. The results confirmed the 2:1 stoichiometry. A combustion analysis was performed on this compound as well. The relative percent errors for carbon, hydrogen and nitrogen were 1.6 %, 2.3 %, and 0.3 % respectively (Table 3). The TGA results for this compound also strongly suggested the $[(\text{CuI})_2\text{Pym}]$ formulation (Table 5, Figure 24). At 154 °C, the compound began to lose mass. A steady decline continued until 234 °C, by which point a 17 % total mass loss was seen in

the material. This phase was identified to be due to a loss of a complete pyrimidine unit from the material. It was stable to about 397 °C, at which point a very slow mass loss began. This mass loss gradually accelerated until it reached 627 °C, after which it abruptly leveled out again. The last mass loss was equal to a 62 % total mass loss from the original material. At this point, a reductive elimination of CuI has occurred to form copper metal at 45.8 % of the mass of the CuI phase.

A thermodynamic stability test was run using the components CuI and pyrimidine to discover if another phase could be formed (Table 7). Various ratios of CuI and pyrimidine were mixed in acetonitrile solutions in vials at 20 °C. It was found that each combination formed the [(CuI)₂Pym] precipitate within a short period of time. The mixtures formed solids in sequential order from the most concentrated to the least concentrated. The 10 mM CuI : 20 mM Pym (10:20) vial formed a neon yellow powder after only 10 seconds, while the 10:1 mixture formed the same solid after 5 minutes. The amount of the neon yellow powder present increased from the 10:1 to the 10:20 vial. Once formed, these compounds did not change composition. Raising the temperature to 70 °C caused the powder of the 10:1 vial to dissolve, while the remaining mixtures lost a minimal amount of mass. Thus the only stoichiometry formed from the components, CuI and pyrimidine was [(CuI)₂Pym].

Figure 24. Thermogravimetric Analysis of [(CuI)₂Pym].Table 7. Thermodynamic Stability Test for [(CuI)₂Pym].

CuI:Pym (mM)	25 °C			70 °C		
	t = 0 (hrs)	t = 2 (hrs)	t = 24 (hrs)	t = 0 (hrs)	t = 2 (hrs)	t = 24 (hrs)
10:1	solution	[(CuI) ₂ Pym]	[(CuI) ₂ Pym]	solution	solution	solution
10:2	solution	[(CuI) ₂ Pym]	[(CuI) ₂ Pym]	[(CuI) ₂ Pym]	[(CuI) ₂ Pym]	[(CuI) ₂ Pym]
10:3	solution	[(CuI) ₂ Pym]	[(CuI) ₂ Pym]	[(CuI) ₂ Pym]	[(CuI) ₂ Pym]	[(CuI) ₂ Pym]
10:4	solution	[(CuI) ₂ Pym]	[(CuI) ₂ Pym]	[(CuI) ₂ Pym]	[(CuI) ₂ Pym]	[(CuI) ₂ Pym]
10:5	solution	[(CuI) ₂ Pym]	[(CuI) ₂ Pym]	[(CuI) ₂ Pym]	[(CuI) ₂ Pym]	[(CuI) ₂ Pym]
10:6	solution	[(CuI) ₂ Pym]	[(CuI) ₂ Pym]	[(CuI) ₂ Pym]	[(CuI) ₂ Pym]	[(CuI) ₂ Pym]
10:7	solution	[(CuI) ₂ Pym]	[(CuI) ₂ Pym]	[(CuI) ₂ Pym]	[(CuI) ₂ Pym]	[(CuI) ₂ Pym]
10:8	solution	[(CuI) ₂ Pym]	[(CuI) ₂ Pym]	[(CuI) ₂ Pym]	[(CuI) ₂ Pym]	[(CuI) ₂ Pym]
10:9	solution	[(CuI) ₂ Pym]	[(CuI) ₂ Pym]	[(CuI) ₂ Pym]	[(CuI) ₂ Pym]	[(CuI) ₂ Pym]
10:10	solution	[(CuI) ₂ Pym]	[(CuI) ₂ Pym]	[(CuI) ₂ Pym]	[(CuI) ₂ Pym]	[(CuI) ₂ Pym]
10:12	solution	[(CuI) ₂ Pym]	[(CuI) ₂ Pym]	[(CuI) ₂ Pym]	[(CuI) ₂ Pym]	[(CuI) ₂ Pym]
10:14	solution	[(CuI) ₂ Pym]	[(CuI) ₂ Pym]	[(CuI) ₂ Pym]	[(CuI) ₂ Pym]	[(CuI) ₂ Pym]
10:16	solution	[(CuI) ₂ Pym]	[(CuI) ₂ Pym]	[(CuI) ₂ Pym]	[(CuI) ₂ Pym]	[(CuI) ₂ Pym]
10:18	solution	[(CuI) ₂ Pym]	[(CuI) ₂ Pym]	[(CuI) ₂ Pym]	[(CuI) ₂ Pym]	[(CuI) ₂ Pym]
10:20	solution	[(CuI) ₂ Pym]	[(CuI) ₂ Pym]	[(CuI) ₂ Pym]	[(CuI) ₂ Pym]	[(CuI) ₂ Pym]

[(CuCl)₂(PPh₃)₂Pym]

A pale yellow powder was collected in 89 % yield from the addition of one half of an equivalent of pyrimidine to a solution of [(CuCl)(PPh₃)] in chloroform. This product was analyzed using AAS, yielding an experimental value of 16.94 % copper by mass. The theoretical copper percentage of [(CuCl)₂(PPh₃)₂Pym] was 15.83 % (Table 4). The TGA data exhibited further evidence for the [(CuCl)₂(PPh₃)₂Pym] formulation (Table 6). At 98 °C a gradual mass loss began and leveled out at 192 °C, after about 10 % of the initial mass had been lost (Figure 25). This mass loss correlates directly to the loss of all of the pyrimidine ligand from the material, leaving [(CuCl)(PPh₃)]. This phase quickly degraded to form CuCl by 377 °C, then the copper chloride quickly sublimed to the expected low mass percentage of copper. The drastic increase in mass at high temperatures was not an expected outcome of the analysis and is probably not reproducible.

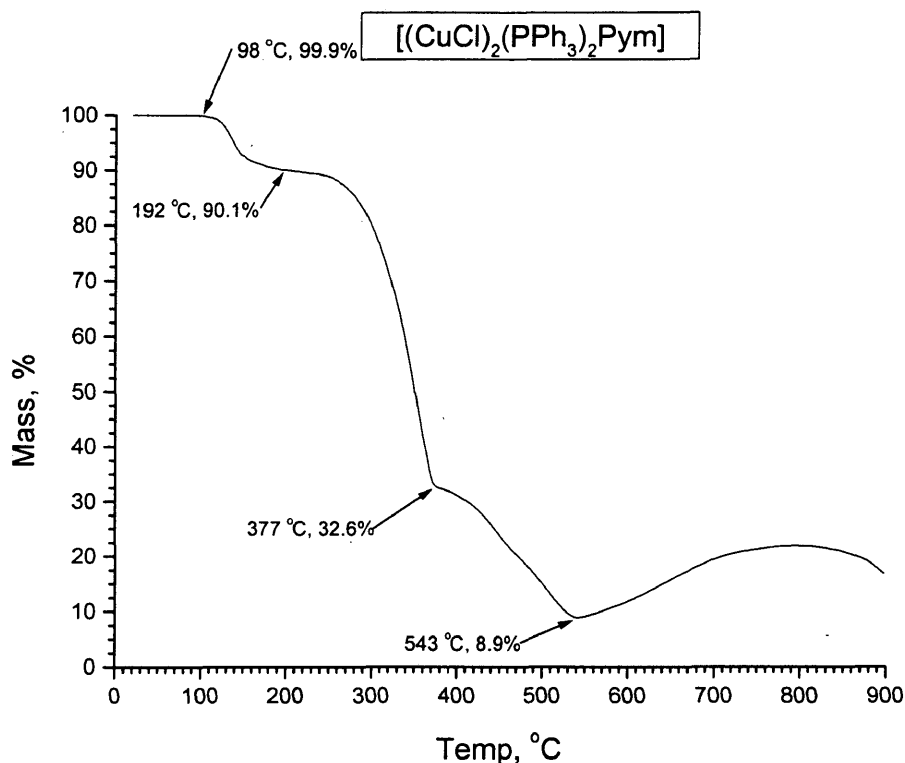


Figure 25. Thermogravimetric Analysis of [(CuCl)₂(PPh₃)₂Pym].

[(CuCl)₂(P(OPh)₃)₂Pym]

A light yellow powder was collected in 42 % yield from the addition of one half of an equivalent of pyrimidine to a solution of [(CuCl)(P(OPh)₃)] in chloroform. This compound was then analyzed by AAS to discover the percentage of copper in the substance. It was found that the material was 13.53 % copper by mass. This was then compared to the theoretical copper percentage of 14.14 % (Table 4). The two copper percentages differed by a relative error of 4.5 %. The compound was then analyzed for carbon, hydrogen, and nitrogen, giving relative errors of 0.5 %, 0.0 %, and 6.9 %, respectively. The relative error for nitrogen is high when compared to carbon and

hydrogen, but the absolute difference between the theoretical and experimental results is only 0.33 %. TGA was used to verify the results found from AAS and combustion analysis (Table 6, Figure 26). The compound began to lose pyrimidine by 107 °C and thus had formed $[(\text{CuCl})(\text{P}(\text{OPh})_3)]$ by 212 °C. This phase was stable for a short temperature range and promptly began to degrade to form CuCl by 348 °C. The CuCl began to sublime shortly afterward to form the usual trace residue by 578 °C.

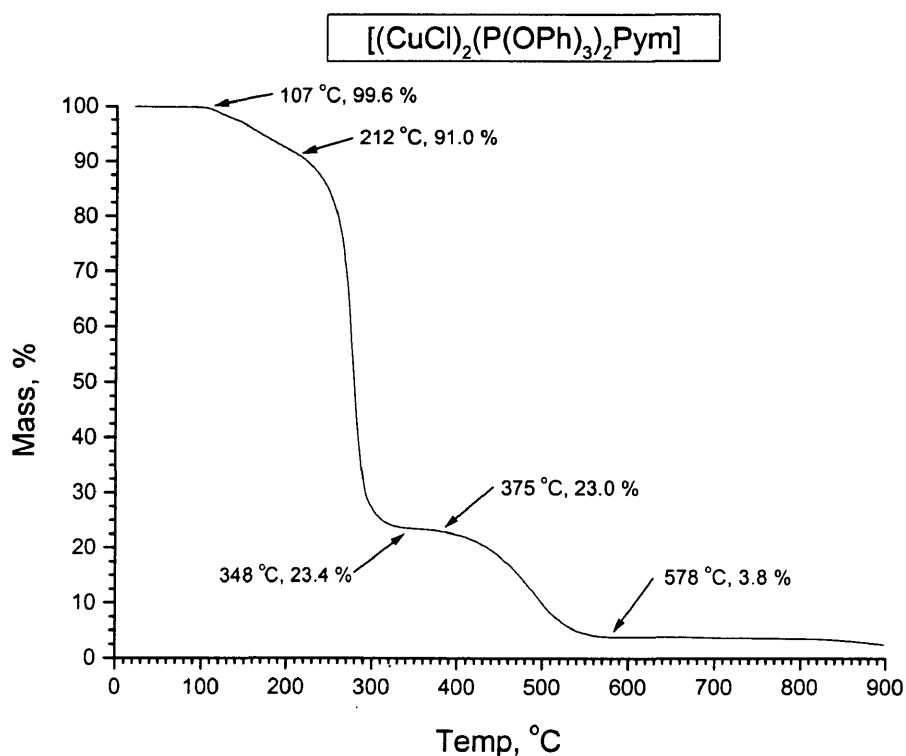


Figure 26. Thermogravimetric Analysis of $[(\text{CuCl})_2(\text{P}(\text{OPh})_3)_2\text{Pym}]$.

$[(\text{CuBr})_2(\text{PPh}_3)_2\text{Pym}]$

A yellow solid was obtained in 98 % yield from a reaction in which one half of an equivalent of pyrimidine was added to a stirring solution of $[(\text{CuBr})(\text{PPh}_3)]$ in

chloroform. The substance was analyzed for copper using AAS. The results of this analysis indicated that the compound was 14.64 % copper by mass. The theoretical copper percentage of 14.26 % corresponded with this value with a relative error of 2.6 % (Table 4). The sample was then analyzed by TGA (Table 6, Figure 27). The compound lost one-half of a unit of pyrimidine from 77 °C to 95 °C. This plateau was stable to 117 °C, at which point it lost the remainder of the pyrimidine. It was stable as [(CuBr)(PPh₃)] for a short temperature range and then quickly began to lose the phosphine at 176 °C. This process was completed when the temperature reached 379 °C and CuBr was remaining. The final loss of mass is due to the sublimation of the remaining CuBr. The final phase formed was 9.6 % of the CuBr phase, which agrees with the CuBr thermal degradation data.

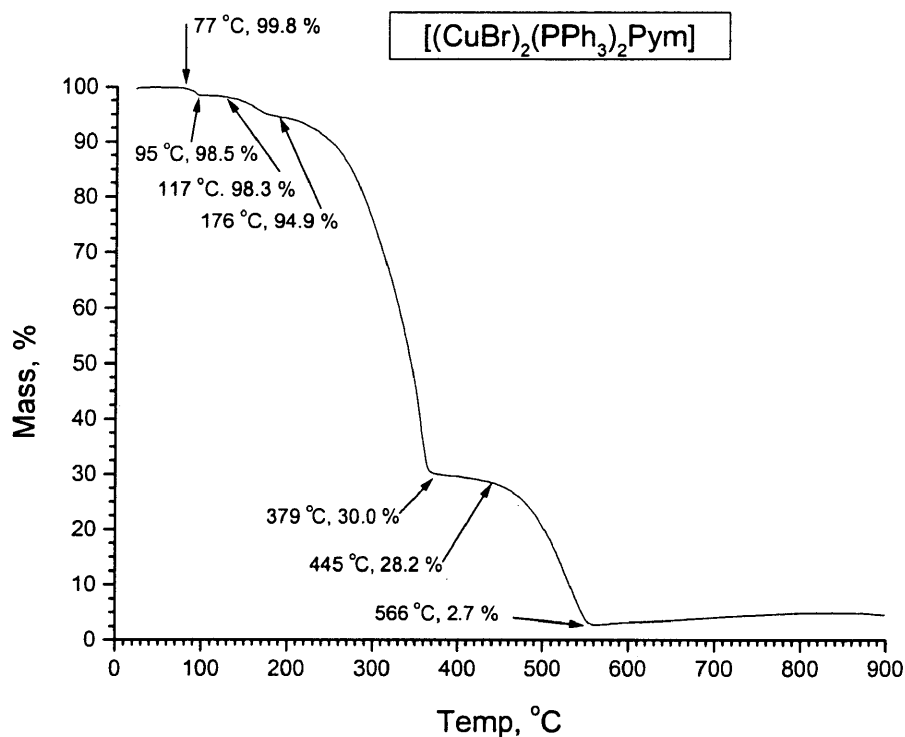


Figure 27. Thermogravimetric Analysis of [(CuBr)₂(PPh₃)₂Pym].

[(CuBr)₂(P(OPh)₃)₂Pym]

A light yellow powder was collected at 71 % yield upon reacting one half equivalent of pyrimidine with a stirring solution of [(CuBr)(P(OPh)₃)] in chloroform. A copper percentage of 12.94 % was obtained from AAS analysis. The theoretical copper percentage by mass for [(CuBr)₂(P(OPh)₃)₂Pym] was 12.87 % (Table 4). The relative error between these two figures was 0.5 %. A combustion analysis was performed on this sample to obtain more information. The carbon, hydrogen, and nitrogen relative errors were 1.2 %, 3.6 %, and 6.9 % respectively. During TGA analysis, the material began to decompose at 101 °C and steadily lost pyrimidine from the sample until the temperature reached 192 °C, at which point the mass loss rate increased (Table 6, Figure 28). There was a noticeable inflection point during the pyrimidine loss step that corresponds well to the loss of one-half of an equivalent of pyrimidine to form [(CuBr)₄(P(OPh)₃)₄Pym] at 143 °C. The material had formed [(CuBr)(P(OPh)₃)] when the temperature reached 192 °C. The material then lost all of the triphenylphosphite at an increased rate until the temperature reached 279 °C. At this temperature the remaining CuBr was stable up to 372 °C, whereupon the CuBr began to sublime steadily up to 545 °C. At this temperature, the phase formed was 11.0 % of the CuBr phase by mass. This compares well to the known CuBr thermal degradation pattern.

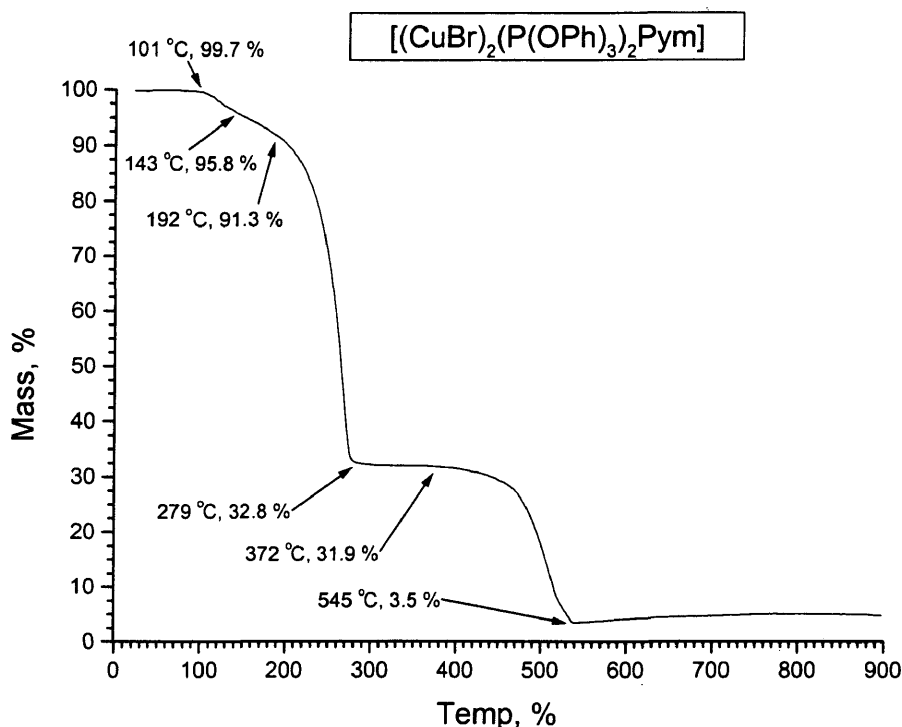


Figure 28. Thermogravimetric Analysis of [(CuBr)₂(P(OPh)₃)₂Pym].

[(CuI)₂(PPh₃)₂Pym]

A reaction of one half equivalent of pyrimidine added to a stirring solution of [(CuI)(PPh₃)] in chloroform resulted in a 36 % yield of a neon yellow powder. The low yield of the reaction and the color of the compound suggested that the reaction had formed [(CuI)₂Pym]. However, AAS analysis gave a value of 13.11 % copper by mass for the substance. In comparison to the possible formations, theoretical copper percentages of [(CuI)₂Pym] and [(CuI)₂(PPh₃)₂Pym] were 27.57 % and 12.90 % respectively. These data suggested that the substance was very similar to the intended compound. Combustion analysis for carbon, hydrogen, and nitrogen was run on the sample. The results paralleled the AAS data, suggesting the [(CuI)₂(PPh₃)₂Pym] product.

The relative percent errors carbon, hydrogen, and nitrogen were 1.8 %, 0.9 %, and 2.2 % respectively (Table 4). The TGA analysis agreed with the former results (Table 6, Figure 29). The compound lost pyrimidine between the temperatures of 127 °C and 177 °C. There was no significant loss of mass until the temperature reached 209 °C, at which point the meta-stable compound $[(\text{CuI})(\text{PPh}_3)]$ lost triphenylphosphine to become CuI. At this point, the temperature had reached 407 °C and the CuI was stable until 450 °C at which point it began to lose I_2 through reductive elimination and form copper metal.

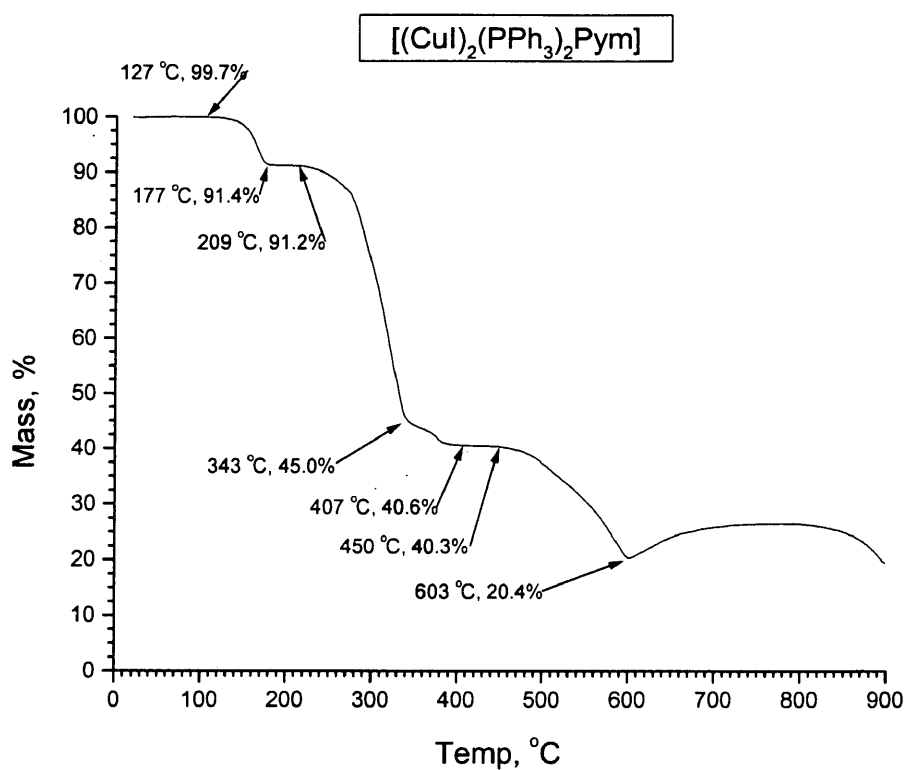


Figure 29. Thermogravimetric Analysis of $[(\text{CuI})_2(\text{PPh}_3)_2\text{Pym}]$.

[(CuI)₂(P(OPh)₃)₂Pym]

A lemon yellow powder was collected in 39 % yield from reacting one half equivalent of pyrimidine with a stirring solution of [(CuI)(P(OPh)₃)] in chloroform. This substance was analyzed for copper using AAS and was found to contain 27.33 % copper by mass. This data confirmed that the expected product was not formed and that the actual product was [(CuI)₂Pym].

Pyridazine**[(CuCl)Pd_z]**

A dark red powder was obtained in 79 % yield by the reaction of one equivalent of CuCl with one equivalent of pyridazine in an acetonitrile solution. The sample was analyzed using AAS and corresponded with the theoretical copper percentage of [(CuCl)Pd_z] to within 2.5 % (Table 3). A TGA was run and the results seemed to agree with the AAS information (Table 5, Figure 30). The [(CuCl)Pd_z] phase was stable up to 102 °C, at which point it began to lose half of its pyridazine and formed [(CuCl)₂Pd_z] by 185 °C. This phase was stable for a limited temperature range and quickly proceeded to lose pyridazine until it seemed that a total of two-thirds of a pyridazine had been lost. This intermediate phase was very short-lived and corresponds to [(CuCl)₃Pd_z]. The next phase that was formed was CuCl at 426 °C after the loss of all the remaining pyridazine. The remaining mass was less than the possible mass percentage of Cu alone and was a result of the sublimation of CuCl.

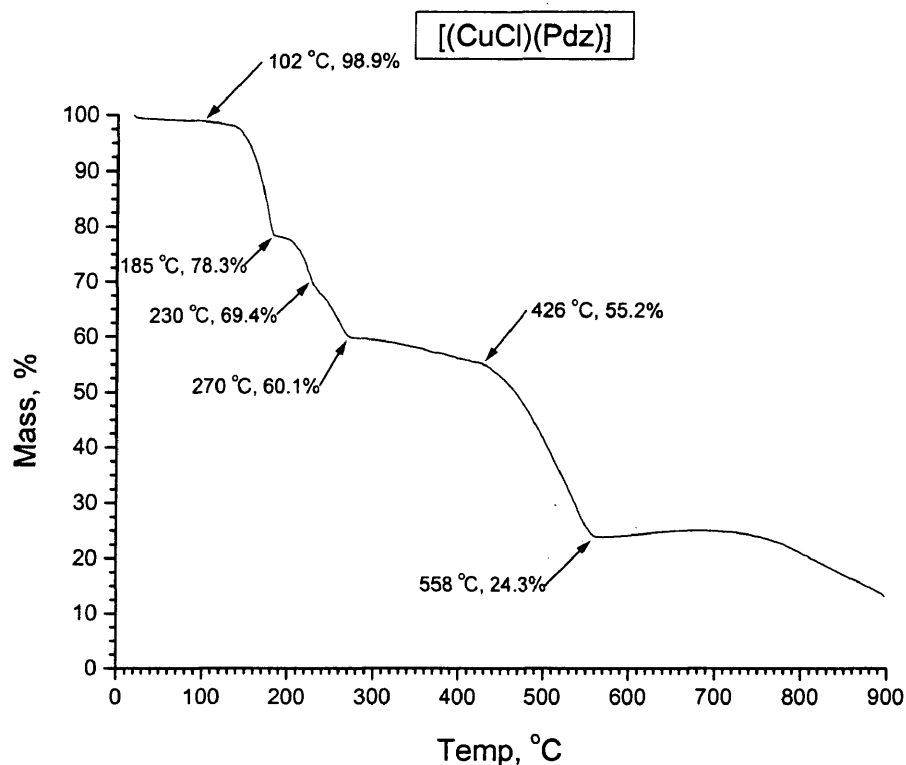


Figure 30. Thermogravimetric Analysis of $[(\text{CuCl})\text{Pdz}]$.

$[(\text{CuBr})\text{Pdz}]$

A red-brown powder was collected in 88 % yield after adding a one equivalent solution of pyridazine in acetonitrile to a stirring acetonitrile solution of one equivalent of CuBr. Atomic absorption spectroscopy analysis yielded a 2.0 % difference between the experimental and the theoretical copper percent of the intended compound, $[(\text{CuBr})\text{Pdz}]$. The sample was then analyzed using combustion analysis for carbon, hydrogen, and nitrogen. These results confirmed that the intended compound had been synthesized. The relative error for carbon was 2.4 %, for hydrogen 4.7 %, and for nitrogen was 3.4 % (Table 3). The compound was analyzed using TGA and found to be stable to 121 °C, at which point it began to lose one half unit of pyridazine (Table 5, Figure 31). The mass

then leveled out after 196 °C. At this temperature, the compound was stable as [(CuBr)₂Pdz] for a short time. It then continued to lose the bridging ligand and showed an inflection point at 258 °C. This required a loss of three-fourths of a pyridazine unit and corresponds to [(CuBr)₄Pdz]. At 470 °C, the last of the pyridazine had finally been lost and the remaining mass corresponded to that of CuBr. The final plateau temperature was at a lower mass percentage than that of copper. This was due to the expected percentage of the CuBr being lost through sublimation.

A thermodynamic stability test similar to that for CuI-Pym was run using CuBr and pyridazine to discover what possible compositions could be formed (Table 8). At 20 °C, all of the vials initially formed solutions that varied from light yellow to yellow orange as the concentration of pyridazine increased. At 3 and 17 hours, the first 7 vials contained solutions while the last 8 showed a fluffy red precipitate. Raising the temperature of the experiment to 70 °C resulted in all of the red solid dissolving after 3 hours. [(CuBr)Pdz] was the only material formed from the combination of CuBr and pyridazine under the conditions studied.

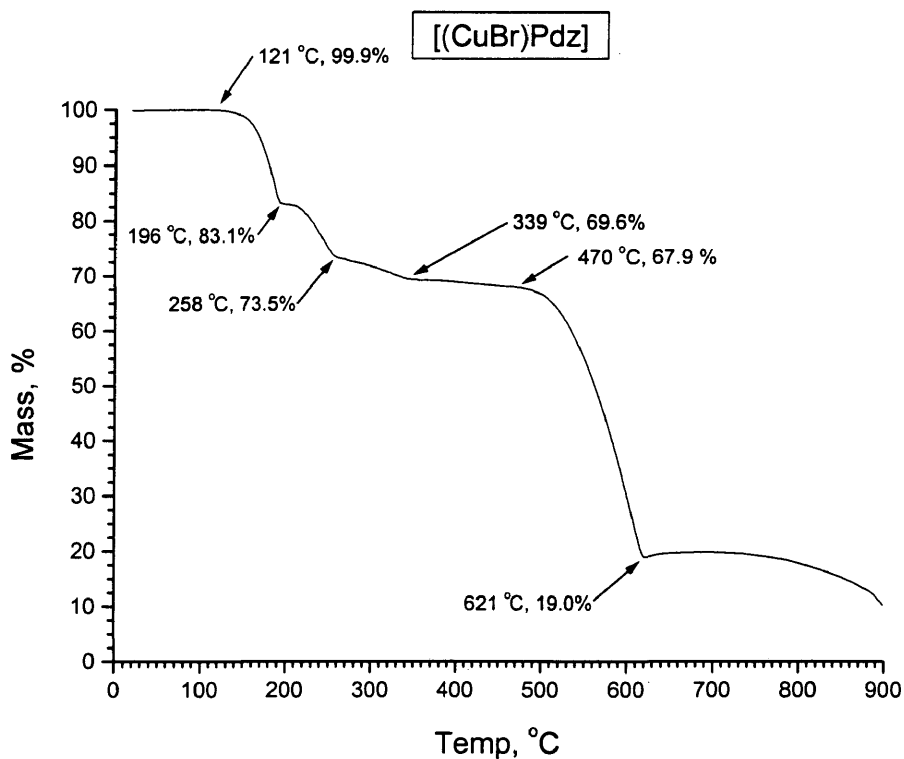


Figure 31. Thermogravimetric Analysis of $[(\text{CuBr})\text{Pdz}]$.

Table 8. Thermodynamic Stability Test for $[(\text{CuBr})\text{Pdz}]$.

CuBr:Pd _z (mM)	25 °C			70 °C		
	t = 0 (hrs)	t = 3 (hrs)	t = 17 (hrs)	t = 0 (hrs)	t = 3 (hrs)	t = 17 (hrs)
10:1	solution	solution	solution	solution	solution	solution
10:2	solution	solution	solution	solution	solution	solution
10:3	solution	solution	solution	solution	solution	solution
10:4	solution	solution	solution	solution	solution	solution
10:5	solution	solution	solution	solution	solution	solution
10:6	solution	solution	solution	solution	solution	solution
10:7	solution	solution	solution	solution	solution	solution
10:8	solution	$[(\text{CuBr})\text{Pdz}]$	$[(\text{CuBr})\text{Pdz}]$	$[(\text{CuBr})\text{Pdz}]$	solution	solution
10:9	solution	$[(\text{CuBr})\text{Pdz}]$	$[(\text{CuBr})\text{Pdz}]$	$[(\text{CuBr})\text{Pdz}]$	solution	solution
10:10	solution	$[(\text{CuBr})\text{Pdz}]$	$[(\text{CuBr})\text{Pdz}]$	$[(\text{CuBr})\text{Pdz}]$	solution	solution
10:12	solution	$[(\text{CuBr})\text{Pdz}]$	$[(\text{CuBr})\text{Pdz}]$	$[(\text{CuBr})\text{Pdz}]$	solution	solution
10:14	solution	$[(\text{CuBr})\text{Pdz}]$	$[(\text{CuBr})\text{Pdz}]$	$[(\text{CuBr})\text{Pdz}]$	solution	solution
10:16	solution	$[(\text{CuBr})\text{Pdz}]$	$[(\text{CuBr})\text{Pdz}]$	$[(\text{CuBr})\text{Pdz}]$	solution	solution
10:18	solution	$[(\text{CuBr})\text{Pdz}]$	$[(\text{CuBr})\text{Pdz}]$	$[(\text{CuBr})\text{Pdz}]$	solution	solution
10:20	solution	$[(\text{CuBr})\text{Pdz}]$	$[(\text{CuBr})\text{Pdz}]$	$[(\text{CuBr})\text{Pdz}]$	solution	solution

[(CuI)Pd_z]

One equivalent of CuI was dissolved in acetonitrile and added to an acetonitrile solution of one equivalent of pyridazine. The resultant orange powder was collected in 86 % yield. AAS analysis revealed that the compound had a copper percentage that was within 3.7% relative error of the intended compound's percent copper by mass (Table 3). A very sharp and definitive trace was produced from the TGA analyses of this sample (Table 5, Figure 32). The initial compound was stable up to 110 °C. Once it reached this temperature, pyridazine began to be lost. A short-lived plateau formed starting at 198 °C. This occurred after a total of one half pyridazine had been lost. The formulation of the new material was [(CuI)₂Pd_z]. Shortly after this transformation, the remainder of the bridging ligand was lost to form CuI. This CuI state was stable from 248 °C to 409 °C. The next stable state formed at 617 °C and represented 31.6 % of the original sample mass. The expected residual mass of copper would have been 23.5 % of the original mass. This plateau was formed due to the partial sublimation of the CuI, representing 44.9 % the mass of the CuI phase. This correlates well with the CuI thermal degradation behavior.

A thermodynamic stability test was set up using the components CuI and pyridazine (Table 9). At room temperature, the dominant compound formed was [(CuI)₂Pd_z] after 19 hours. The orange precipitate, [(CuI)Pd_z], was formed in the five vials with the greatest concentration of pyridazine present. The experiment was then heated to 70 °C and stirred for 20 hours. At this time, about half of the mixtures were in solution, and the others formed a varying amount of yellow precipitate, [(CuI)₂Pd_z]. With increased temperature, the 1:1 precipitates of the first experiment had formed the

2:1 powder, while the 2:1 precipitates had dissolved. This test demonstrated that [(CuI)Pd₂] and [(CuI)₂Pd₂] were the only phases formed under the conditions studied.

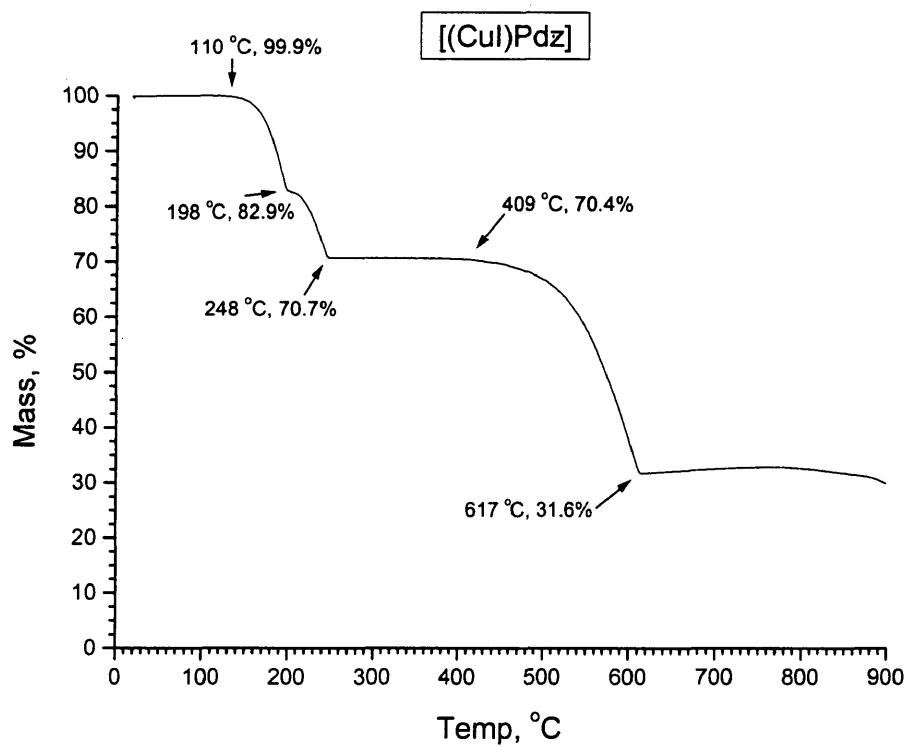


Figure 32. Thermogravimetric Analysis of [(CuI)Pd₂].

Table 9. Thermodynamic Stability Test for $[(\text{CuI})_x\text{PdZ}]$ ($x = 1,2$).

CuI:PdZ (mM)	25 °C			70 °C		
	t = 0 (hrs)	t = 2 (hrs)	t = 19 (hrs)	t = 0 (hrs)	t = 2 (hrs)	t = 19 (hrs)
10:1	solution	solution	solution	solution	solution	solution
10:2	solution	$[(\text{CuI})_2\text{PdZ}]$	$[(\text{CuI})_2\text{PdZ}]$	$[(\text{CuI})_2\text{PdZ}]$	solution	solution
10:3	solution	$[(\text{CuI})_2\text{PdZ}]$	$[(\text{CuI})_2\text{PdZ}]$	$[(\text{CuI})_2\text{PdZ}]$	solution	solution
10:4	solution	$[(\text{CuI})_2\text{PdZ}]$	$[(\text{CuI})_2\text{PdZ}]$	$[(\text{CuI})_2\text{PdZ}]$	solution	solution
10:5	solution	$[(\text{CuI})_2\text{PdZ}]$	$[(\text{CuI})_2\text{PdZ}]$	$[(\text{CuI})_2\text{PdZ}]$	solution	solution
10:6	solution	$[(\text{CuI})_2\text{PdZ}]$	$[(\text{CuI})_2\text{PdZ}]$	$[(\text{CuI})_2\text{PdZ}]$	solution	solution
10:7	solution	$[(\text{CuI})_2\text{PdZ}]$	$[(\text{CuI})_2\text{PdZ}]$	$[(\text{CuI})_2\text{PdZ}]$	solution	solution
10:8	solution	$[(\text{CuI})_2\text{PdZ}]$	$[(\text{CuI})_2\text{PdZ}]$	$[(\text{CuI})_2\text{PdZ}]$	$[(\text{CuI})_2\text{PdZ}]$	solution
10:9	solution	$[(\text{CuI})\text{PdZ}]$	$[(\text{CuI})_2\text{PdZ}]$	$[(\text{CuI})_2\text{PdZ}]$	$[(\text{CuI})_2\text{PdZ}]$	$[(\text{CuI})_2\text{PdZ}]$
10:10	solution	$[(\text{CuI})\text{PdZ}]$	$[(\text{CuI})_2\text{PdZ}]$	$[(\text{CuI})_2\text{PdZ}]$	$[(\text{CuI})_2\text{PdZ}]$	$[(\text{CuI})_2\text{PdZ}]$
10:12	solution	$[(\text{CuI})\text{PdZ}]$	$[(\text{CuI})\text{PdZ}]$	$[(\text{CuI})\text{PdZ}]$	$[(\text{CuI})_2\text{PdZ}]$	$[(\text{CuI})_2\text{PdZ}]$
10:14	$[(\text{CuI})\text{PdZ}]$	$[(\text{CuI})\text{PdZ}]$	$[(\text{CuI})\text{PdZ}]$	$[(\text{CuI})\text{PdZ}]$	$[(\text{CuI})_2\text{PdZ}]$	$[(\text{CuI})_2\text{PdZ}]$
10:16	$[(\text{CuI})\text{PdZ}]$	$[(\text{CuI})\text{PdZ}]$	$[(\text{CuI})\text{PdZ}]$	$[(\text{CuI})\text{PdZ}]$	$[(\text{CuI})_2\text{PdZ}]$	$[(\text{CuI})_2\text{PdZ}]$
10:18	$[(\text{CuI})\text{PdZ}]$	$[(\text{CuI})\text{PdZ}]$	$[(\text{CuI})\text{PdZ}]$	$[(\text{CuI})\text{PdZ}]$	$[(\text{CuI})_2\text{PdZ}]$	$[(\text{CuI})_2\text{PdZ}]$
10:20	$[(\text{CuI})\text{PdZ}]$	$[(\text{CuI})\text{PdZ}]$	$[(\text{CuI})\text{PdZ}]$	$[(\text{CuI})\text{PdZ}]$	$[(\text{CuI})_2\text{PdZ}]$	$[(\text{CuI})_2\text{PdZ}]$

$[(\text{CuI})_2\text{PdZ}]$

A reaction of two equivalents of CuI with one equivalent of pyridazine resulted in a yellow powder in 95 % yield. This compound was analyzed for copper using AAS. The copper percentage was found to be within 1.0 % relative error of the copper percentage for the expected $[(\text{CuI})_2\text{PdZ}]$ (Table 3). From TGA data it was found that the sample was thermally stable up to 170 °C (Table 5, Figure 33). The material lost all of the pyridazine after this point and only CuI was left by 249 °C. The CuI was stable to 383 °C, at which point the CuI degraded to 42.4 % of its mass via reductive elimination.

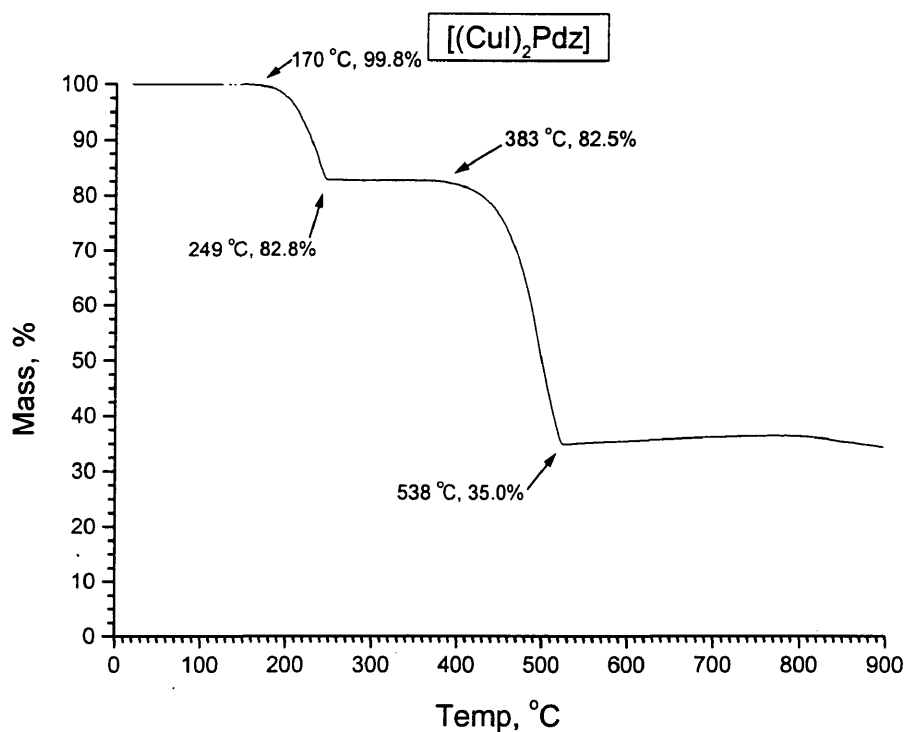


Figure 33. Thermogravimetric Analysis of $[(\text{CuI})_2\text{PdZ}]$.

$[(\text{CuCl})_2(\text{PPh}_3)_2\text{PdZ}]$

A reaction of one half of an equivalent of pyridazine added to a stirring solution of $[(\text{CuCl})(\text{PPh}_3)]$ in chloroform resulted in a 72 % yield of a light yellow powder. This reaction was run following the guidelines used for forming $[(\text{CuCl})_2(\text{PPh}_3)_2\text{Pym}]$. We, therefore, initially believed that $[(\text{CuCl})_2(\text{PPh}_3)_2\text{PdZ}]$ (2:2:1) had formed. Atomic absorption spectroscopy analysis of the sample provided surprising results. The theoretical copper percentages for the 1:1:1 and 2:2:1 stoichiometries are 14.40 % and 15.83 % respectively and were compared to the experimental value of 13.74 %. The sample was analyzed for carbon, hydrogen, and nitrogen to help clarify this result. The relative errors for the 1:1:1 stoichiometry for carbon, hydrogen, and nitrogen were 1.1 %, 1.1 %, and 1.1 % respectively.

2.4 %, and 56.0 % respectively. The same comparison utilizing the 2:2:1 stoichiometry resulted in relative errors of 1.1 %, 0.2 %, and 14.3 %. These data suggested the 2:2:1 material had been formed (Table 4). Analysis by TGA was the final step in discerning the correct stoichiometry of the sample (Table 6, Figure 34). The material began to lose pyridazine by 116 °C and continued to lose mass until the temperature reached 179 °C, at which point 92.1 % of the original mass still remained. If the material had the 2:2:1 stoichiometry, the loss of the pyridazine would leave 90.0 % of the residual mass. The loss of bridging ligand for the 1:1:1 stoichiometry would result in only 81.9 % mass remaining. This result was more consistent with the 2:2:1 formulation, $[(\text{CuCl})_2(\text{PPh}_3)_2\text{PdZ}]$. The large loss of mass from 179 °C to 397 °C was due to the loss of all of the phosphine to form CuCl, after which the residual mass was 23.8 % of the original mass. The residual masses for the 2:2:1 and 1:1:1 stoichiometries would be 24.7 % and 22.4 % correspondingly. The final loss of mass was due to the sublimation of the CuCl to form the expected copper metal at 5.7 % original mass. In summary, the results from TGA and combustion analysis suggested a 2:2:1 stoichiometry and were deemed more reliable than the AAS results, which suggested the 1:1:1 ratio.

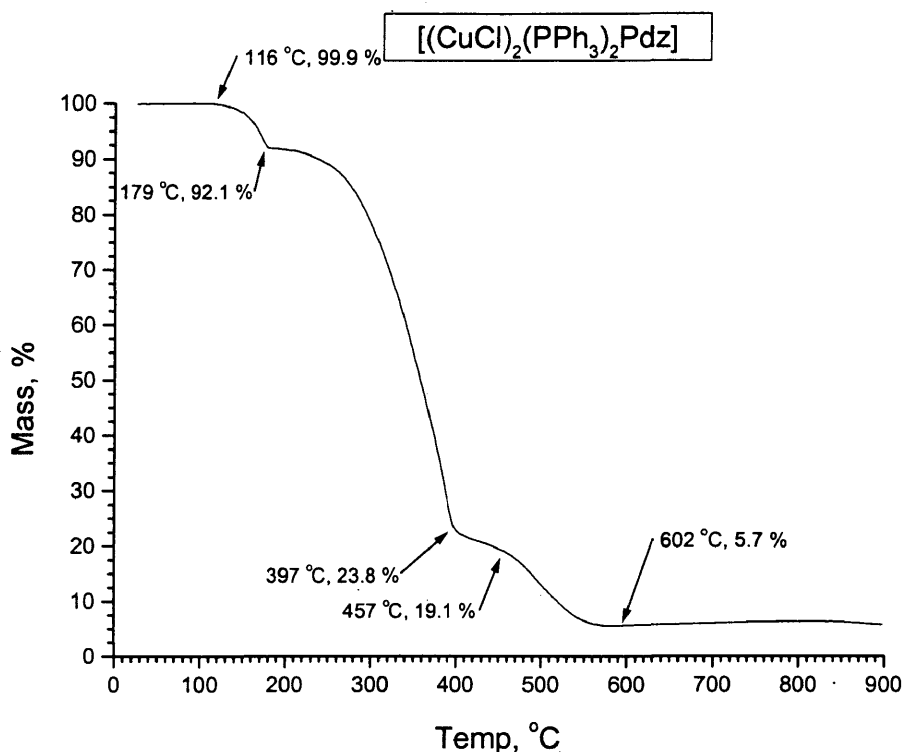


Figure 34. Thermogravimetric Analysis of $[(\text{CuCl})_2(\text{PPh}_3)_2\text{PdZ}]$.

$[(\text{CuCl})(\text{P}(\text{OPh})_3)\text{PdZ}]$

The addition of one half equivalent of pyridazine to a stirring solution of $[(\text{CuCl})(\text{P}(\text{OPh})_3)]$ formed a yellow powder in 27 % yield based on a 2:2:1 product formulation. Atomic absorption spectroscopy analysis of this sample provided a copper percentage of 12.55 % for the material. The 2:2:1 material would have had a copper percentage of 14.14 %, a relative error of 12.7 %. On the other hand, the comparison to the 1:1:1 stoichiometry copper percentage of 12.99 % to the sample, gave a relative error of only 3.5 % (Table 4). The TGA of the same sample did not yield any intermediate phases that resembled reasonable losses (Figure 35). The sample degraded early, commencing at 80 °C, and lost mass steadily until it reached 315 °C (Table 6). The

remaining material represented only 27.7 % of the beginning total mass. The copper percentage of CuCl is 20.2 % of the total mass of $[(\text{CuCl})(\text{P}(\text{OPh})_3)\text{Pdz}]$. The next phase at 579 °C represented 10.9 % of the original mass. A mass percentage of 13.0 % was calculated for the mass percentage of Cu from the original mass. Thus TGA did not provide conclusive information on the formulation of the sample material for either the 1:1:1 or 2:2:1 stoichiometries.

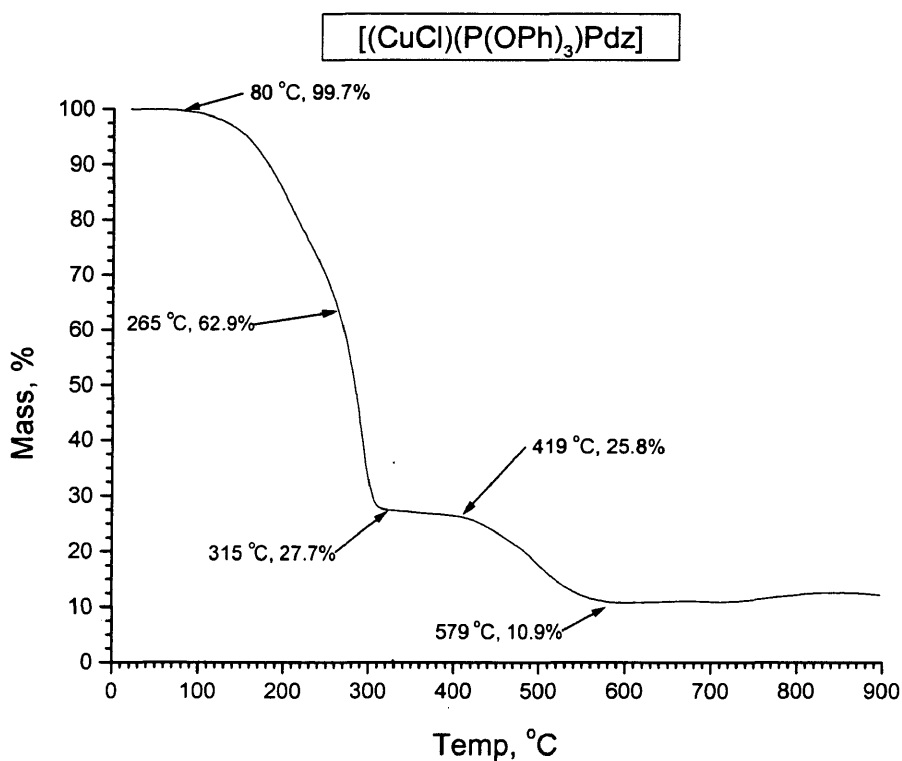


Figure 35. Thermogravimetric Analysis of $[(\text{CuCl})(\text{P}(\text{OPh})_3)\text{Pdz}]$.

$[(\text{CuBr})(\text{PPh}_3)\text{Pdz}]$

One half of an equivalent of pyridazine, diluted in chloroform, was added to a stirring solution of $[(\text{CuBr})(\text{PPh}_3)]$ in chloroform. This reaction resulted in a light

yellow-orange powder. This compound was expected to form a 2:2:1 phase, but was found to be 1:1:1 instead. The theoretical copper percentage had a relative error of only 0.5 % for the 1:1:1 stoichiometry when compared to the actual value obtained from AAS. Combustion analysis was performed on the sample for carbon, hydrogen, and nitrogen analysis. The error value for carbon was 1.0 %, for hydrogen was 3.4 %, and for nitrogen was 3.6 %. Thus, the results of AAS and combustion analysis strongly supported the [(CuBr)(PPh₃)PdZ] formulation (Table 4). The TGA data gave additional information on the identity of the sample (Table 6, Figure 36). The first mass loss of 6 % represented a mass loss of one half unit of pyridazine to form [(CuBr)₂(PPh₃)₂PdZ]. The next mass loss concluded at 200 °C and imparted a total mass loss of 21 %. At this point the remainder of the pyridazine bridge had been lost, to form [(CuBr)(PPh₃)]. At 260 °C, a large mass loss of about 43 % of the original mass began and continued until 368 °C. At this point the remainder of the compound was CuBr. The CuBr was stable for only a short temperature range before it began to decompose in the usual way. Sublimation and reductive elimination ended by 581 °C, leaving 4.5 % of the original mass.

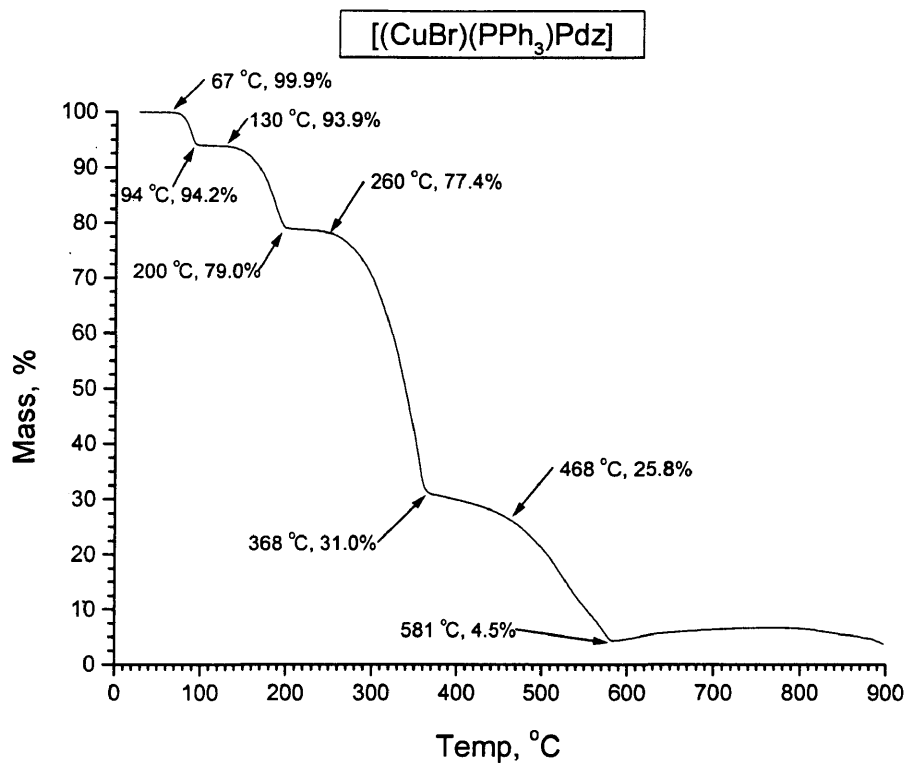


Figure 36. Thermogravimetric Analysis of [(CuBr)(PPh₃)PdZ].

[(CuBr)(P(OPh)₃)PdZ]

The attempted synthesis of [(CuBr)₂(P(OPh)₃)₂PdZ] resulted in a light yellow powder. It was found from AAS and combustion analysis that the material formed matched the 1:1:1 stoichiometry. An experimental copper percentage of 12.08 % was found from AAS. The theoretical value for copper percentage of [(CuBr)(P(OPh)₃)PdZ] is 11.90 %, while the copper percentage of [(CuBr)₂(P(OPh)₃)₂PdZ] is 12.87 %. Combustion analysis was performed on the sample to collect further information on the composition of the material. The carbon and hydrogen analyses were within 2.0 % relative error of the theoretical percentages for both formulations and, therefore, were inconclusive in determining the stoichiometry. The nitrogen analysis, however, gave

decisive data in determining the formula. The percent nitrogen in the sample was 5.11 % of the total mass of the material. The theoretical mass percents of nitrogen for the 1:1:1 and 2:2:1 stoichiometries are 5.25 % and 2.84 % respectively (Table 4). The TGA data for this sample was not helpful in confirming the correct formulation of the material. The graph closely resembled the $[(\text{CuCl})(\text{P}(\text{OPh})_3)\text{PdZ}]$ TGA results (Table 6). Apparently the problem was that the phosphite and pyridazine are lost at roughly the same temperature (Figure 37). The phase formed by 328 °C was expected to be CuBr. For the 2:2:1 stoichiometry, CuBr would be 29.1 % of its original mass, while the CuBr phase for the 1:1:1 stoichiometry would have been 26.9 % of the original mass. These two values are much too similar to come to provide definitive data on the composition of the sample.

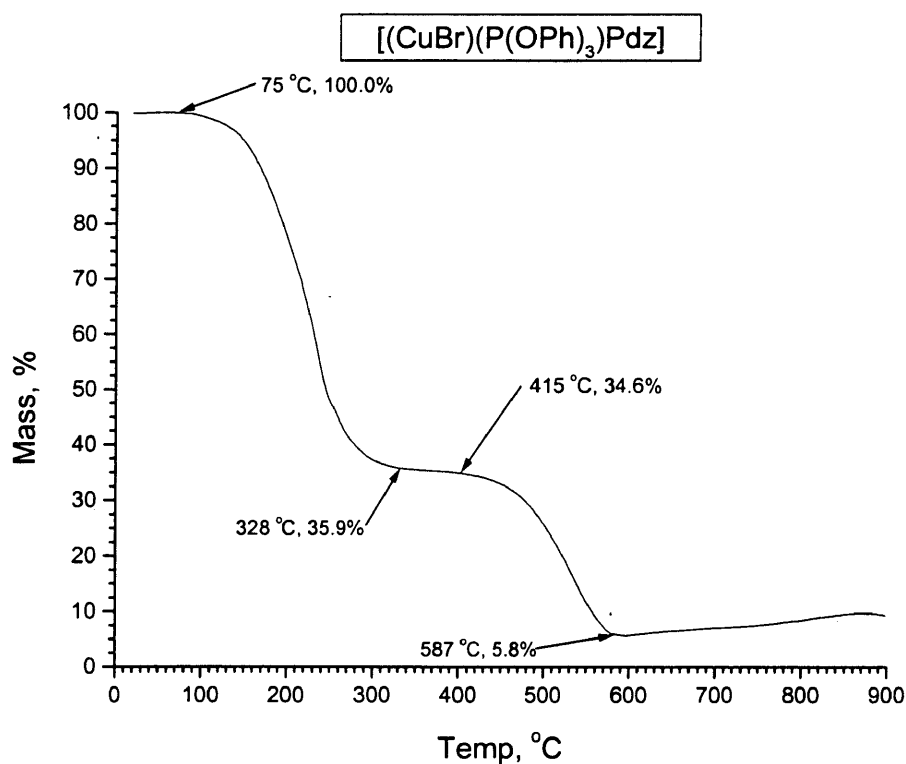


Figure 37. Thermogravimetric Analysis of $[(\text{CuBr})(\text{P}(\text{OPh})_3)\text{PdZ}]$.

[(CuI)(PPh₃)Pd₂]

A reaction of one half of an equivalent of pyridazine added to a stirring solution of [(CuI)(PPh₃)] in chloroform resulted in a 65 % yield of a yellow-orange powder. The AAS analysis of this sample suggested that the product was [(CuI)₂(PPh₃)₂Pd₂]. The experimental result and the theoretical value had a relative difference of only 2.2 % (Table 4). If the sample is compared to the theoretical value for [(CuI)(PPh₃)Pd₂] the relative error is 5.5 %. However, analysis by TGA produced a disparity with the AAS results (Table 6, Figure 38). If the sample was assumed to have the 2:2:1 stoichiometry, the first mass loss between 70 °C and 110 °C would compare well to a loss of pyridazine to form [(CuI)(PPh₃)]. The mass loss from 110 °C to 335 °C was equal to a mass loss of the remaining phosphine to form CuI, which then degraded in the expected way. The problem in this degradation analysis was the apparent formation of a phase by 111 °C, which further degraded by 160 °C. When this TGA is evaluated according to the 1:1:1 stoichiometry, the first mass loss represented removal of one half unit of pyridazine to form [(CuI)₂(PPh₃)₂Pd₂]. The next decrease was the loss of the remainder of the pyridazine to form [(CuI)(PPh₃)]. The next mass loss started by 199 °C and ended by 381 °C was due to the loss of the phosphine to form the CuI phase, which then began to sublime by 450 °C. The data from the TGA compared much more reasonably to the 1:1:1 stoichiometry. Each mass loss could be accounted for when compared to this stoichiometry. By comparison, the 2:2:1 formulation is consistent with the plateau between 158 °C and 199 °C. It also required higher CuI percentage than was represented by the plateau between 381 °C and 450 °C.

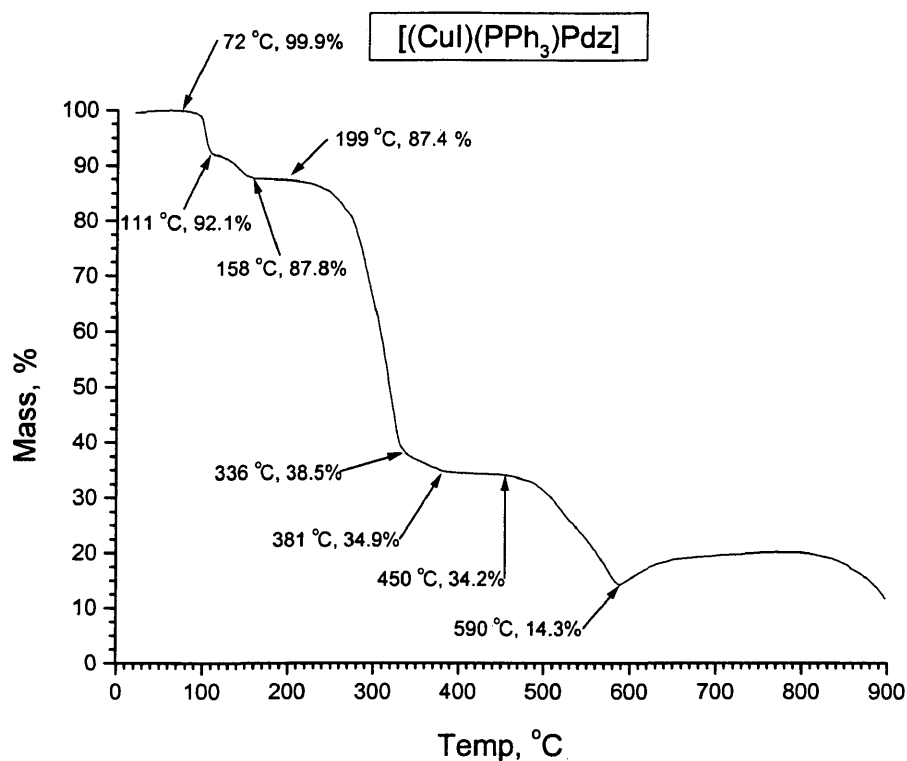


Figure 38. Thermogravimetric Analysis of [(CuI)(PPh₃)PdZ].

[(CuI)₂(P(OPh)₃)₂PdZ]

A yellow powder was collected upon reacting one half equivalent of pyridazine with a stirring solution of [(CuI)(P(OPh)₃)] in chloroform. This substance was analyzed for copper using AAS and was found to contain 27.21 % copper by mass. This data confirmed that the expected product was not formed and that the resultant product was actually [(CuI)₂PdZ].

Triazine

[(CuCl)₂Trz]

All attempts to synthesize this 2:1 compound directly resulted in the formation of other stoichiometries. However, the [(CuCl)₂Trz] product was formed at 70 % yield

during the attempted synthesis of $[(\text{CuCl})_3(\text{Trz})_2]$. The copper percentage for the sample was found to be 46.22 %. The theoretical copper percentage for $[(\text{CuCl})_2\text{Trz}]$ was 45.54 % resulting in a relative error of 1.5 % (Table 3). The TGA data for this sample was consistent with this formulation. The compound began to decompose at 111 °C and lost about 10 % of its original mass (Table 5, Figure 39). The first plateau at 90 % original mass would correspond to a loss of one-third of a triazine to form $[(\text{CuCl})_3\text{Trz}]$. Loss of the remainder of the triazine would have formed CuCl at 71 % of the original mass. By 429 °C, the CuCl began to sublime. The information from TGA and AAS gave substantial evidence that the 2:1 stoichiometry had been formed.

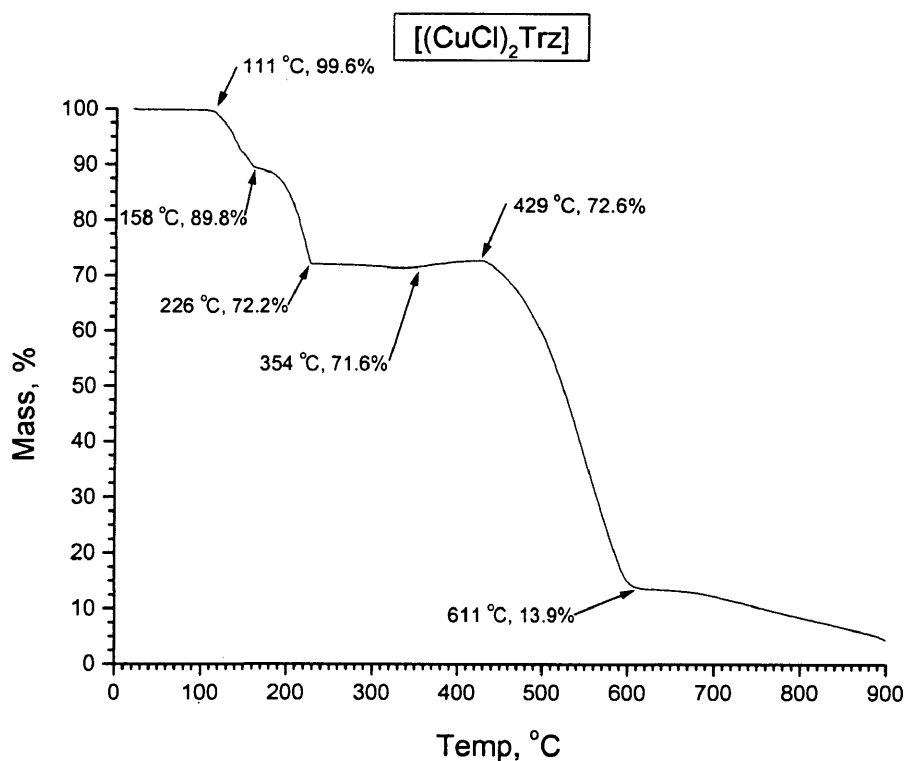


Figure 39. Thermogravimetric Analysis of $[(\text{CuCl})_2\text{Trz}]$.

[(CuCl)₃Trz]

A brown-orange powder was collected from the addition of two-thirds of an equivalent of triazine to one equivalent of CuCl dissolved in acetonitrile. This sample was analyzed using AAS, and the copper percentage was found to be 47.45 %. This value was between the copper percentages of [(CuCl)₂Trz] and [(CuCl)₃Trz], 45.51 % and 50.43 % respectively. A combustion analysis was performed on this material to determine percentages of carbon, hydrogen, and nitrogen. The resultant data were remarkably inconsistent with the theoretical mass percentages of the 2:1 species. The relative errors for carbon, hydrogen, and nitrogen were 30.54 %, 8.00 %, and 34.95 %. The 3:1 stoichiometry was then compared to the same experimental results to afford relative errors of 3.7 %, 20.0 %, and 0.4 % for carbon, hydrogen, and nitrogen. The hydrogen error seemed very substantial, but considering that the mass percents differed by only 0.20 %, the discrepancy was not considered to be serious (Table 3). The TGA data for this sample helped to support the combustion analysis information (Table 5, Figure 40). The thermal degradation of the compound began at 118 °C and continued to 176 °C, whereupon one-fourth of a unit of triazine had been lost to convert the [(CuCl)₃Trz] to [(CuCl)₄Trz], a previously unknown phase. The remainder of the triazine was lost quickly thereafter to form CuCl by 250 °C. The mass percent remaining was 77 % and corresponded well to the theoretical mass percentage of 79 %. Formation of CuCl provided fairly definitive information for both of the CuCl-Trz complexes. In both cases, the remaining mass percent for pure CuCl was stable over a long temperature range. Thus, the CuCl mass percentages for both of the products: 2:1 (71 %) and 3:1 (79 %) served as a sort of fingerprint for the original materials.

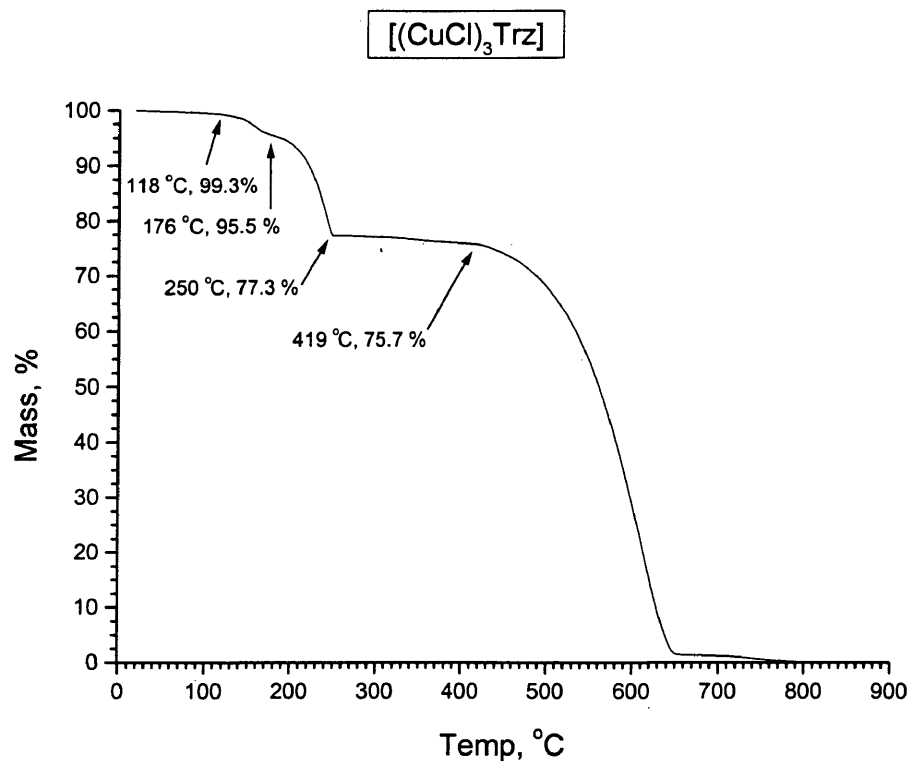


Figure 40. Thermogravimetric Analysis of [(CuCl)₃Trz].

[(CuBr)₃(Trz)₂]

All attempts to synthesize this 3:2 compound directly resulted in the formation of other products. The [(CuBr)₃(Trz)₂] formulation was formed in 15 % yield from the attempted formation of [(CuBr)₃Trz]. The copper percentage for the sample was found to be 32.20 %. The theoretical copper percentage for [(CuBr)₃(Trz)₂] was 32.18 %, an error of 0.1 % (Table 3). The sample was analyzed by TGA to confirm the AAS results (Table 5, Figure 41). The compound began to degrade by 92 °C and lost one half unit of triazine by 145 °C to form [(CuBr)₂Trz]. This phase was stable for only a short temperature range. The next phase at 175 °C, [(CuBr)₃Trz], was formed from the loss of another half unit of triazine. The remainder of the triazine had degraded by 245 °C, to leave a CuBr

phase. This phase was stable up to 484 °C, at which point it began to decompose in the expected fashion.

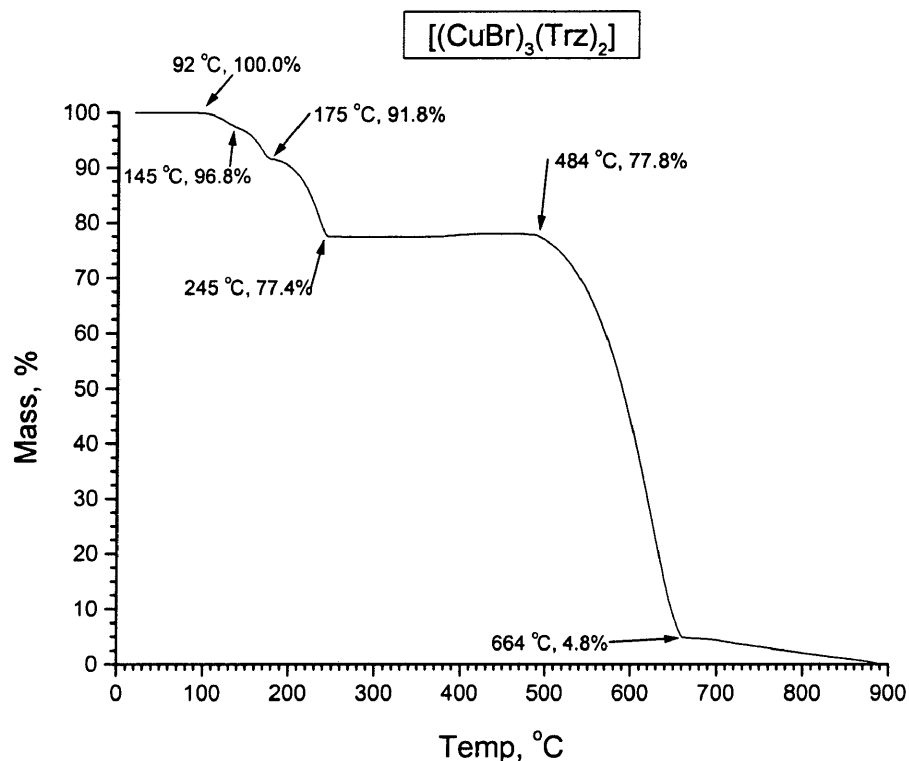


Figure 41. Thermogravimetric Analysis of [(CuBr)₃(Trz)₂].

[(CuBr)₂Trz]

An orange powder was formed from the attempted synthesis of [(CuBr)₃(Trz)₂] and was discovered to be [(CuBr)₂Trz] after combustion analysis. The theoretical copper percentage of the [(CuBr)₃(Trz)₂] material is 32.18 % and of the [(CuBr)₂Trz] material is 34.54 %. The experimental AAS copper percentage was 35.00 %. The material was analyzed by combustion as well. The relative errors of carbon, hydrogen, and nitrogen for [(CuBr)₂Trz] were found to be 1.3 %, 10.9 %, and 3.9 % respectively (Table 3). The

thermal degradation of the compound was then probed using TGA (Table 5, Figure 42). The results clearly showed a loss of one-third of a triazine unit to form a short-lived $[(\text{CuBr})_3\text{Trz}]$ phase. The next step in the thermal degradation was the formation of CuBr , after the remainder of the triazine was lost. The CuBr was stable up to $485\text{ }^\circ\text{C}$, whereupon the CuBr began to sublime and decompose to the expected copper metal residue.

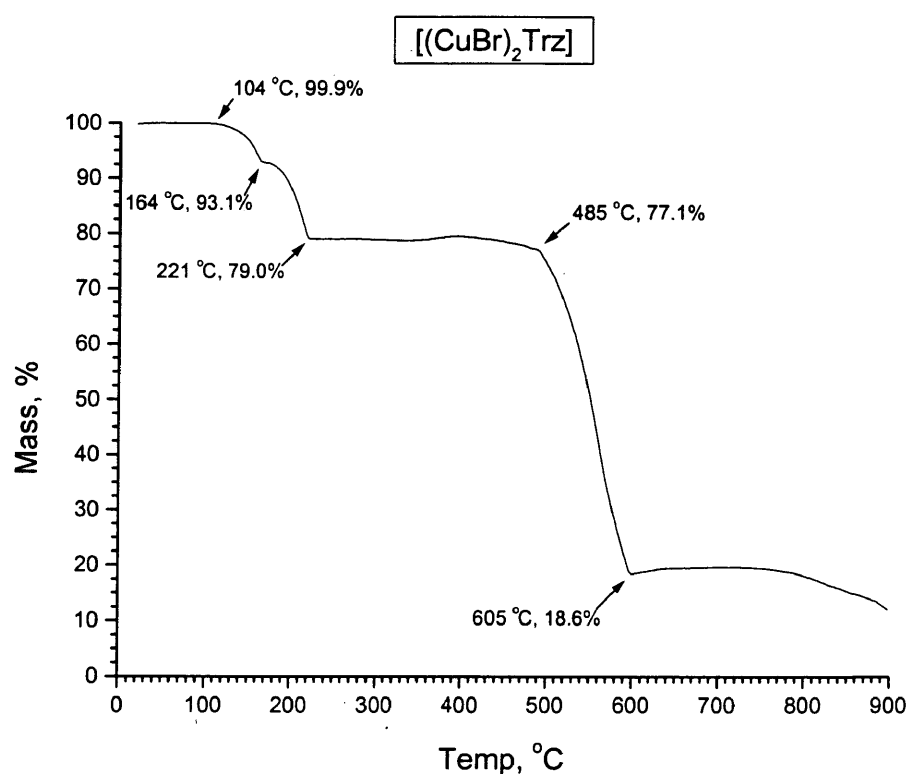


Figure 42. Thermogravimetric Analysis of $[(\text{CuBr})_2\text{Trz}]$.

$[(\text{CuBr})_3\text{Trz}]$

The attempted formation of $[(\text{CuBr})_3(\text{Trz})_2]$ through reacting CuBr and triazine at a 1:1 ratio instead produced $[(\text{CuBr})_3\text{Trz}]$ in 76 % yield. The sample was analyzed using AAS to obtain a copper percentage of 37.19 % (Table 3). The theoretical copper

percentage is 37.28 % (a 0.2 % relative error). TGA analysis of the sample revealed an initial loss of mass by 77 °C (Table 5, Figure 43). At this temperature, one half unit of triazine was lost and $[(\text{CuBr})_6\text{Trz}]$ had formed by 150 °C. The remainder of the triazine was then lost to form CuBr by 233 °C. This phase was stable up to 529 °C, whereupon, the CuBr began to sublime to form the expected amount of residue. The TGA data corresponds well to the information reported from AAS. A thermodynamic stability test was run using the components CuBr and triazine in the concentrations previously employed (see Tables 6, 7, 8, and 9). The mixtures all initially formed green solutions. After 17 hours, no precipitate was seen and it was determined that the concentrations used were too low.

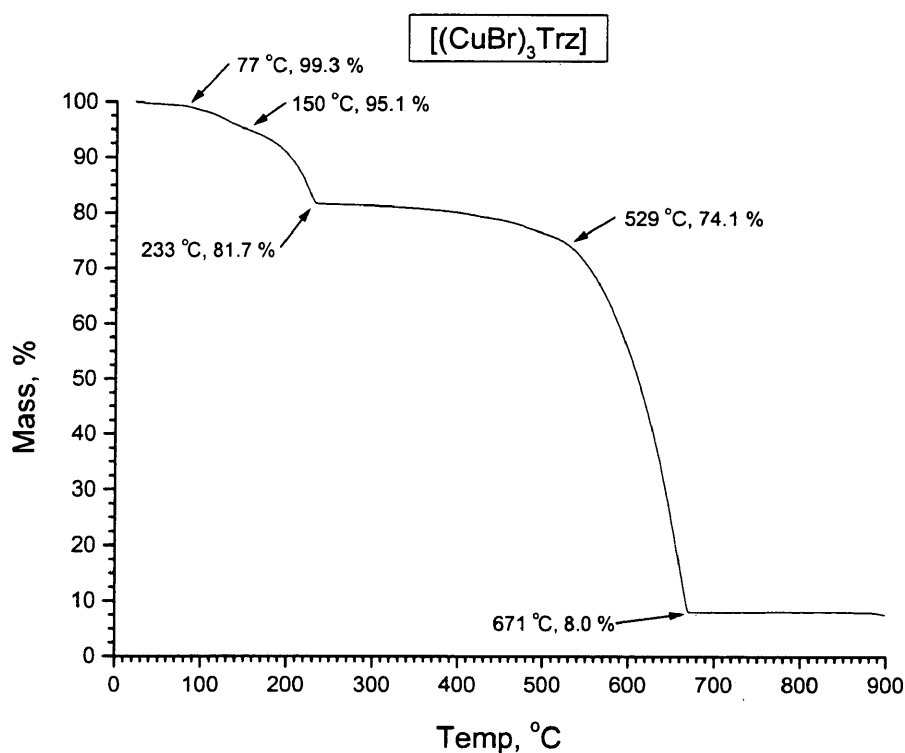


Figure 43. Thermogravimetric Analysis of $[(\text{CuBr})_3\text{Trz}]$.

[(CuI)₂Trz]

A neon-yellow powder was collected in 94 % from a reaction of three equivalents of CuI and two equivalents of triazine in acetonitrile solution. Atomic absorption spectroscopy analysis of this sample gave very good results for the copper percentage of [(CuI)₂Trz] with only a 0.3 % relative error based on the theoretical copper percentage (Table 3). The TGA degradation of the sample began at 126 °C with a loss of one unit of triazine (Table 5, Figure 44). The remaining material, CuI, was stable from 202 °C to 392 °C. At this temperature, the CuI began to be lost through reductive elimination. The final material at 36 % of the original mass was the expected copper metal residue. A stability test was run with CuI and triazine as the components (Table 10). Initially, all of the mixtures formed yellow solutions. After 3 hours, the six mixtures with the lowest concentration of triazine remained in solution, while the other nine had formed a neon yellow precipitate (with increasing mass as triazine concentration increased). The only stoichiometry formed from these two components was [(CuI)₂Trz].

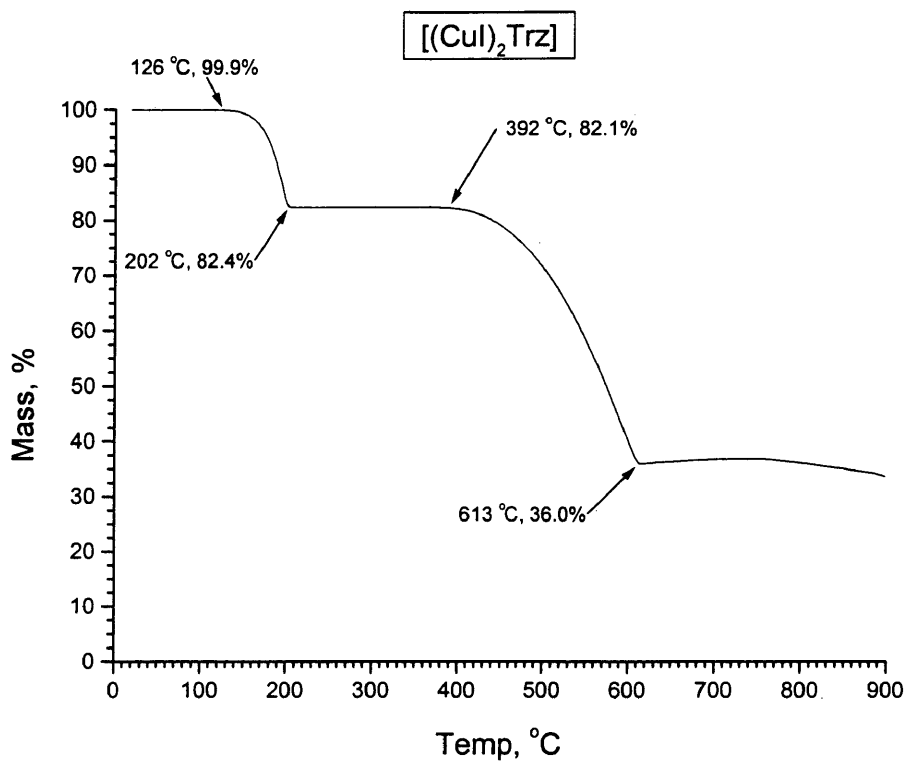


Figure 44. Thermogravimetric Analysis of [(CuI)₂Trz].

Table 10. Thermodynamic Stability Test of [(CuI)₂Trz].

CuI:Trz (mM)	25 °C		
	t = 0 (hrs)	t = 3 (hrs)	t = 17 (hrs)
10:1	solution	solution	solution
10:2	solution	solution	solution
10:3	solution	solution	solution
10:4	solution	solution	solution
10:5	solution	solution	solution
10:6	solution	solution	solution
10:7	solution	[(CuI) ₂ Trz]	[(CuI) ₂ Trz]
10:8	solution	[(CuI) ₂ Trz]	[(CuI) ₂ Trz]
10:9	solution	[(CuI) ₂ Trz]	[(CuI) ₂ Trz]
10:10	solution	[(CuI) ₂ Trz]	[(CuI) ₂ Trz]
10:12	solution	[(CuI) ₂ Trz]	[(CuI) ₂ Trz]
10:14	solution	[(CuI) ₂ Trz]	[(CuI) ₂ Trz]
10:16	solution	[(CuI) ₂ Trz]	[(CuI) ₂ Trz]
10:18	solution	[(CuI) ₂ Trz]	[(CuI) ₂ Trz]
10:20	solution	[(CuI) ₂ Trz]	[(CuI) ₂ Trz]

[(CuCl)₃(PPh₃)₃Trz]

One-third of an equivalent of triazine was dissolved in chloroform and added to a 1:1 mixture of CuCl and PPh₃ in chloroform. This resulted in a light brown-orange suspension. The light orange solid was removed from the yellow solution and discarded. The yellow solution was then concentrated and allowed to crystallize. Yellow-orange crystals formed and were washed with ether to remove white particles (PPh₃) from their surface. This yellow-orange powder was determined to have a copper percentage of 16.39 % by AAS. The theoretical copper percentage for the 2:1 product is 15.82 % (a relative error of 3.5 %). The copper percentage for the 3:1 stoichiometry is 16.37 %, producing a relative error of 0.1 % (Table 4). The results from TGA were compared to the expected decomposition stages of both the 2:2:1 and the 3:3:1 products to help clarify the sample composition (Figure 45). The sample was first compared to the 2:2:1 formulation. The first mass loss from 98 °C to 123 °C would represent a loss of one-third of an equivalent of triazine to leave 97 % of the original mass remaining (Table 6). The actual mass percent loss at this point was 98 %. The loss of the remaining triazine would result in 90 % residual mass. The actual percent mass remaining at the next meta-stable phase was 92 %. For the 3:3:1 compound, the first mass loss was comparable to a loss of one-fourth of an equivalent of triazine at 98 % residual mass. The loss of the remaining triazine would have left 93 % of the original sample. The data compiled from both AAS and TGA seem to resemble the 3:3:1 stoichiometry more closely, but a definitive determination of the formula could not be made.

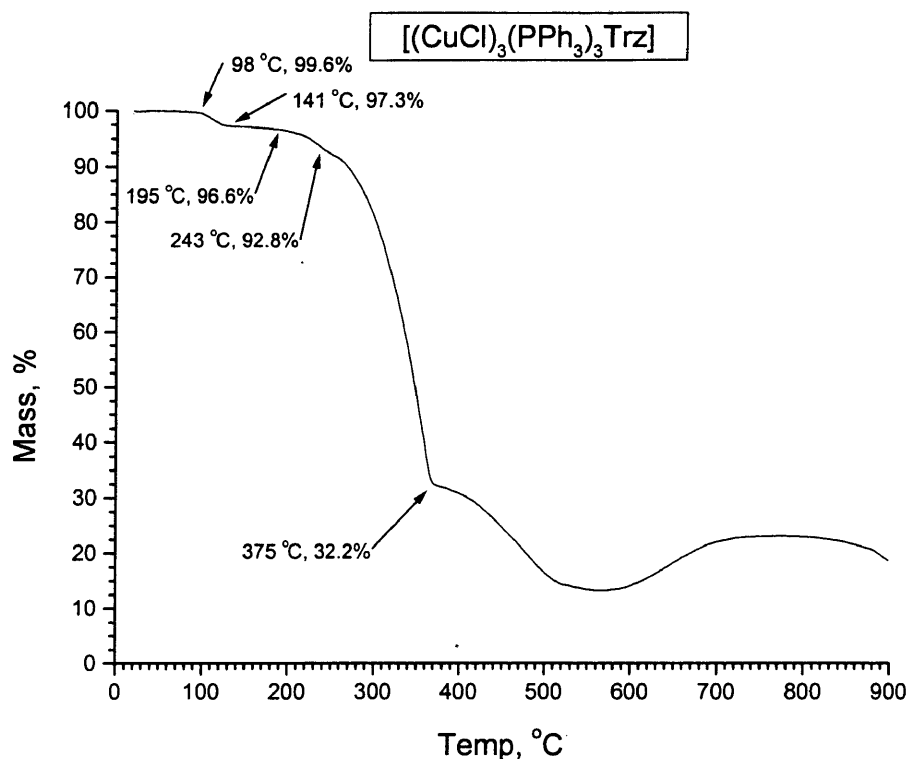


Figure 45. Thermogravimetric Analysis of [(CuCl)₃(PPh₃)₃Trz].

[(CuCl)₂(P(OPh)₃)₂Trz]

A yellow-orange powder was collected in 69 % yield from the addition of one-half of an equivalent of triazine to a solution of [(CuCl)(P(OPh)₃)] in chloroform. The sample was discovered to contain 13.93 % copper by mass. This corresponded to a relative error of 1.4 % when compared to the theoretical value of 14.13 % copper for the intended compound (Table 4). The sample was analyzed by TGA and it was found that the sample began to degrade by 41 °C (Table 6, Figure 46). This low temperature degradation leveled off by 87 °C, at which point one half unit of triazine had been lost to form [(CuCl)₄(P(OPh)₃)₄Trz]. The compound continued to degrade gradually and had lost all of the triazine by 170 °C to form [(CuCl)(P(OPh)₃)]. The phosphite lost mass

promptly to form CuCl by 290 °C. The CuCl phase was stable up to 366 °C, at which point it began to decompose normally.

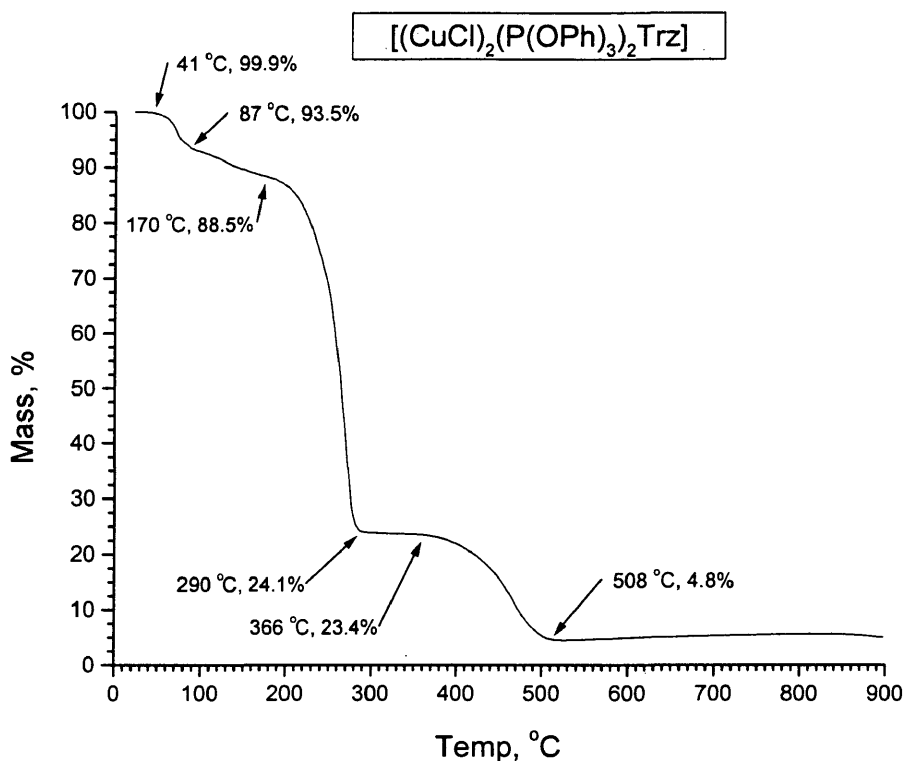


Figure 46. Thermogravimetric Analysis of [(CuCl)₂(P(OPh)₃)₂Trz].

[(CuBr)₂(PPh₃)₂Trz]

This material was formed from an attempted reaction to produce [(CuBr)₃(PPh₃)₃Trz]. One-third of an equivalent of triazine was dissolved in chloroform and added to a 1:1 mixture of CuCl and PPh₃ in chloroform. A yellow solid was formed in 51 % yield, and from later analyses found to be [(CuBr)₂(PPh₃)₂Trz]. The direct reaction to form this product produced a yellow solid in 81 % yield, but the product did not analyze as well as that of the former reaction. The copper percentage of the sample was 14.52 %. The relative error was 2.0 % when compared to the theoretical copper

percentage of 14.24 %. The same sample was analyzed for percentages of carbon, hydrogen, and nitrogen. The comparisons between theoretical and experimental results for these three elements were excellent (Table 4). The thermal degradation of this material began at 115 °C and slowed drastically at 150 °C (Table 6, Figure 47). This mass loss was equivalent to a complete loss of triazine from the sample to form $[(\text{CuBr})(\text{PPh}_3)]$. The loss of the phosphine from 240 °C to 370 °C, would have resulted in the formation of CuBr at a mass percentage of 32 %, but the actual sample had an inflection point near 38 %. The CuBr meta-stable phase was found to be a short-lived stage of the thermal degradation of the sample.

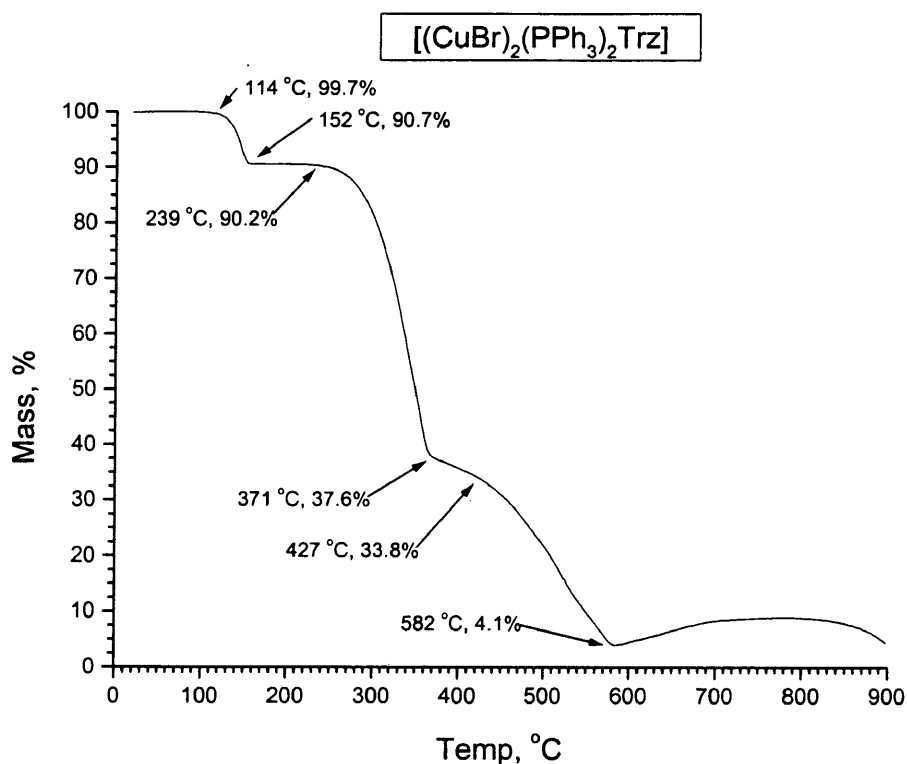


Figure 47. Thermogravimetric Analysis of $[(\text{CuBr})_2(\text{PPh}_3)_2\text{Trz}]$.

[(CuBr)₂(P(OPh)₃)₂Trz]

A yellow powder was collected in 51 % yield upon addition of half an equivalent of triazine to a solution of [(CuBr)(P(OPh)₃)] in chloroform. This compound was analyzed by AAS to determine the percentage of copper in the substance. It was found that the material was 12.83 % copper by mass. This value was compared to the theoretical copper percentage of 12.86 %, a relative error of 0.2 %. The compound was analyzed for carbon, hydrogen, and nitrogen, giving relative errors of 0.3 %, 0.0 %, and 0.5 %, respectively. (Table 4). The thermal degradation of this material began at 76 °C and it continued to lose mass until the temperature reached 184 °C, at which point the compound had lost all of its triazine and had become [(CuBr)(P(OPh)₃)] (Table 6, Figure 48). The loss of the phosphite, theoretically, would leave a mass percentage of only 29 %. The TGA results displayed a meta-stable stage at about 36 %, at which the sample had presumably become CuBr. The next mass loss was due to the sublimation and decomposition of CuBr. Thus, the analyses of this compound confirmed that the 2:2:1 product was prepared.

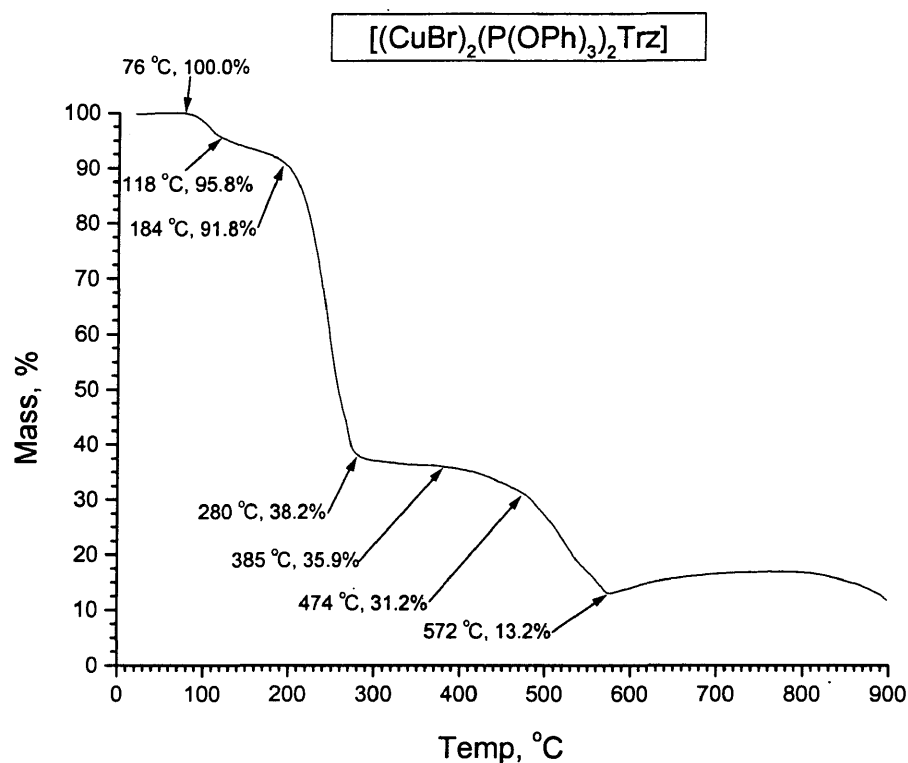


Figure 48. Thermogravimetric Analysis of [(CuBr)₂(P(OPh)₃)₂Trz].

[(CuI)₂(PPh₃)₂Trz]

A light orange powder was collected in 84 % yield by adding one half an equivalent of triazine to a solution of [(CuI)(PPh₃)] in chloroform. This compound was then analyzed by AAS to determine the percentage of copper. It was found that the material was 12.80 % copper by mass. This was compared to the theoretical copper percentage of 12.88 % to obtain a relative difference of 0.6 %. The material was analyzed for carbon, hydrogen, and nitrogen. The relative errors of carbon, hydrogen, and nitrogen for [(CuI)₂(PPh₃)₂Trz] were found to be 1.3 %, 0.6 %, and 1.2 % respectively (Table 4). The thermal degradation of this material began at 121 °C (Figure 49). It continued to lose mass until the temperature reached 166 °C, whereupon the

compound had lost all of its triazine and had become $[(\text{CuI})(\text{PPh}_3)]$ (Table 6). The loss of the triphenylphosphine resulted in a residual mass of 39 %, which was determined to be CuI. The final mass loss to the mass of about 20 % was formed after partial sublimation of the CuI.

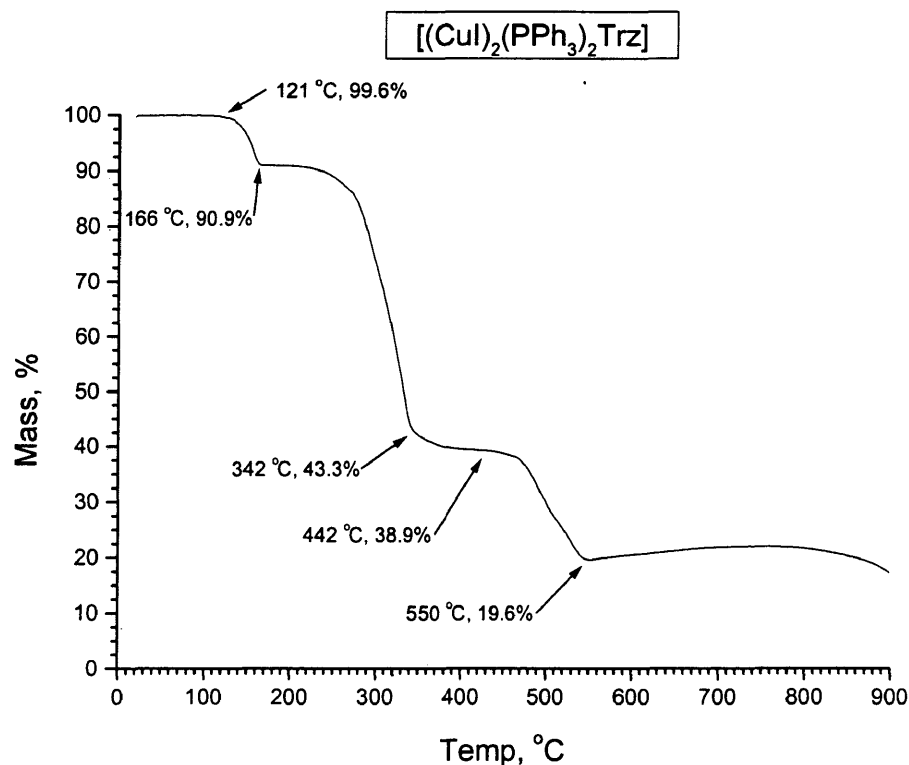


Figure 49. Thermogravimetric Analysis of $[(\text{CuI})_2(\text{PPh}_3)_2\text{Trz}]$.

$[(\text{CuI})_3(\text{P(OPh)}_3)_3\text{Trz}]$

The attempted production of $[(\text{CuI})_2(\text{P(OPh)}_3)_2\text{Trz}]$ resulted in a light cream yellow powder. An experimental copper percentage of 11.77 % was determined from AAS data. The theoretical value for copper percentage of $[(\text{CuI})_2(\text{P(OPh)}_3)_2\text{Trz}]$ is 11.74 %, while the copper percentage of $[(\text{CuI})_3(\text{P(OPh)}_3)_3\text{Trz}]$ is 12.04 %. Thus, the AAS data

suggested that we had successfully formed the 2:2:1 product. The sample was analyzed for carbon, hydrogen, and nitrogen to support the 2:2:1 stoichiometry. The carbon analyses were within 2.0 % relative error of the theoretical percentages for both products and, therefore, were inconclusive in determining the formulation of the sample. Both hydrogen errors for the 2:2:1 and 3:3:1 were near 8 % relative error, which is reasonable for hydrogen. The nitrogen analysis, however, provided the decisive information for the final formulation. The percent nitrogen in the sample was 2.79 % of the total mass of the material. The theoretical mass percents of nitrogen for the 3:3:1 and 2:2:1 stoichiometries are 2.65 % and 3.88 % respectively. Thus, the combustion analysis of the sample was in disagreement with the AAS results (Table 4). The results from TGA were compared to the expected decomposition stages of both the 2:2:1 and the 3:3:1 products to help clarify the sample's composition (Table 6, Figure 50). The sample was first compared to the 2:2:1 stoichiometry. The first mass loss from 31 °C to 101 °C would represent a loss of one equivalent of triazine to leave 93 % of the original mass remaining. The actual mass percent loss at this point was 93 %. The loss of the phosphite from the sample would result in 35 % residual mass. The actual percent mass remaining at the next meta-stable state was 39 %. For the 3:3:1 compound, the first mass loss was comparable to a loss of one equivalent of triazine at 94 % residual mass. The loss of the phosphite would have left 40 % of the original sample. In summary, the data compiled from both combustion analysis and TGA seemed to resemble the 3:3:1 stoichiometry more closely than the 2:2:1, in agreement with the nitrogen analysis. However, it is possible that the "product" is not actually either species, based upon its

pale color and the fact that neither the $[(\text{CuI})_2(\text{P}(\text{OPh})_3)_2\text{Pdz}]$ nor the $[(\text{CuI})_2(\text{P}(\text{OPh})_3)_2\text{Pym}]$ products are formed.

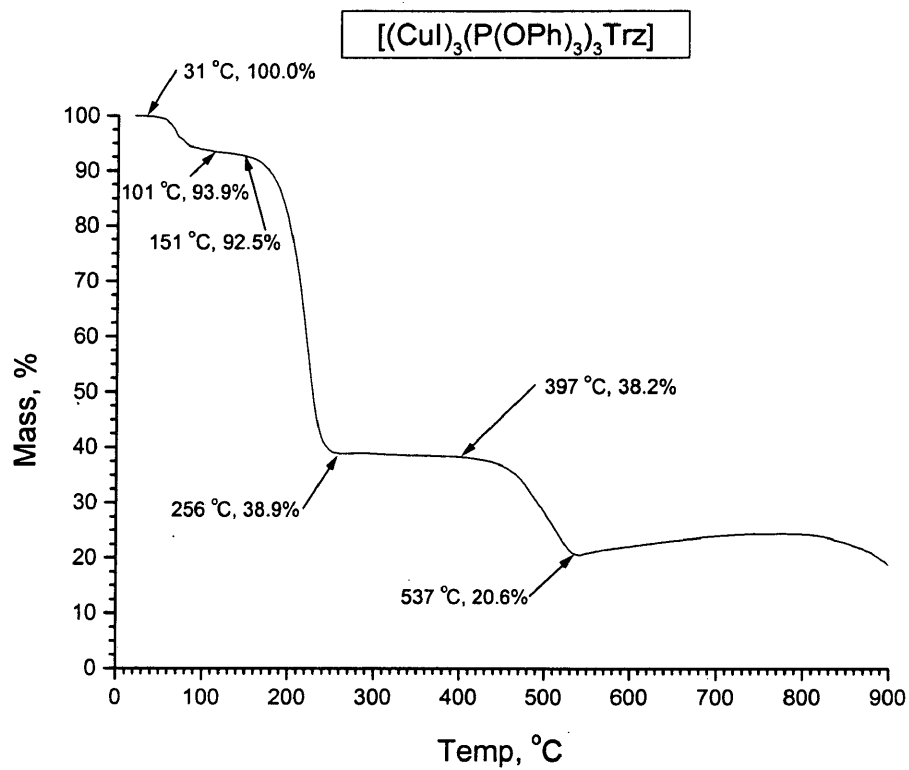


Figure 50. Thermogravimetric Analysis of $[(\text{CuI})_3(\text{P}(\text{OPh})_3)_3\text{Trz}]$.

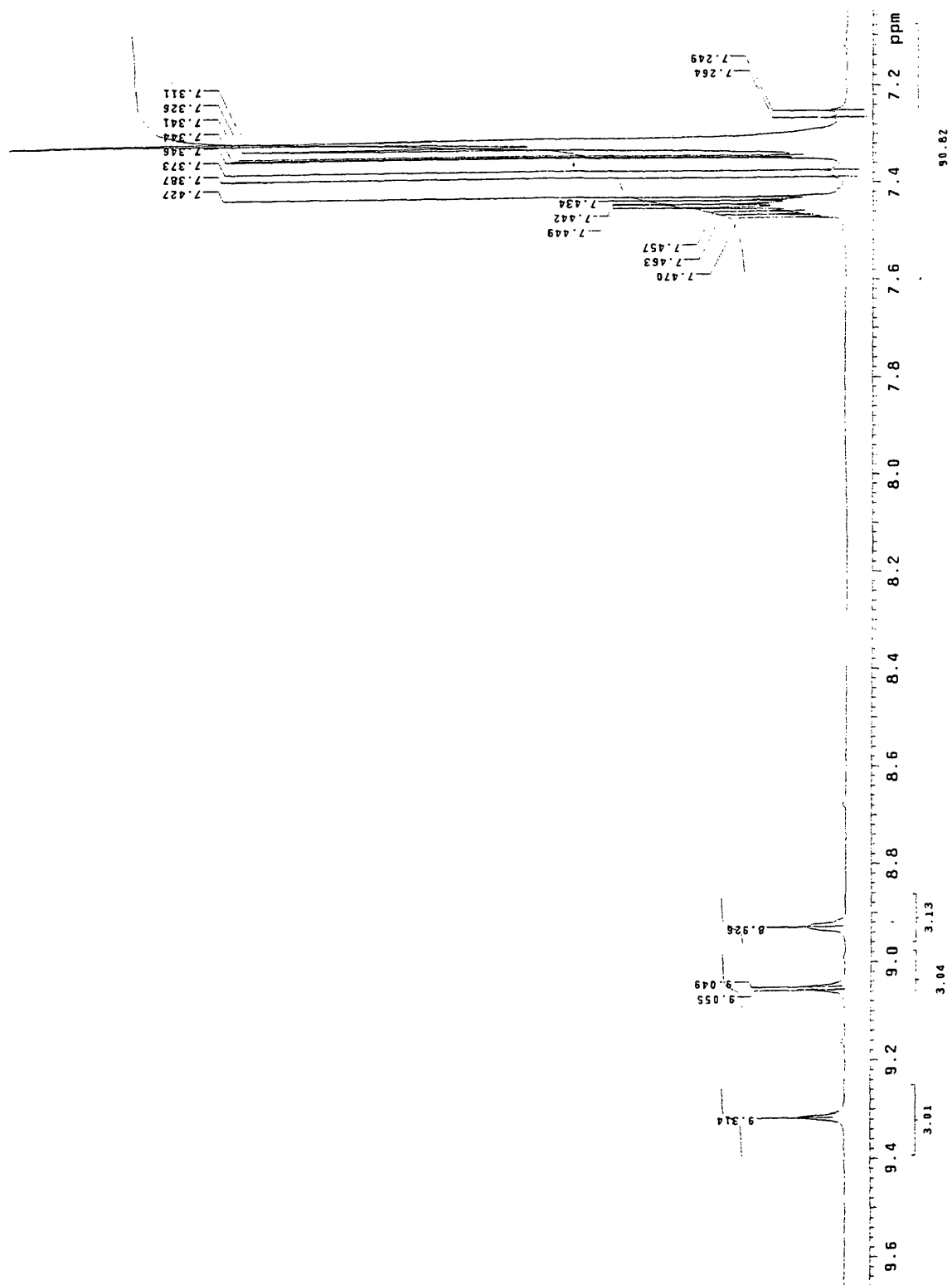
CONCLUSION

Polymeric compounds of the type, $[\text{CuB}(\text{PPh}_3)_2]^+ \text{BF}_4^-$ and dimers of the type $[\text{Cu}_2\text{B}(\text{PPh}_3)_4]^{2+} 2 \text{BF}_4^-$, were synthesized. The pyrazine carboxylic acid and the pyrazine carboxamide bridging ligands both resulted in the formation of oligomers of considerable length. The analogous reactions for the diacid and diamide produced dimers. When each of these oligomers was deprotonated, the chain length remained roughly unchanged, excluding that of pyrazine carboxamide. In this case, the long oligomer converted to a dimer when deprotonated.

Thirteen compounds of the category, $[(\text{CuX})_n\text{B}]$ were synthesized. The stoichiometries formed were particular to the bridging ligand of the species. The pyrimidine series formed only $[(\text{CuX})_2\text{Pym}]$ compounds for all three halides used. The compounds formed using pyridazine were of the type $[(\text{CuX})\text{Pdz}]$ for each halide, but the use of CuI also formed $[(\text{CuI})_2\text{Pdz}]$. The formation of these two stoichiometries was elucidated in a thermodynamic stability test (Table 9). The use of triazine as the bridging ligand resulted in three possible stoichiometries: $[(\text{CuX})_3(\text{Trz})_2]$, $[(\text{CuX})_2\text{Trz}]$, and $[(\text{CuX})_3\text{Trz}]$. Copper chloride was found to form both $[(\text{CuX})_2\text{Trz}]$ and $[(\text{CuX})_3\text{Trz}]$. On the other hand, CuBr formed these two stoichiometries, as well as the previously unreported $[(\text{CuBr})_3(\text{Trz})_2]$ compound. It was found that CuI did not exhibit the same stoichiometric flexibility as CuCl and CuBr. A thermodynamic stability test resulted in forming only $[(\text{CuI})_2\text{Trz}]$.

Through the addition of triphenylphosphine and triphenylphosphite to the [CuXB] networks, numerous new products were formed. For the compounds having pyrimidine as the bridging ligand, the stoichiometry uniformly discovered was [(CuX)₂L₂B]. The only exception was that [(CuI)(P(OPh)₃)₂Pym] was not able to be synthesized. Parallel compounds were synthesized using pyridazine as the bridging ligand to form predominantly [(CuX)LB] stoichiometries. The exceptions found were the formation of [(CuCl)₂(PPh₃)₂Pdz] and the failure to form a [(CuI)(P(OPh)₃)PdZ] product. Triazine formed [(CuX)₂L₂B] stoichiometries in all cases except [(CuCl)₃(PPh₃)₃Trz] and [(CuI)₃(P(OPh)₃)₃Trz]. A correlation can be made from the stoichiometries of the [(CuX)_nB] and the [(CuX)_nL_nB] compounds for each bridging ligand. The 2:1 pyrimidine compounds transfer over as 2:2:1 compounds when a 'capping' ligand is included. The 1:1 pyridazine stoichiometry remains intact and forms 1:1:1 compounds with the 'capping' ligand. The majority of the triazine compounds with 'capping' ligands formed were 2:2:1, with the exception of two showing 3:3:1 stoichiometry. However, given the diverse coordination modes conceivable for triazine, it seems plausible that both 2:2:1 and 3:3:1 stoichiometries should form as well as a possible 3:3:2 stoichiometry.

APPENDIX A

Figure A1. Proton NMR of $[\text{Cu}(\text{Pca})(\text{PPh}_3)_2]^+ \text{BF}_4^-$.

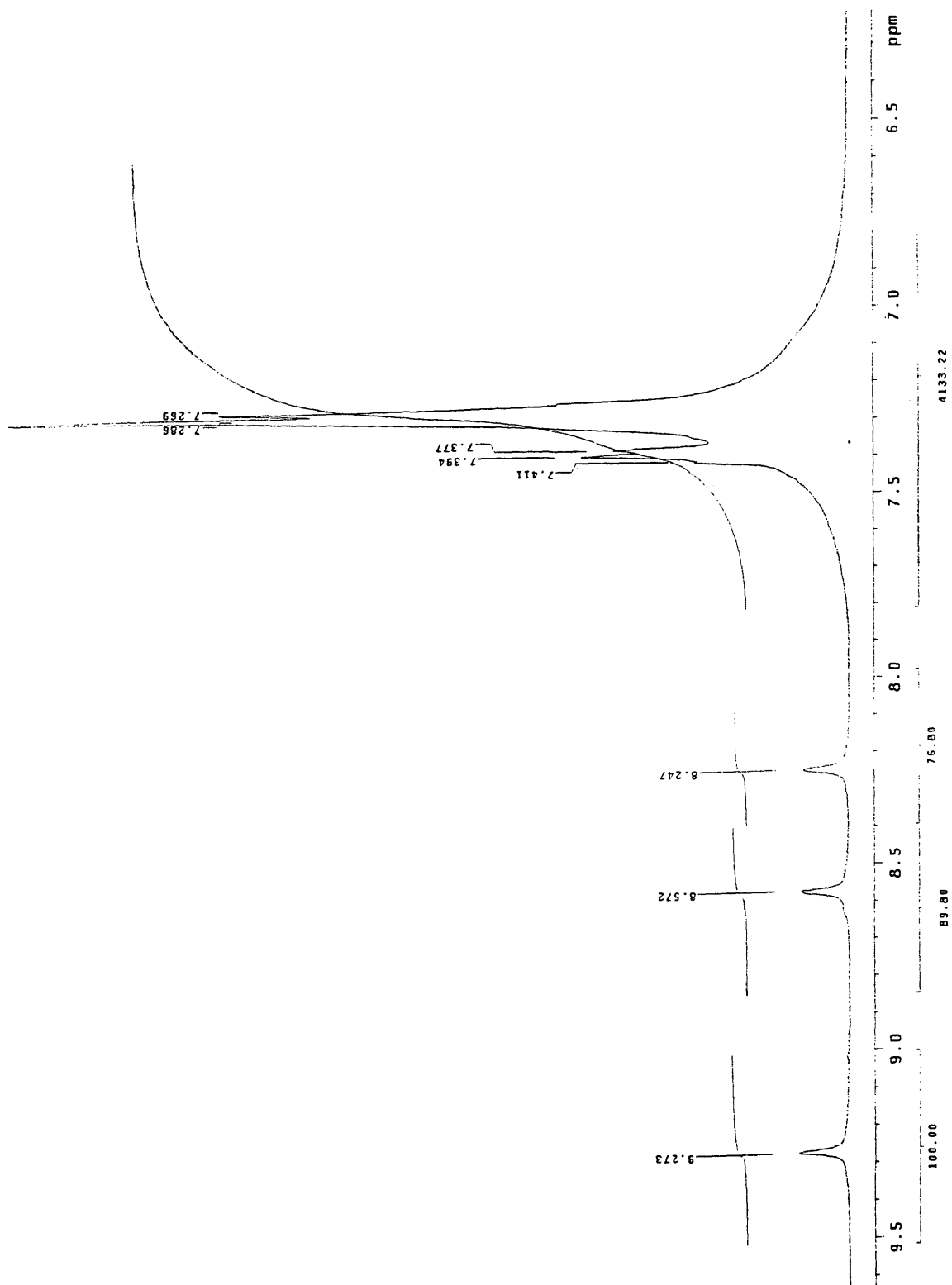


Figure A2. Proton NMR of [Cu(D-Pca)(PPh₃)₂].

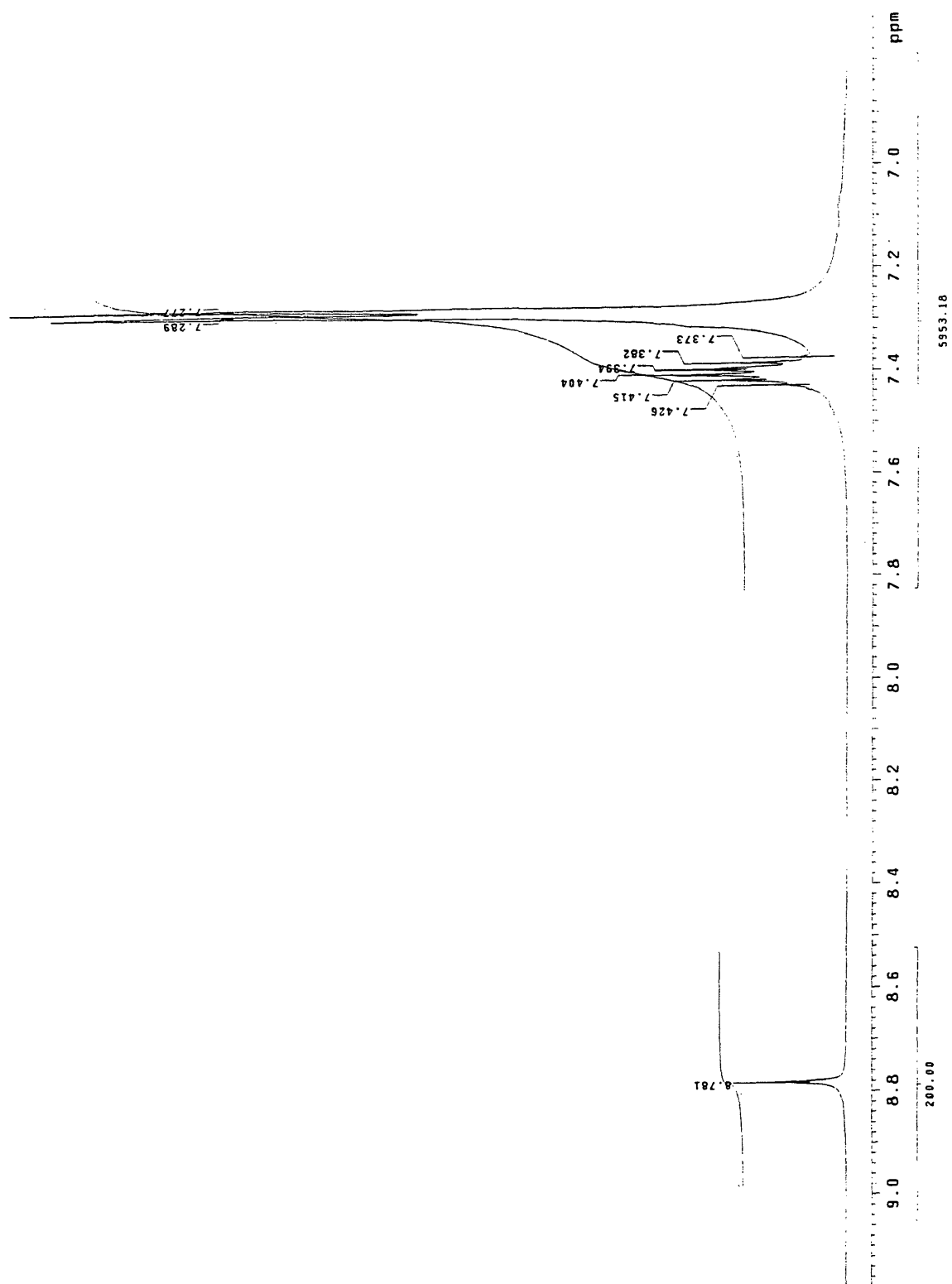


Figure A3. Proton NMR of $[\text{Cu}_2(\text{Pdca})(\text{PPh}_3)_4]^{2+} 2 \text{BF}_4^-$.

REFERENCES

- 1 Hoskins, B. F.; Robson, R. *J. Am. Chem. Soc.* **1990**, *112*, 1546.
- 2 Munakata, M.; Kuroda-Sowa, T.; Maekawa, M.; Honda, A.; Kitagawa, S. *J.*
- 3 Munakata, M.; Wu, L. P.; Kuroda-Sowa, T. *Adv. Inorg. Chem.* **1999**, *46*, 173.
- 4 Munakata, M.; Wu, L. P.; Kuroda-Sowa, T. *Bull. Chem. Soc. Jpn.* **1997**, *70*, 1727.
Chem. Soc., Dalton Trans. **1994**, 2771.
- 5 Graham, P. M.; Pike, R. D.; Sabat, M.; Bailey, R. D.; Pennington, W. T. *Inorg. Chem.* **2000**, *39*, 5121.
- 6 Dyason, J. C.; Engelhardt, L. M.; Healy, P. C.; White, A. H. *Aust. J. Chem.* **1984**, *37*, 2201.
- 7 Kromp, T.; Sheldrick, W. S. *Z. Naturforsch.* **1999**, *54b*, 1175.
- 8 Blake, A. J.; Brooks, N. R.; Champness, N. R.; Hanton, L. R.; Hubberstey, P.; Parsons, S.; Schröder, M. *Pure Appl. Chem.* **1998**, *70*, 2351.
- 9 Blake, A. J.; Brooks, N. R.; Champness, N. R.; Crew, M.; Hanton, L. R.; Hubberstey, P.; Parsons, S.; Schröder, M. *J. Chem. Soc., Dalton Trans.* **1999**, 2813.
- 10 Goher, M. A. S.; Mautner, F. A. *Polyhedron* **1999**, *18*, 1805.
- 11 Lu, J. L.; Crisci, G.; Niu, T.; Jacobson, A. J. *Inorg. Chem.* **1997**, *36*, 5140.
- 12 Henary, H.; Wootton, J. L.; Khan, S. I.; Zink, J. I. *Inorg. Chem.* **1997**, *36*, 796.
- 13 Blake, A. J.; Brooks, N. R.; Champness, N. R.; Cooke, P. A.; Deveson, A. M.; Fenske, D.; Hubberstey, P.; Li, W.; Schroder, M. *J. Chem. Soc., Dalton Trans.* **1999**, 2103.
- 14 Pike, R. D.; Todd, J. L. unpublished results.

- 15 Goher, M. A. S.; Mautner, F. A. *Polyhedron* **2000**, *19*, 601.
- 16 Munakata, M.; Kuroda-Sowa, T.; Maekawa, M.; Hirota, A.; Kitagawa, S. *Inorg. Chem.* **1995**, *34*, 2705.
- 17 Wohlfarth, C. In *CRC Handbook of Chemistry and Physics*; Lide, D. R., Ed.; CRC Press: Boca Raton, FL, 1999, 6-148.
- 18 *CRC Handbook of Chemistry and Physics*; Lide, D. R., Ed.; CRC Press: Boca Raton, FL, 1999, 4-35.

VITA

Born at Bethesda Naval Hospital in Bethesda, Maryland on April 13, 1977. Received high school diploma from Rappahannock County High School in Sperryville, Virginia in June of 1995. Continued education at the College of William and Mary in Williamsburg, Virginia and earned a Bachelor of Science with a concentration in Chemistry in May of 1999. Candidate for a Master of Arts in Chemistry at the College of William and Mary, 1999-2001.